Lessons 7 and 8

- Indirect detection of photons with 50 GeV < E_γ < 100 TeV.
- Detection of VHE γ induced EAS with Imaging Air Cherenkov Telescopes: main results
- “Leptonic” and “Hadronic” sources of high energy photons: the Inverse Compton process
- Long term Measurement of EAS at high quote over sea level over (the ARGO and Milagro experiments)
- Ground based detectors:
- Detection at ground of extensive Air Showers: nature, direction and energy of the primary C.R.
- The KASKADE experiment
- Detection of U.H.E. Cosmic Rays (E>> 100 PeV)

Measuring cosmic-ray and γ-ray air showers

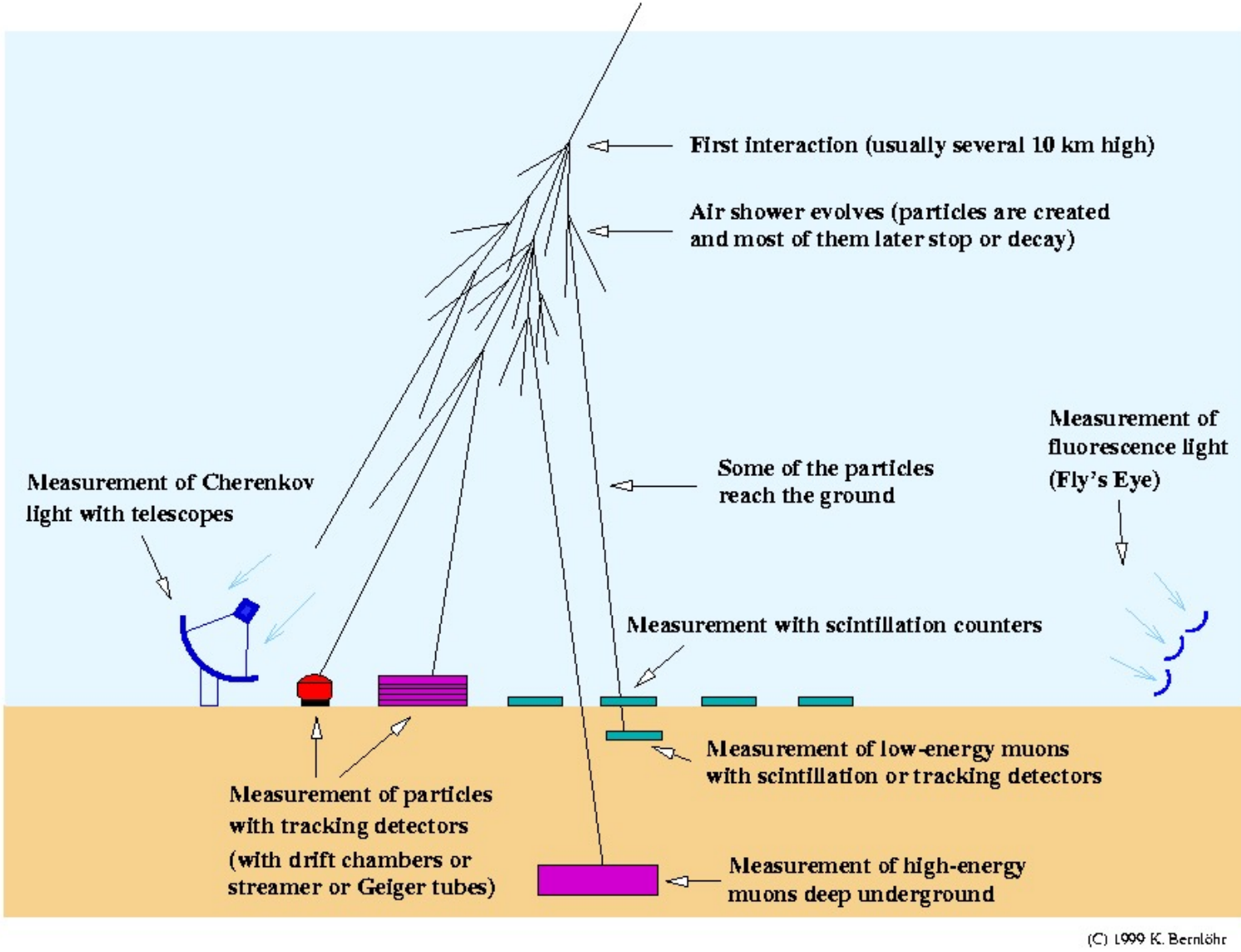

The Imaging Atmospheric Cherenkov technique

- Cherenkov radiation due to secondary particles with speed $v > c/n$.
- Short flashes (5-20 ns).
- Cherenkov photons collected by large ground reflectors and focused onto a camera with fast PMTs.
- The shower is “imaged” by the Cerenkov telescope.

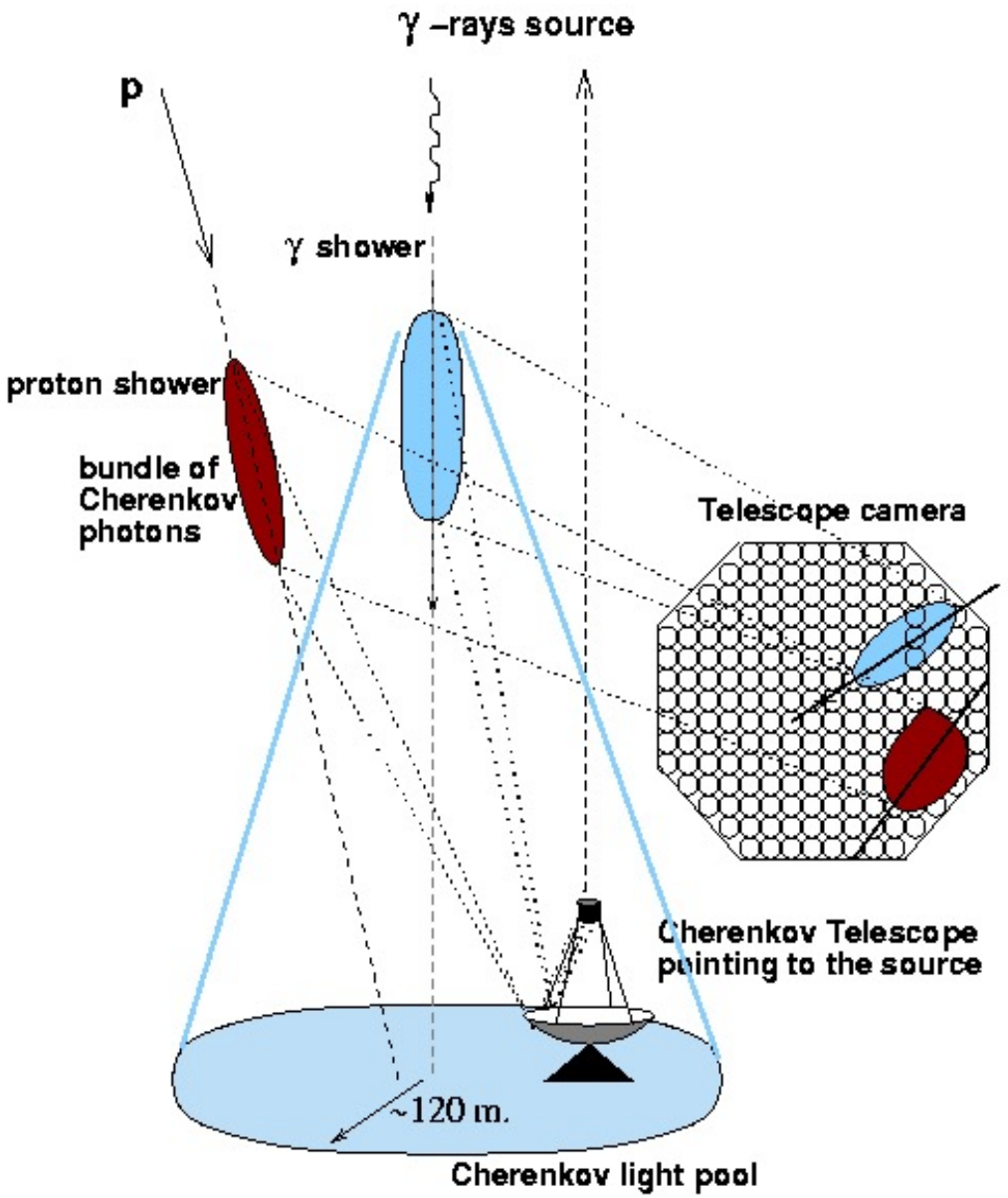

How the image is built-up on the central camera

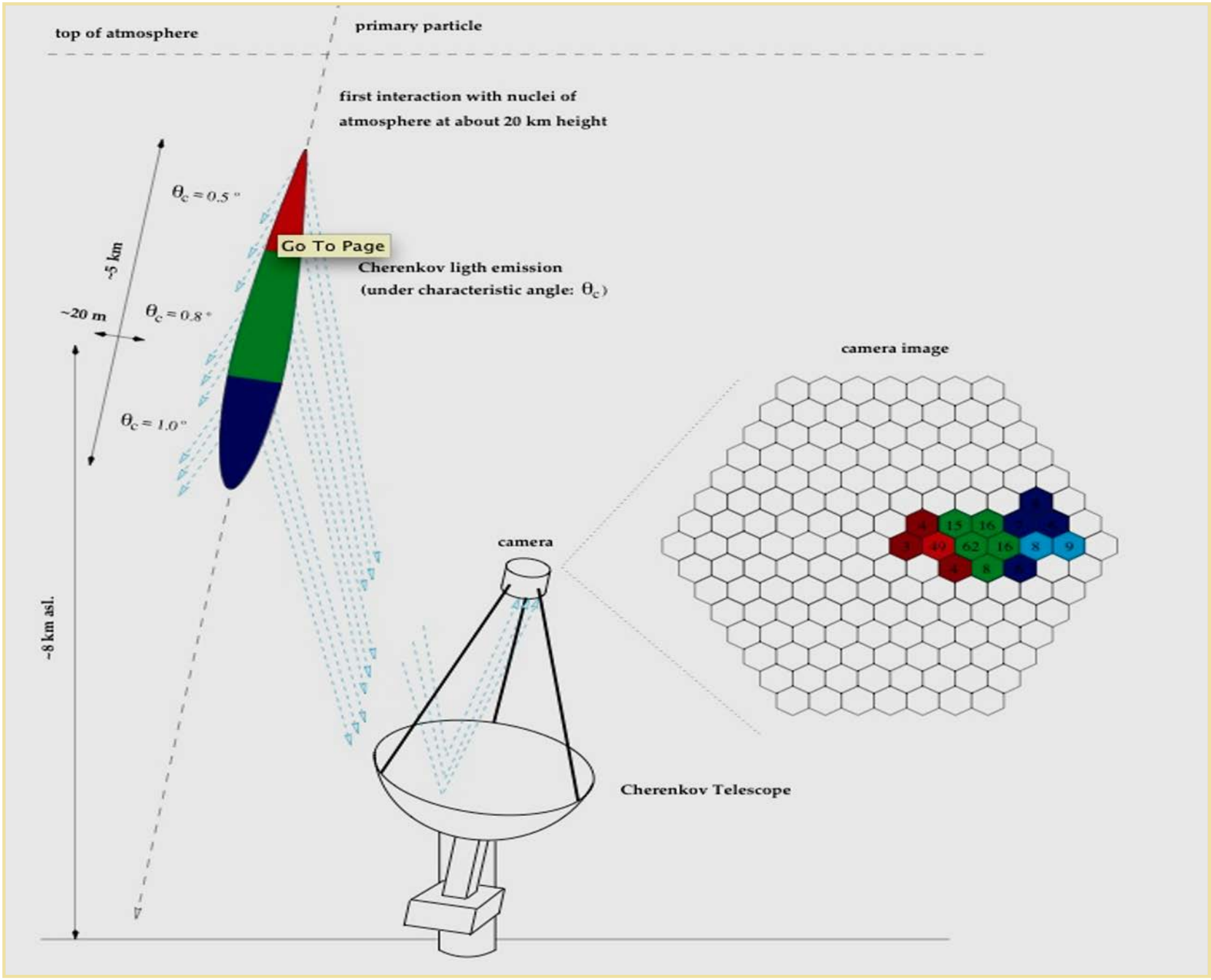

A γ-ray "image" obtained when the telescope points to the source

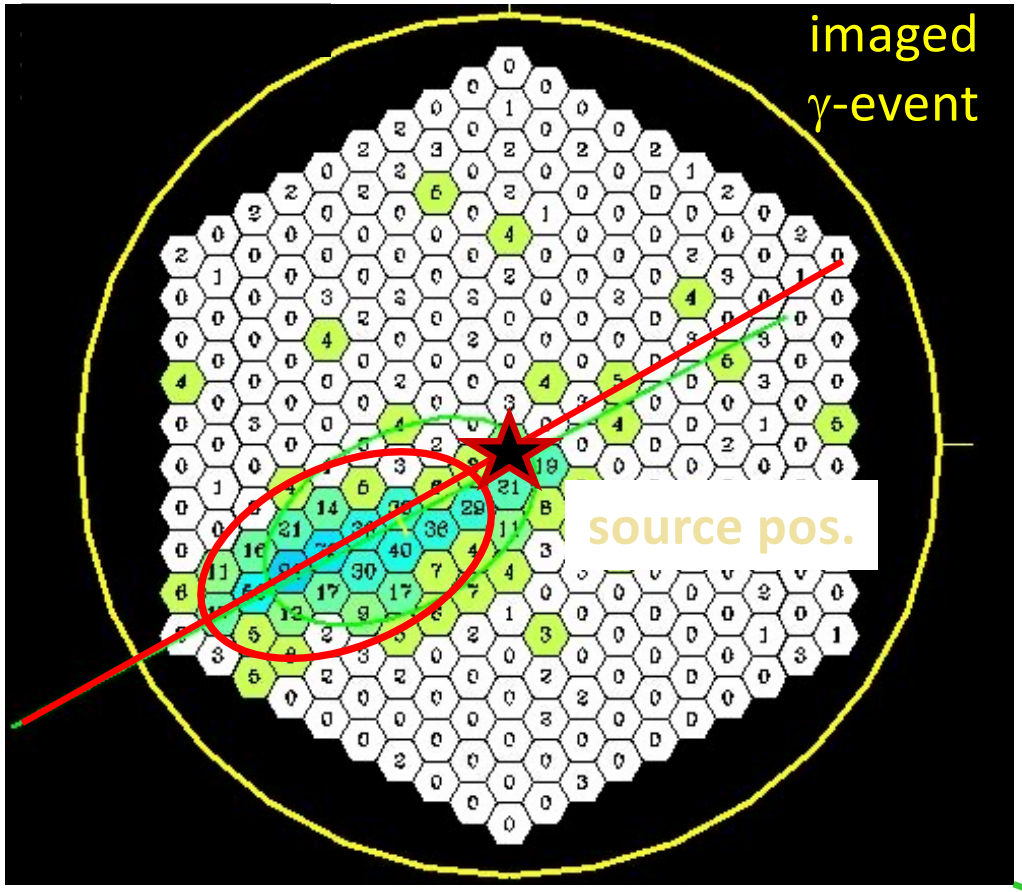

the source is placed at the camera center

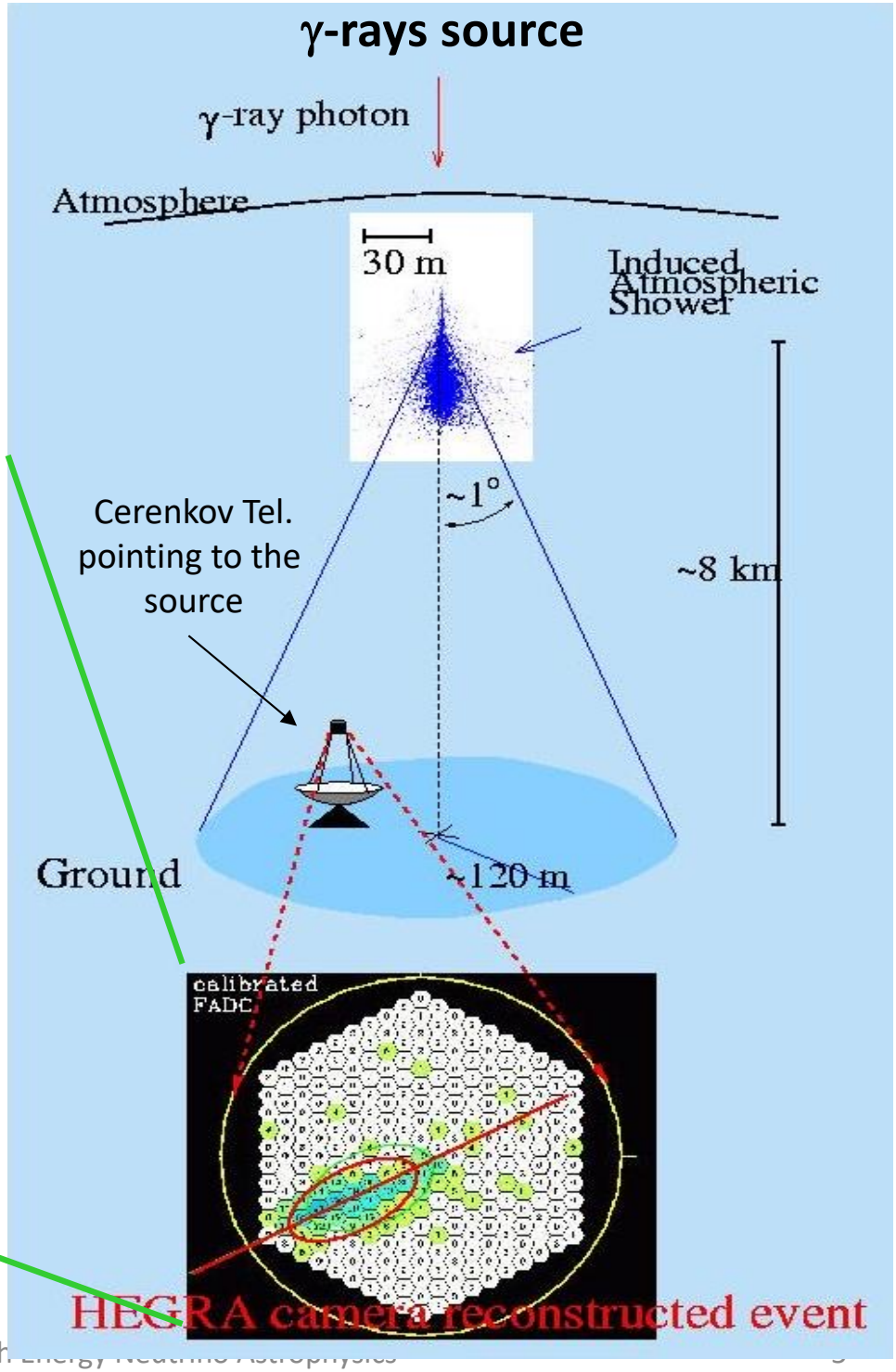

Charged Cosmic Ray “image”

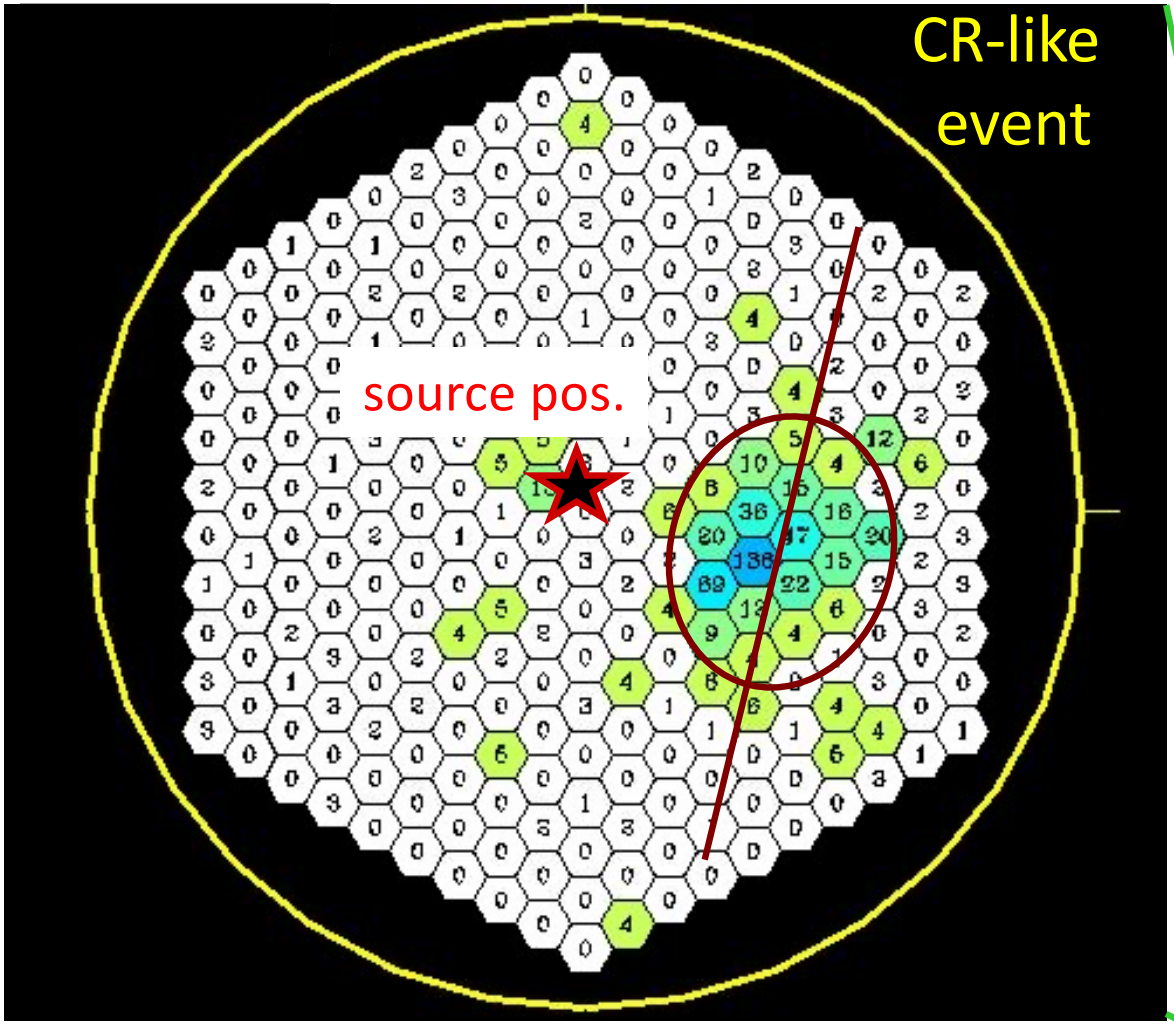

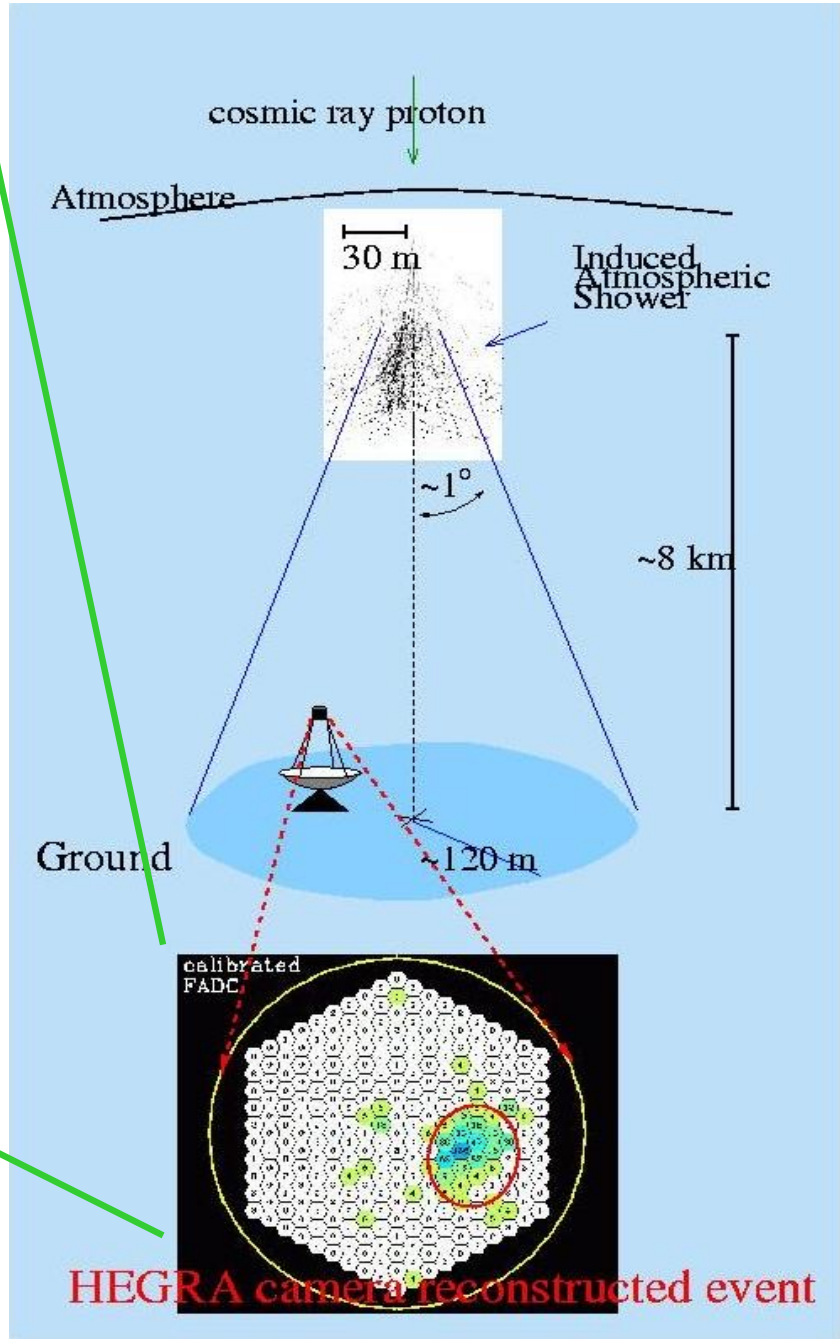

CR-images are randomly distributed so they don't point to the source !!

Experiments for γ astronomy

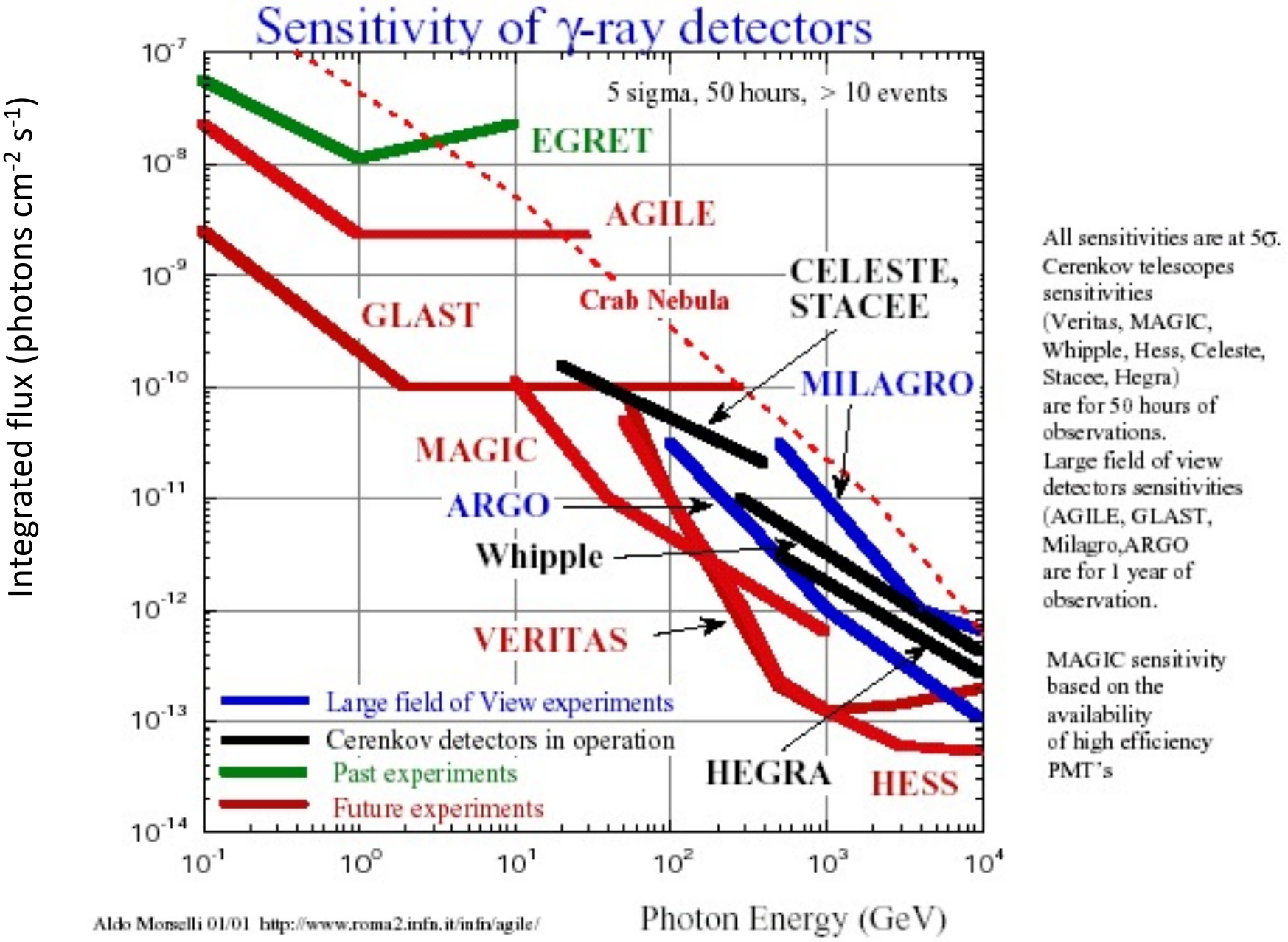

Operating Cherenkov telescopes

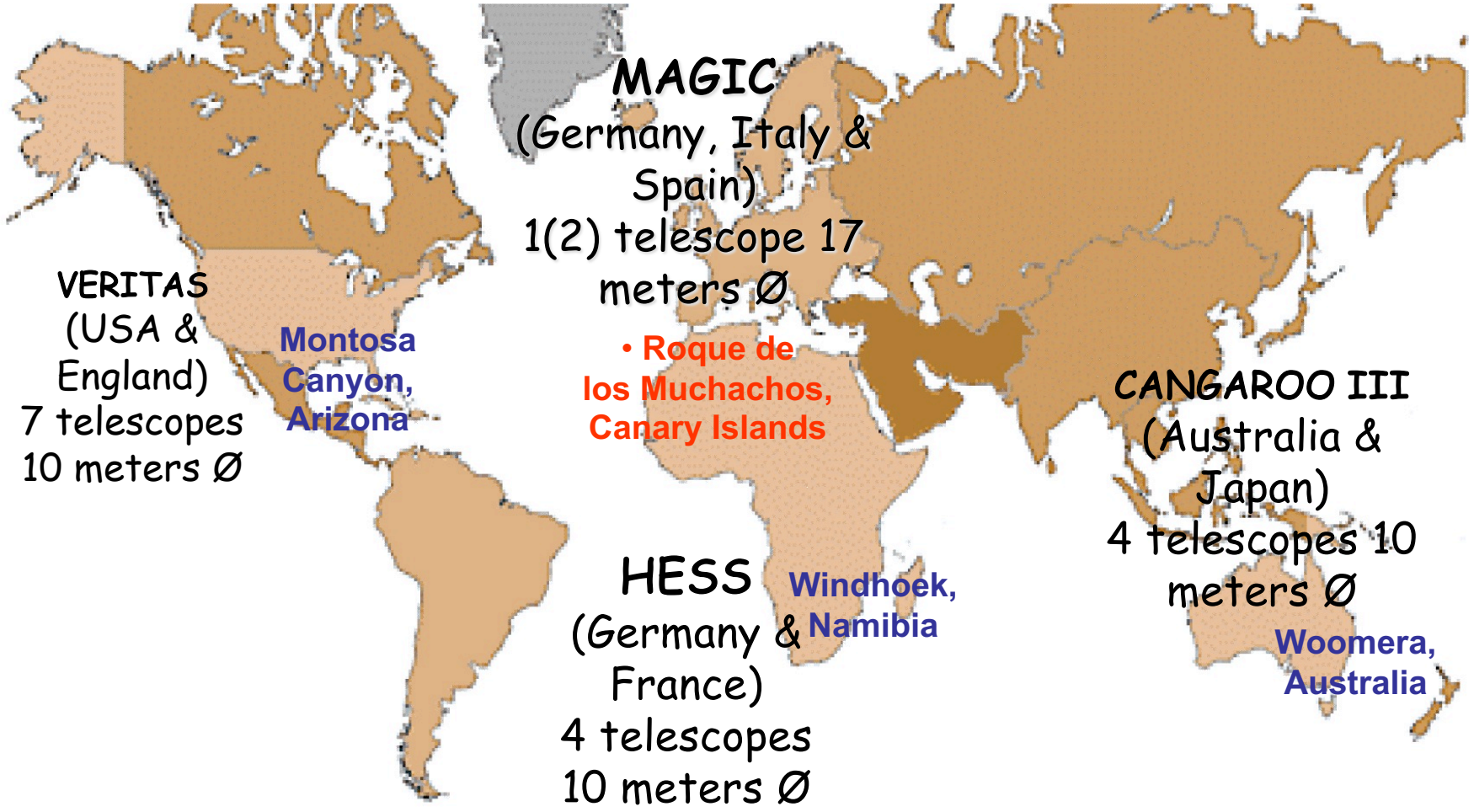

Galactic TeV gamma-ray Sources

- at least 4 source classes:
  - Shell-type SNR
  - Pulsar Wind Nebulae (PWN)
  - X-ray binaries (binary pulsar and microquasars)
  - Molecular Clouds plus SMBH in GC (Sgr A*)?

Many not yet identified!

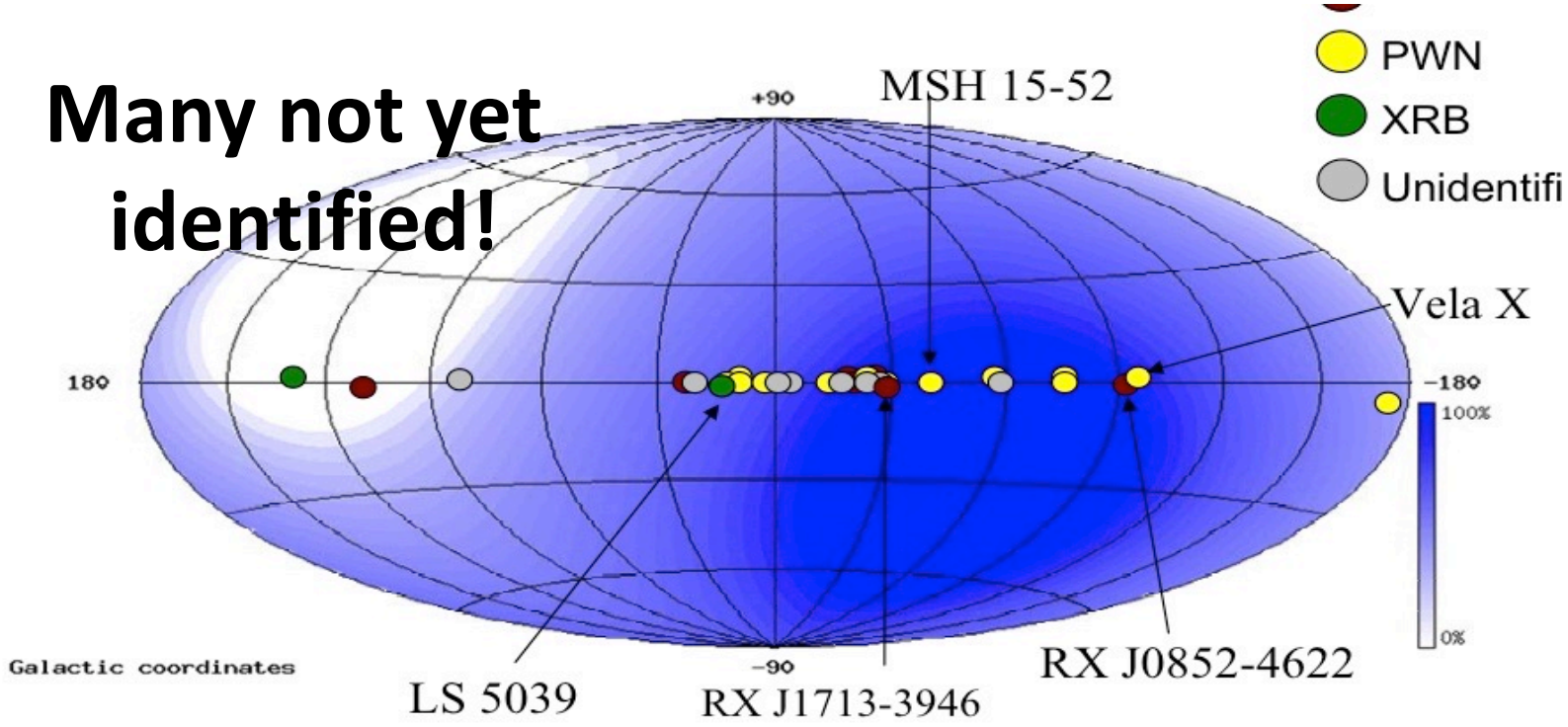

Crab Nebula: the standard candle (I)

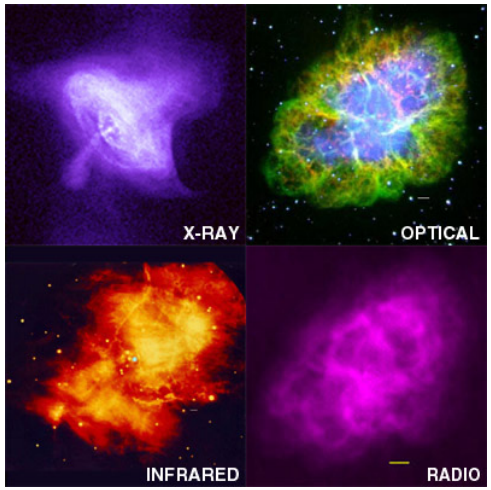

- Remnant of a supernova explosion, occurred in 1054.
- Pulsar injecting relativistic electrons into the nebula.
- Emission predominantly by non-thermal processes, covering a huge energy range (radio to TeV).
- First TeV source (Whipple Telescope, 1989).
- Steady HE γ-ray emission

  → *standard candle*

- $\Phi\,(E>1\ \mathrm{TeV}) = 1.6 \cdot 10^{-11}\ \mathrm{ph\ cm^{-2}\ s^{-1}}$

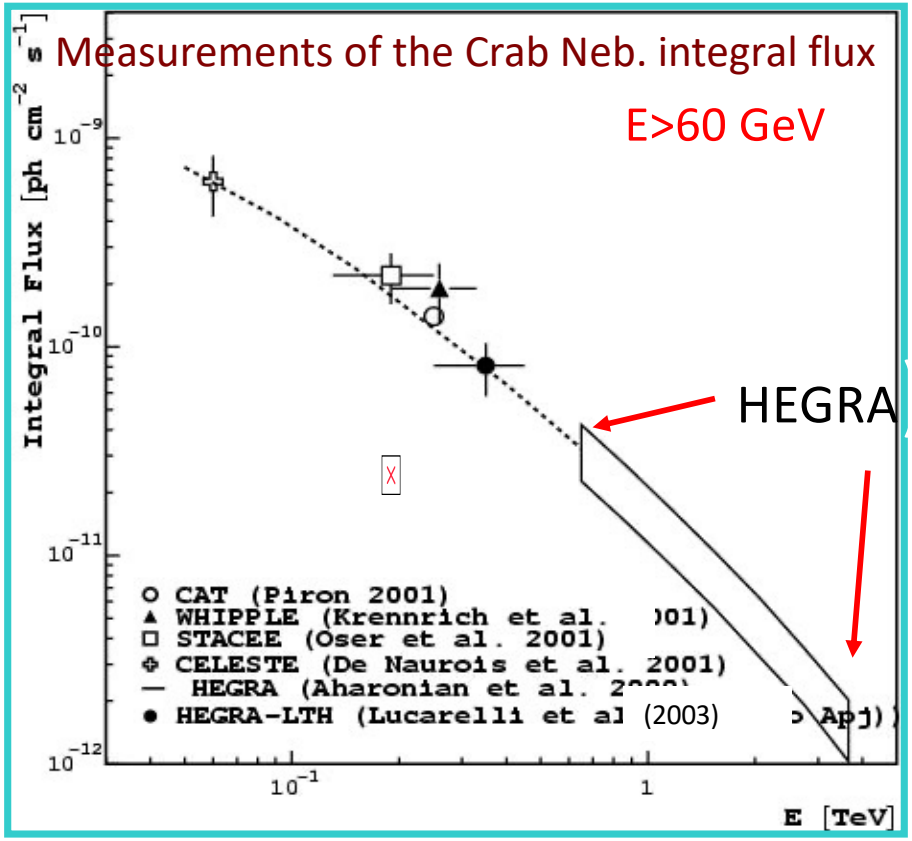

Crab Nebula: the standard candle (II)

☞ **TeV emission from up-scattering of low energy photons (synchrotron, MWB, IR) by electrons in the pulsar wind.**

- **Synchrotron Self-Comtpon** (SSC) model fits the observed spectrum.
- Inverse Compton peak expected below 100 GeV.

No pulsed emission detected so far for E>0.01 TeV

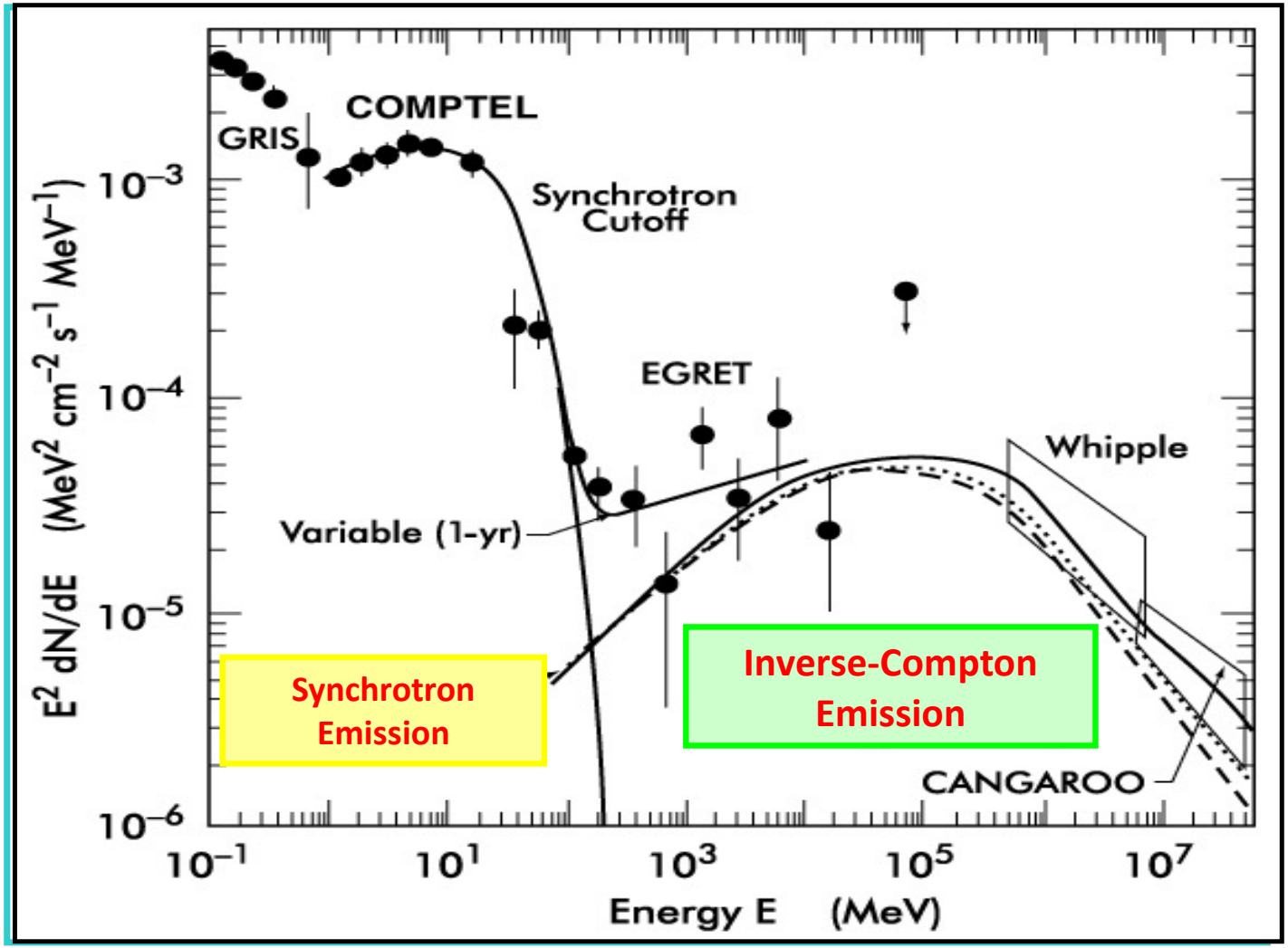

Galactic and Extra-galactic High Energy γ Sources

Observed sky, in galactic coordinates.

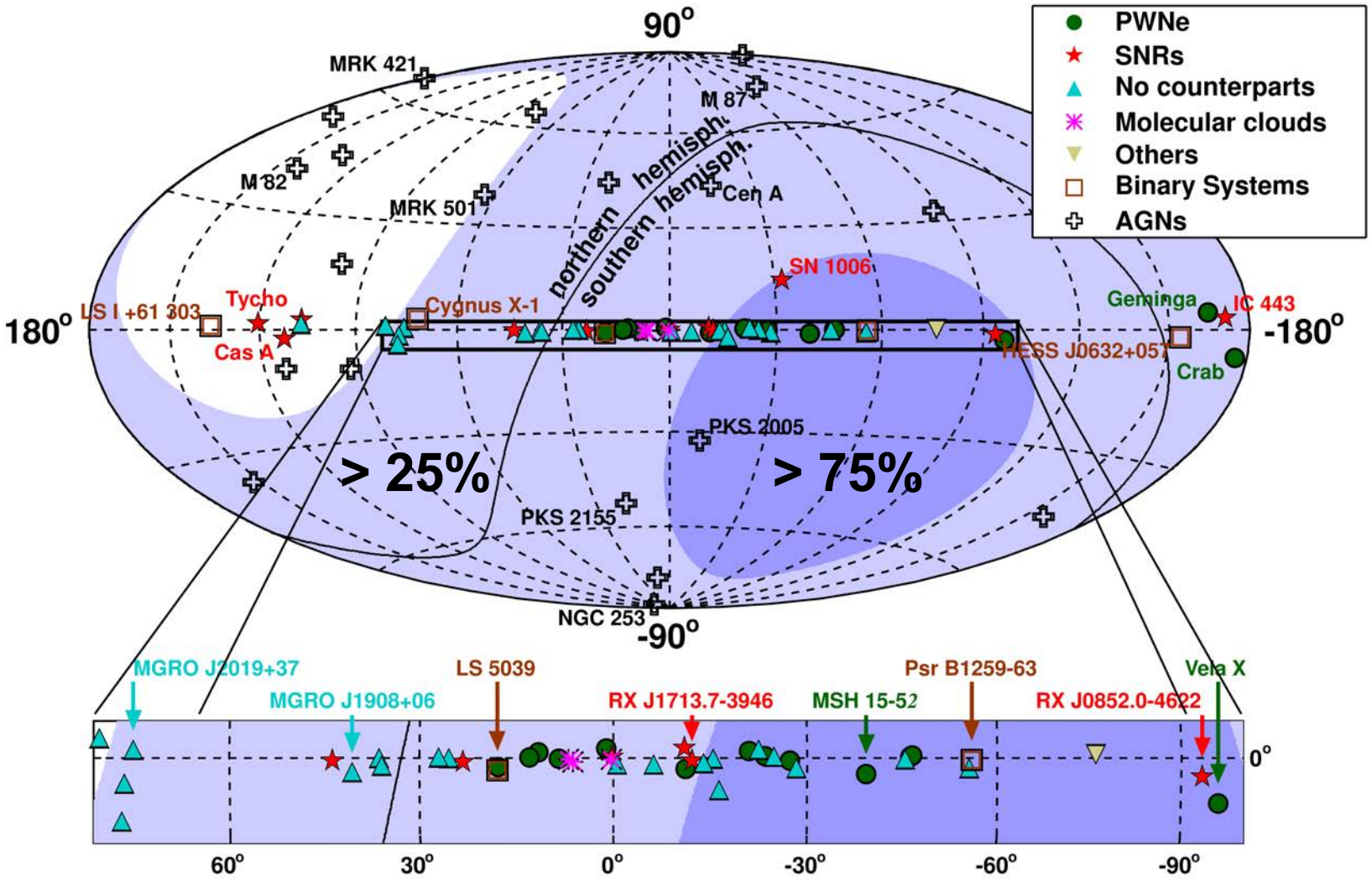

Which processes characterize High Energy sources

leptonic process

Inverse Compton scattering

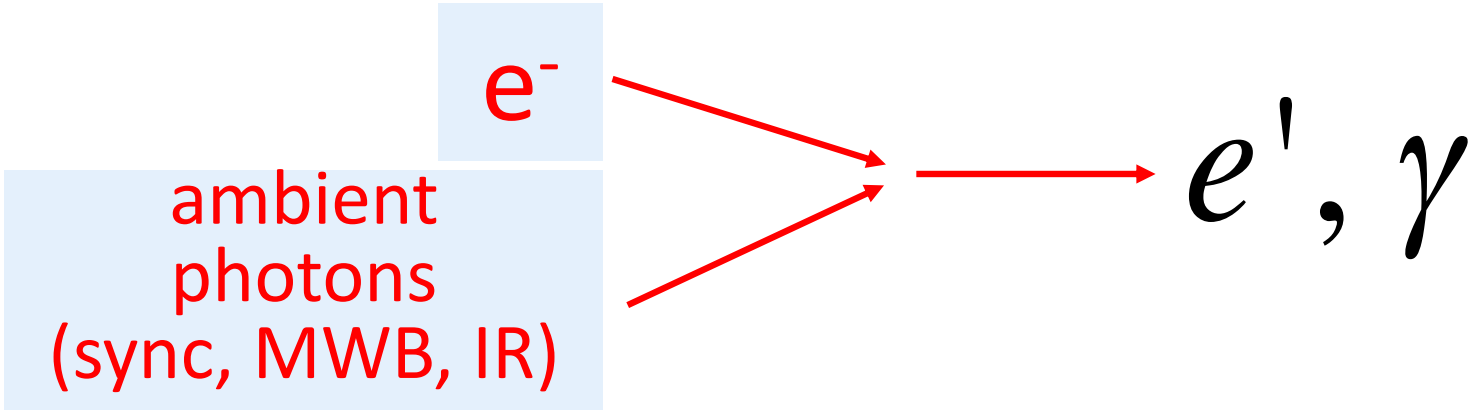

We have to consider also hadronic processes like:

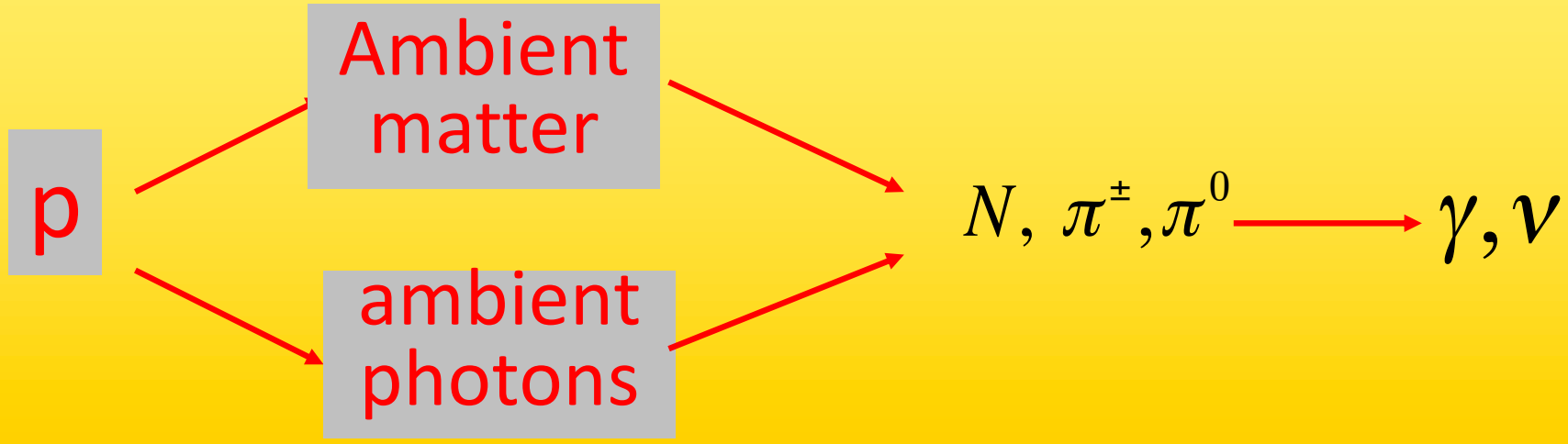

TeV γ-rays from SNRs

High energy gamma observed: not always the Inverse Compton model can explain the observed spectra !

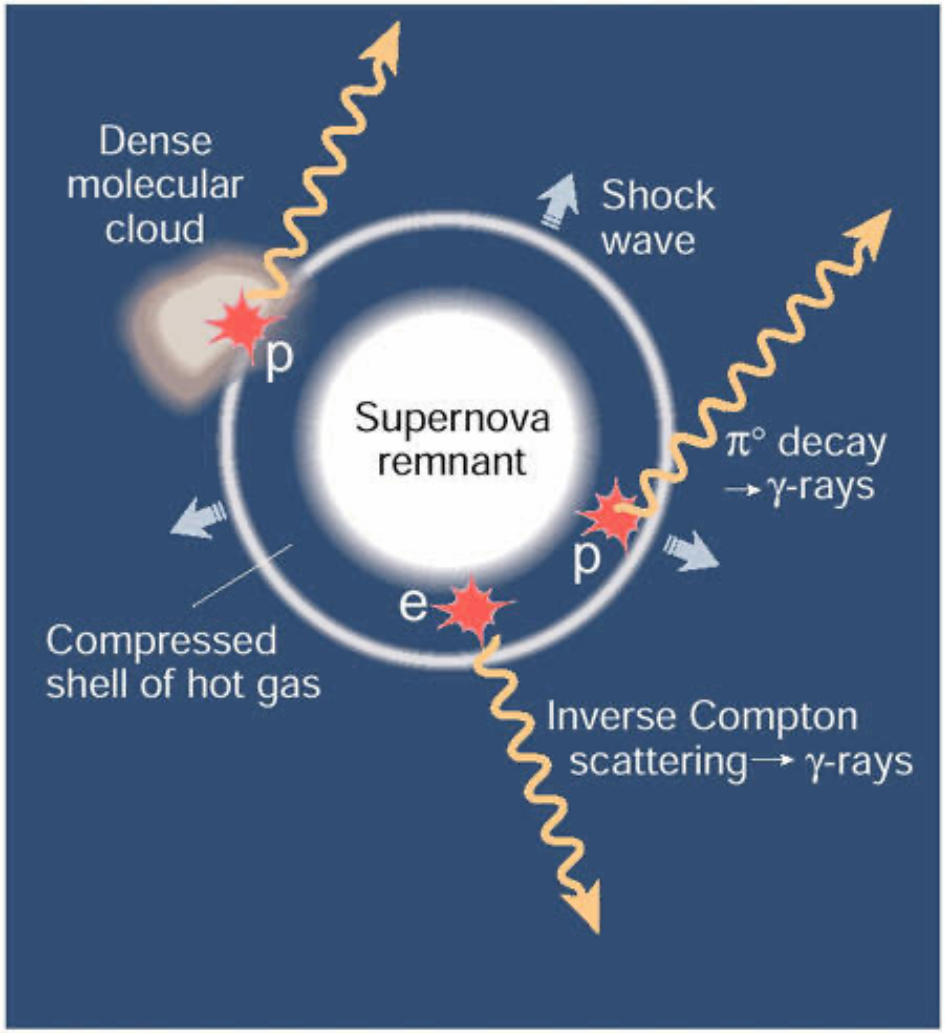

SNR as cosmic particle accelerators

Predicted power law Spectrum:
$dN/dE \sim E^{-2...2.2}$

Imaged using secondary gamma rays created in interactions with ambient medium

A high energy γ source: the Supernova Remnant RX1713-39: an extended source

HESS coll.:Nature 432 (2004) 75

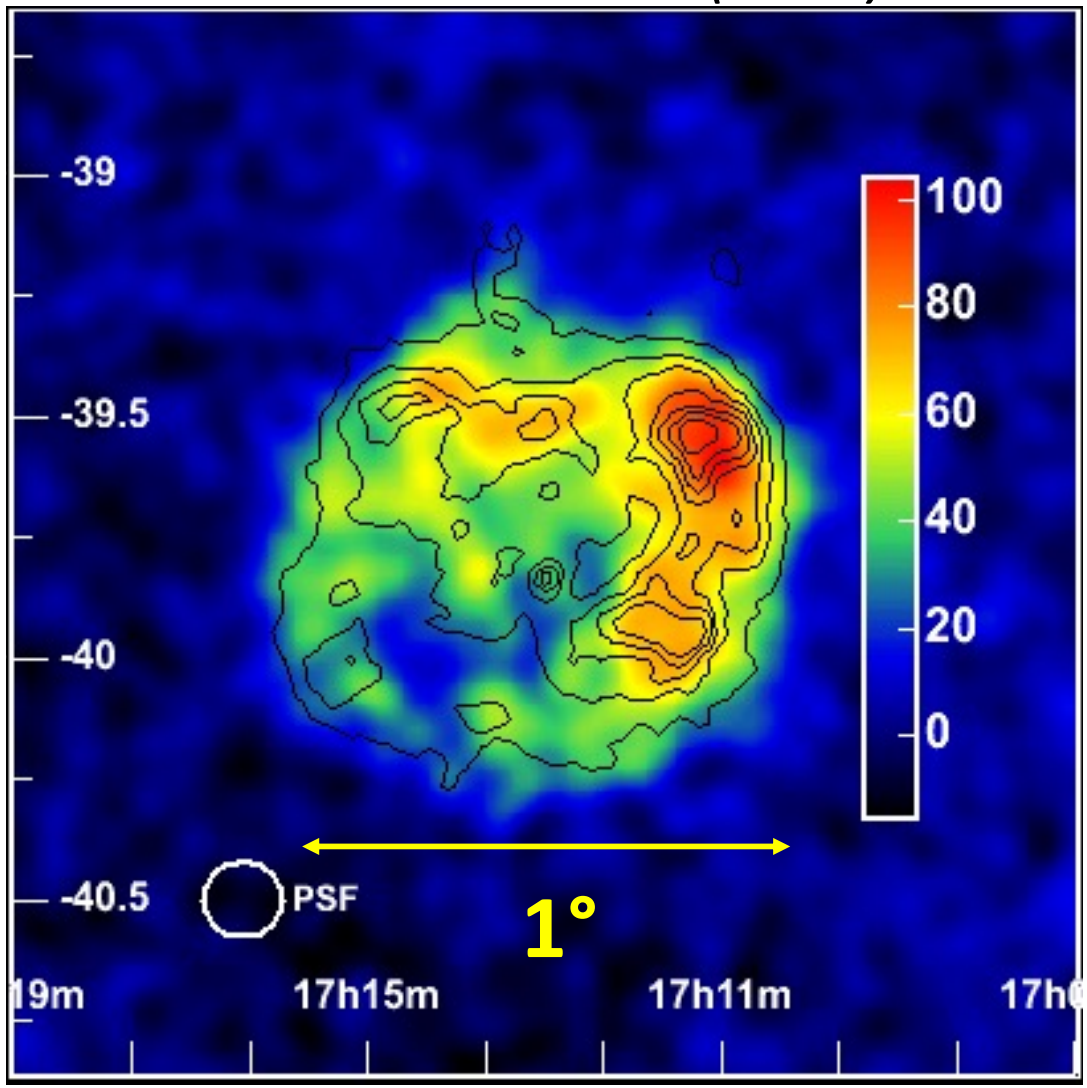

Eγ up to 100 TeV!

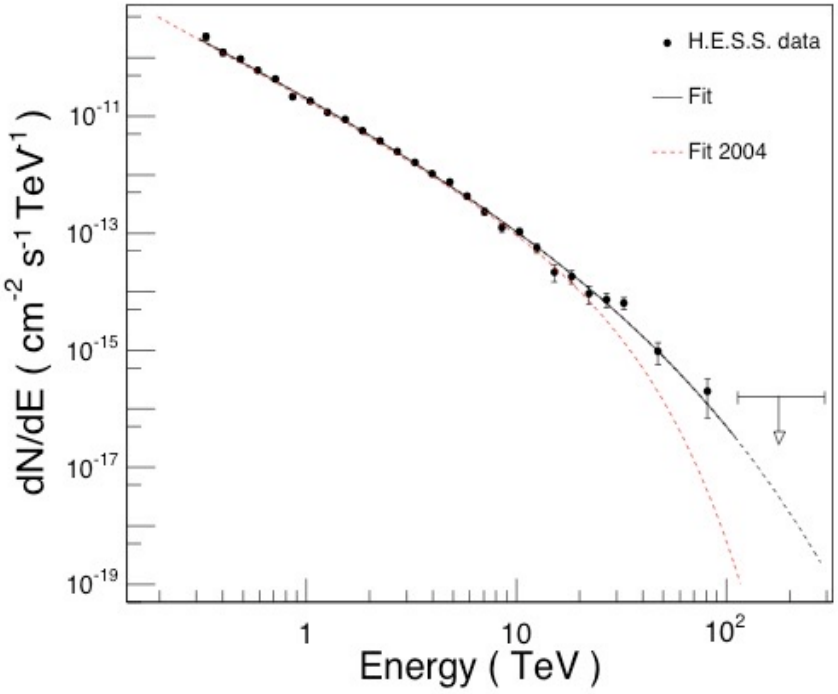

Eγ difficult to justify with Inverse Compton model

“Leptonic” and “Hadronic” origins of High Energy gamma rays

From non thermal extreme dynamic processes:

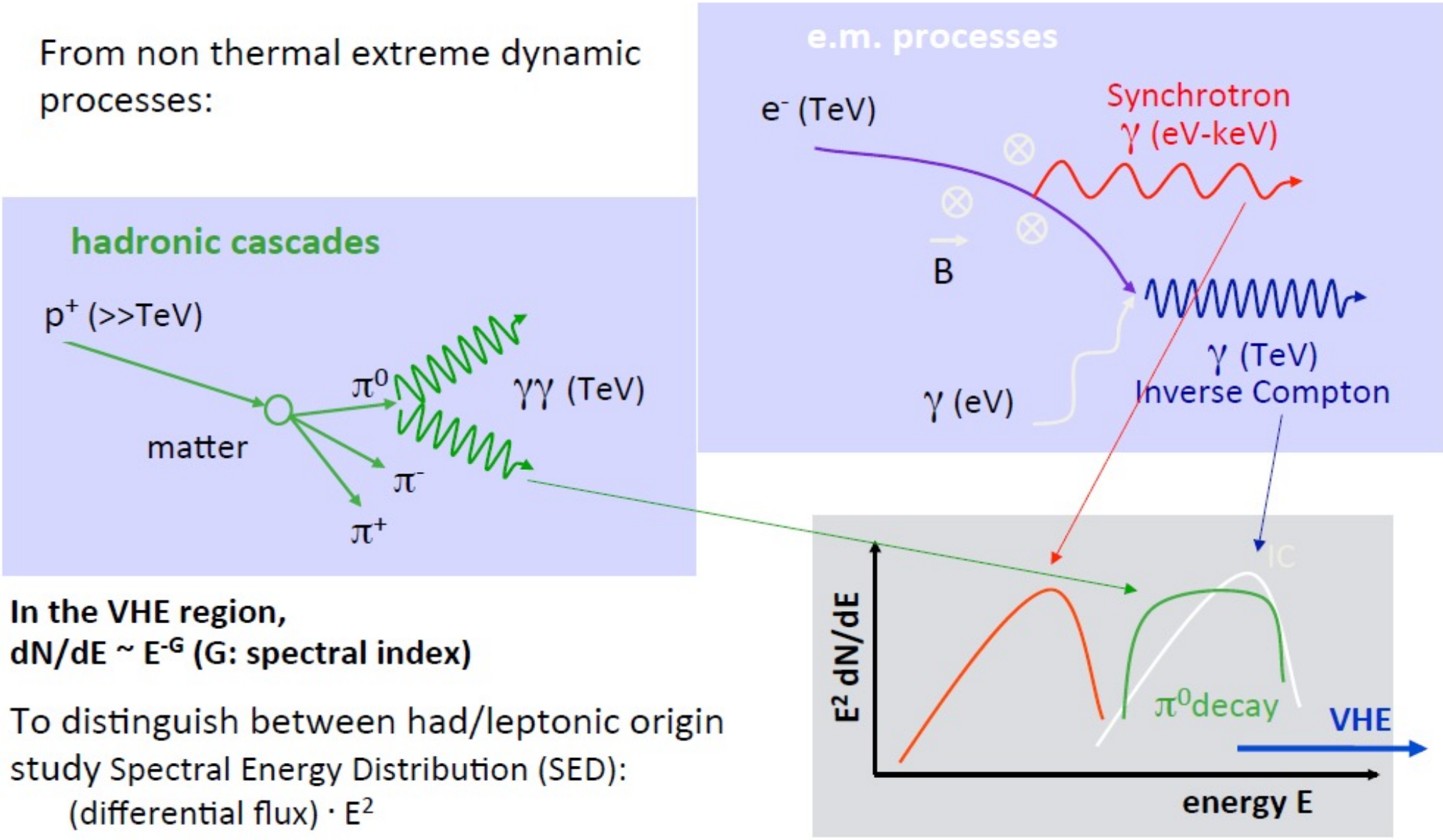

In the VHE region,
$dN/dE \sim E^{-G}$ (G: spectral index)

To distinguish between had/leptonic origin study Spectral Energy Distribution (SED):
(differential flux) · E^2

The π^0-decay bump

- Neutral pion-decay: in the rest-frame of the pion, the two γ rays have 67.5 MeV each (i.e. a line)

Stecker, 1971 (Cosmic gamma rays)

- Transforming into the lab-frame smears the line but keeps it symmetric about 67.5 MeV (in dN/dE)

Dermer, 1986

- Transforming to E2 dN/dE and drop in pion-production cross section destroys symmetry and generates the "bump"

Stecker, 1971 (Cosmic gamma rays)

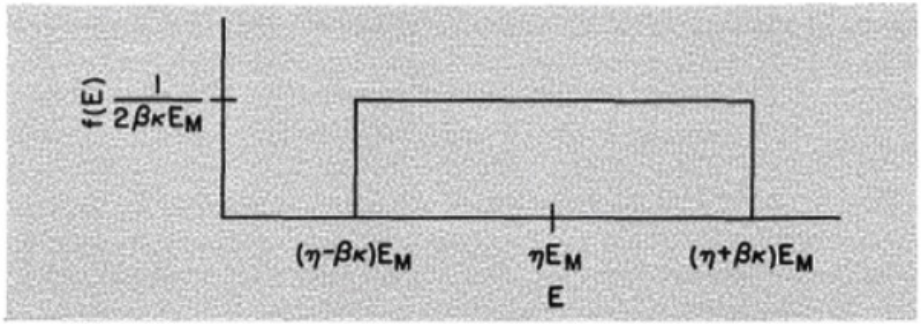

Dermer, 1986

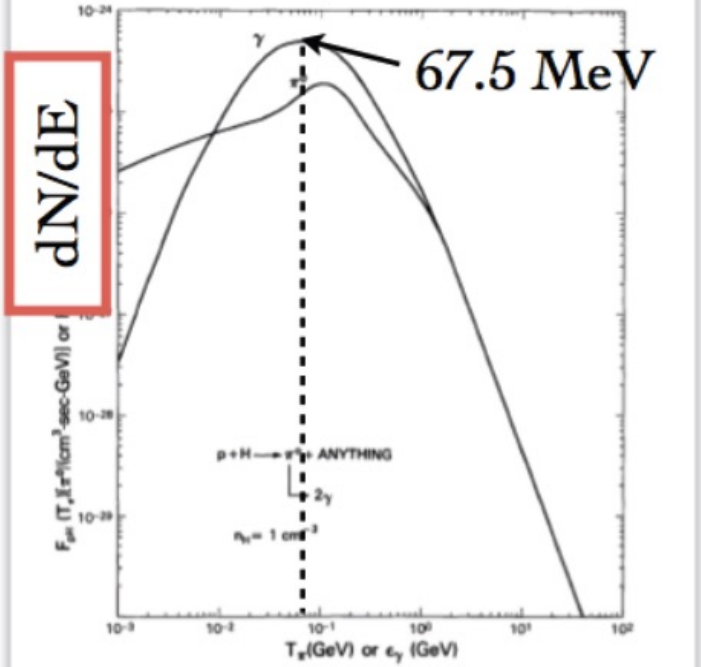

Fig. 7. The secondary π^0 and γ-ray emissivities from the interaction of the local demodulated cosmic ray proton spectrum with unit density of atomic hydrogen

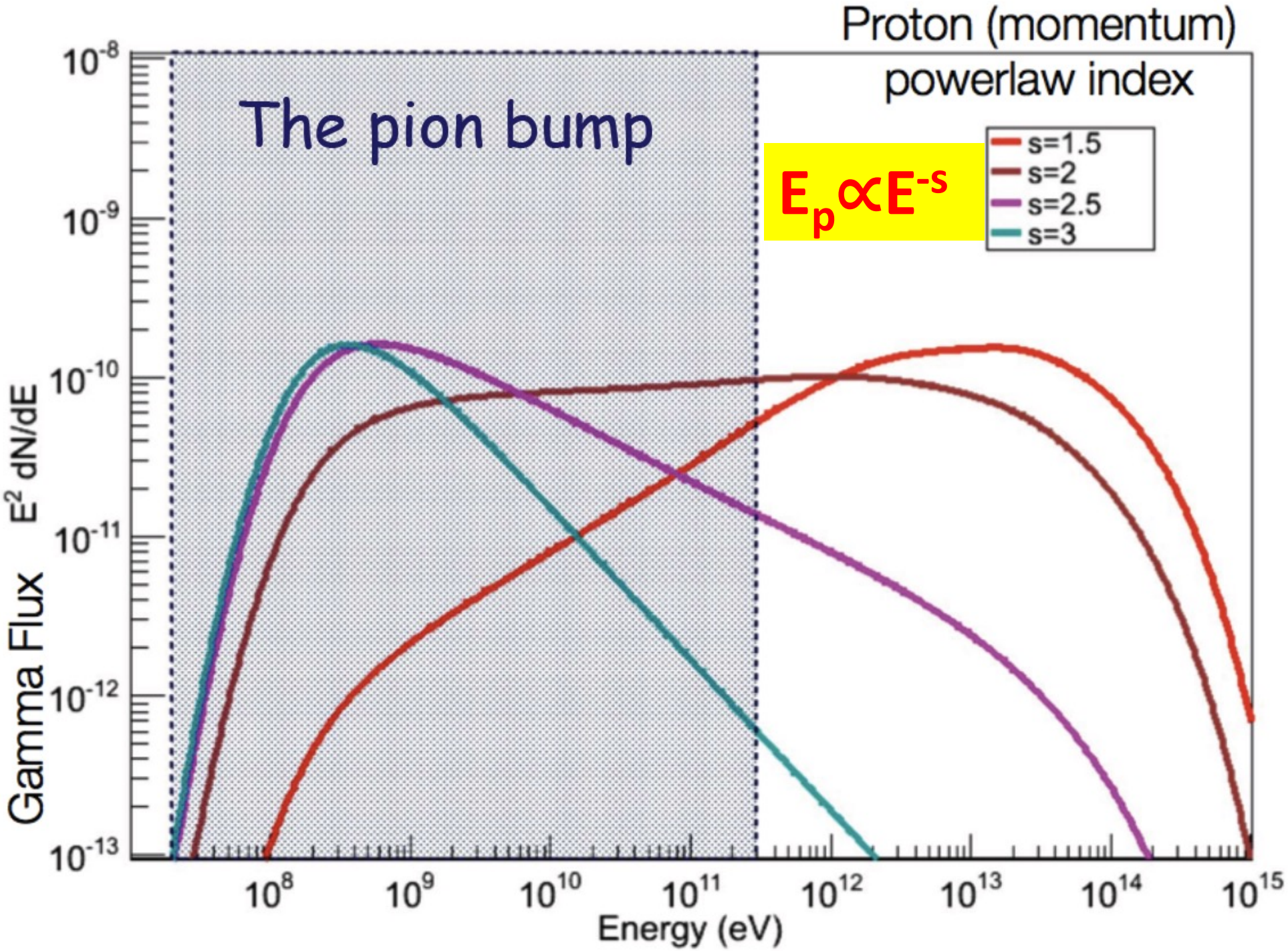

Smoking gun feature for accelerated protons

Hadronic or leptonic?

- possibly hadronic but IC origin not (yet) excluded (requires B-field <10 μG)

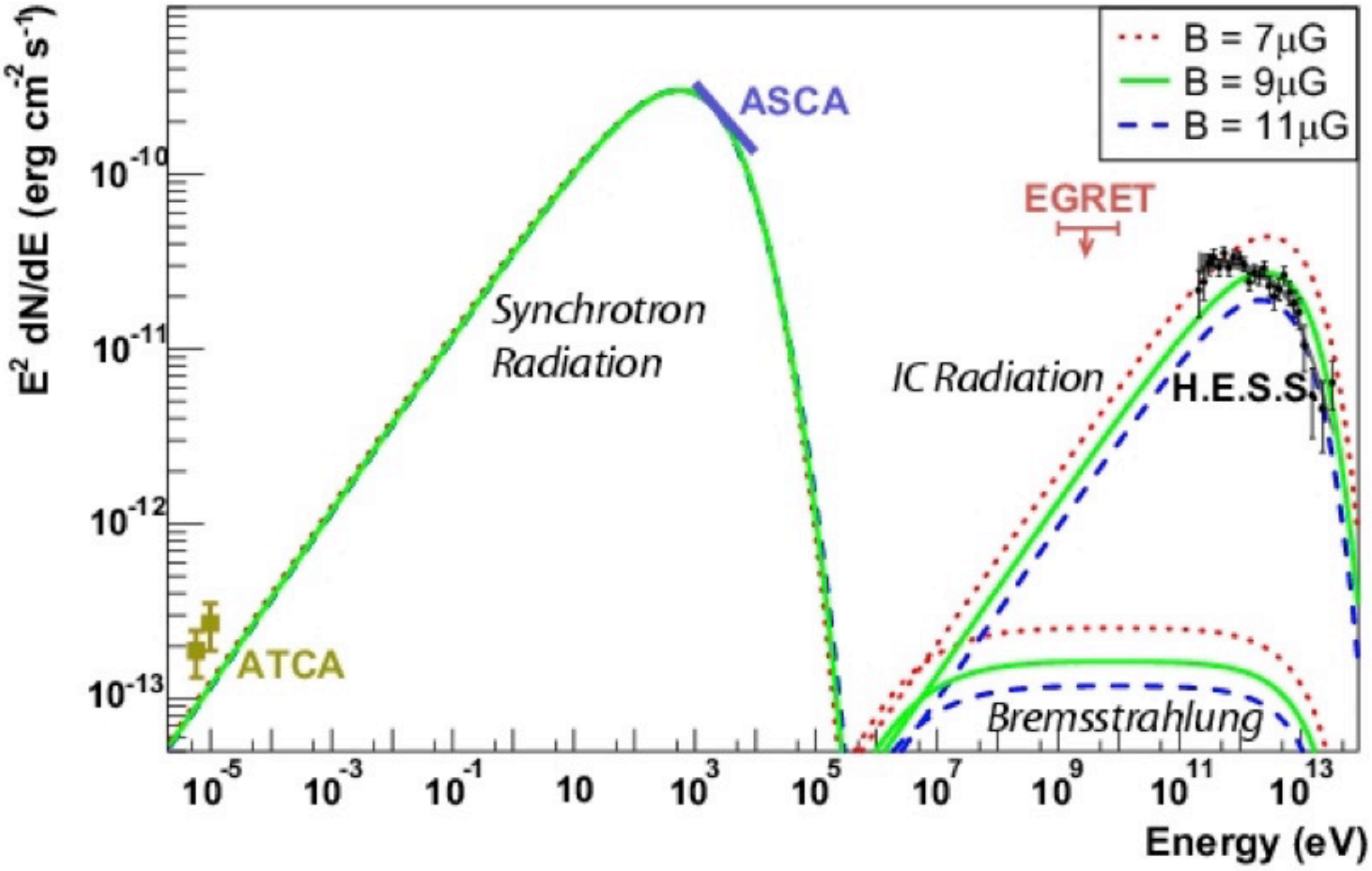

Very High Energy Cosmic Rays detection and measurements (E< 1PeV)

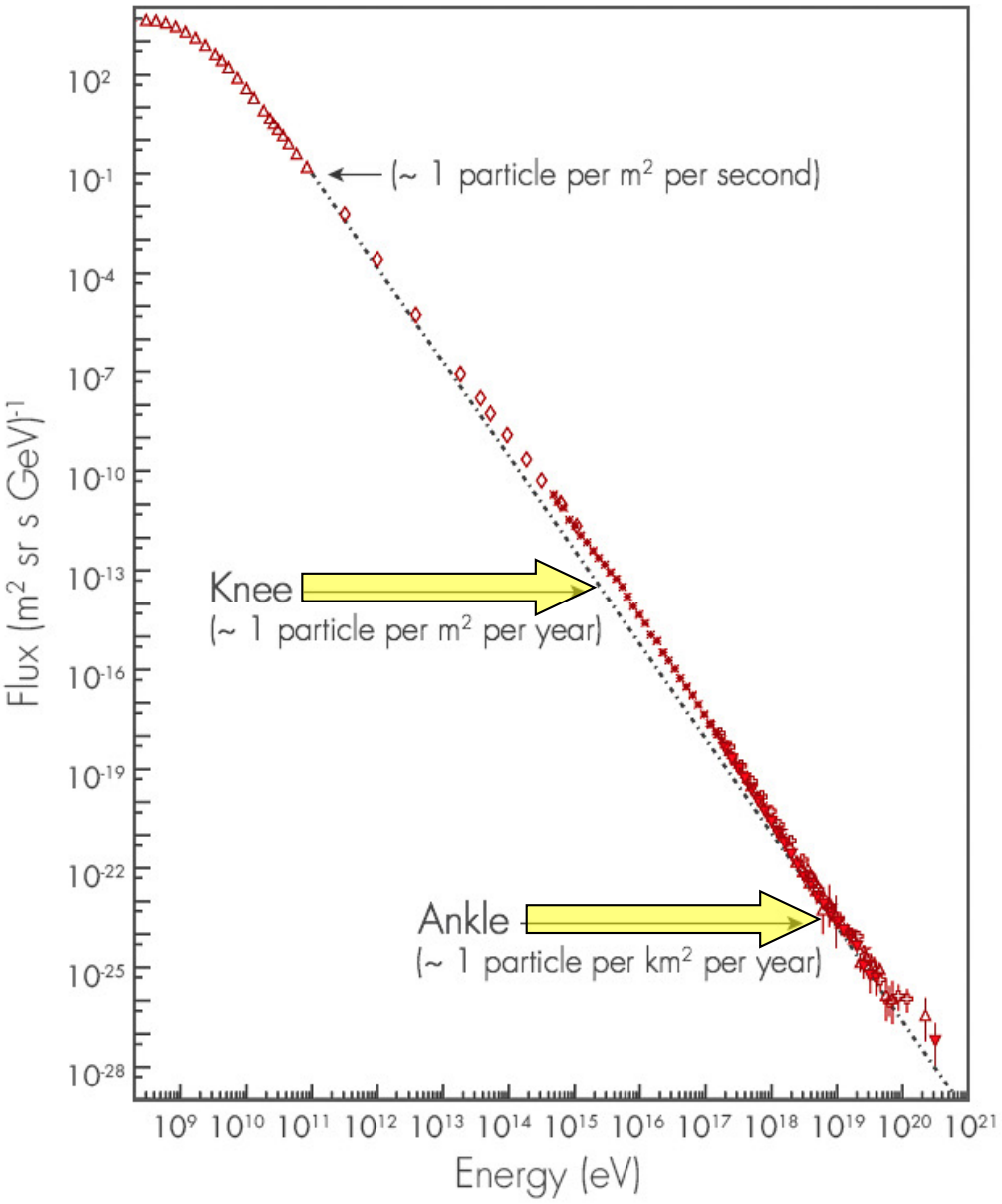

The study of photons and charged C.R. with E> 1TeV requires:

- large equipment (scintillator apparatus, Cherenkov light, tracers, ...)
- on the earth's surface
- the "results" of the interactions of the primary cosmic rays with the atmosphere are studied and allow to go back to E, direction, nature of the "primary"

For example the detector ARGO for γ and C.R. at 4300m (~600g/cm²) height Tibet)

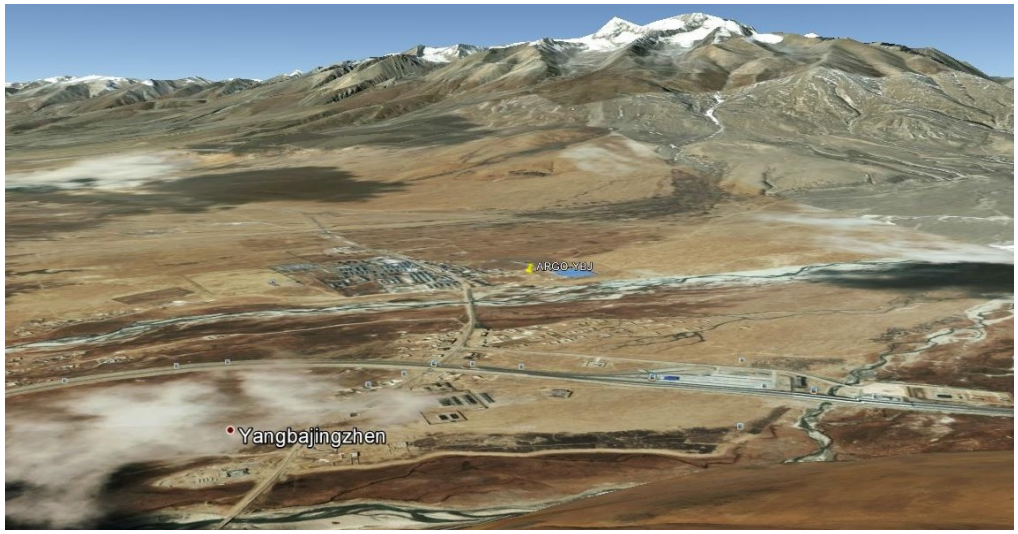

The electromagnetic component of an induced γ shower

Why we want to perform measurements of E-M showers at high quote???

In the air X_0 ~36.6 g/cm^2 at 4300 m above sea level a photon has crossed about 16 X_0

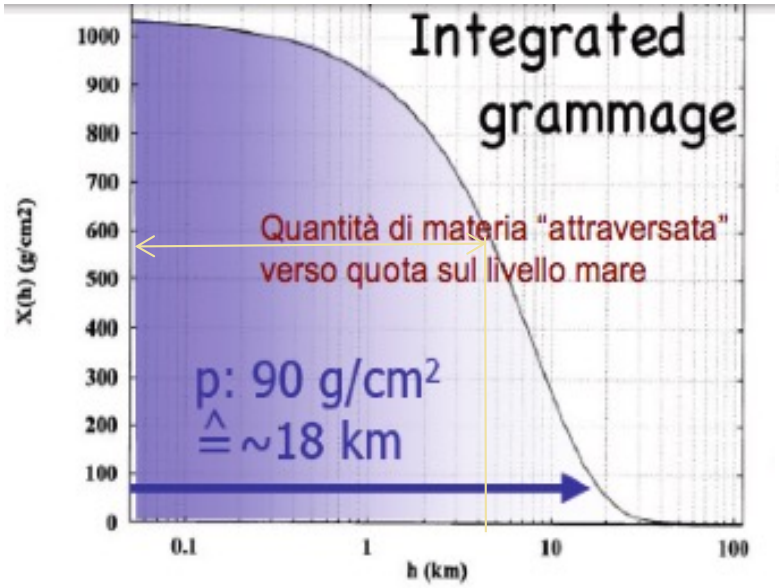

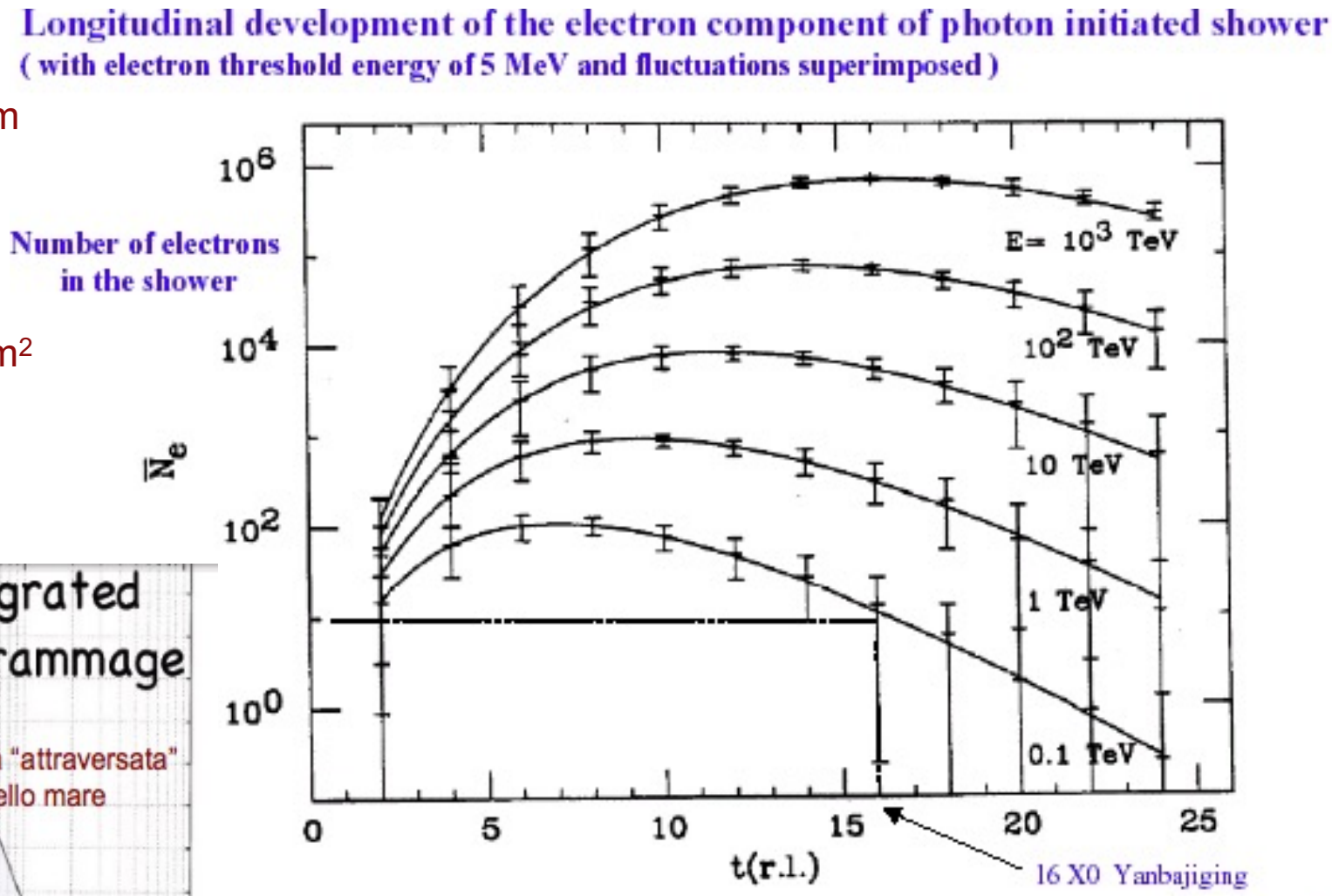

Shower longitudinal development in units of radiation lenghts

ARGO+ Resistive Plate Chamber detector on TIBET

ARGO

Area 5.200 m² (full coverage)
(10.000 m² with guard ring)
Field of view ~ 1 sr
E = 50 GeV - 50 TeV
Location: Tibet 4300m alt.
Scheduled 2002 (final conf.)

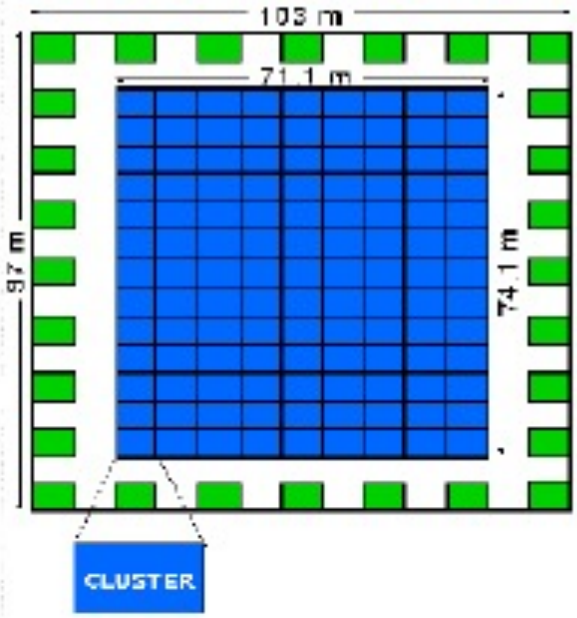

17400 Pads 56 by 60 cm² each of Resistive Plate Chamber (RPC).
Each pad subdivided in pick-up strips 6 cm wide for the space pattern inside the pad.
The CLUSTER is made of 12 RPCs Pads

ARGO-YBJ physics goals

- **VHE γ-Ray Astronomy**:
  (search for)/(study of) point-like (and diffuse) galactic and extra-galactic sources with few hundreds GeV energy threshold

- **Cosmic ray physics**:
  energy spectrum and composition
  study of the shower space-time structure
  flux anisotropies at different angular scales
  p-Air cross section measurement and hadronic interaction studies
  anti-p / p ratio at TeV energies,
  geomagnetic effects
  .....

- **Search for GRB's** (full GeV / TeV energy range)
- **...**

through the…

Observation of *Extensive Air Showers* produced in the atmosphere by primary γ's and nuclei

EAS reconstruction

Data taking with full configuration:
November 2007- February 2013

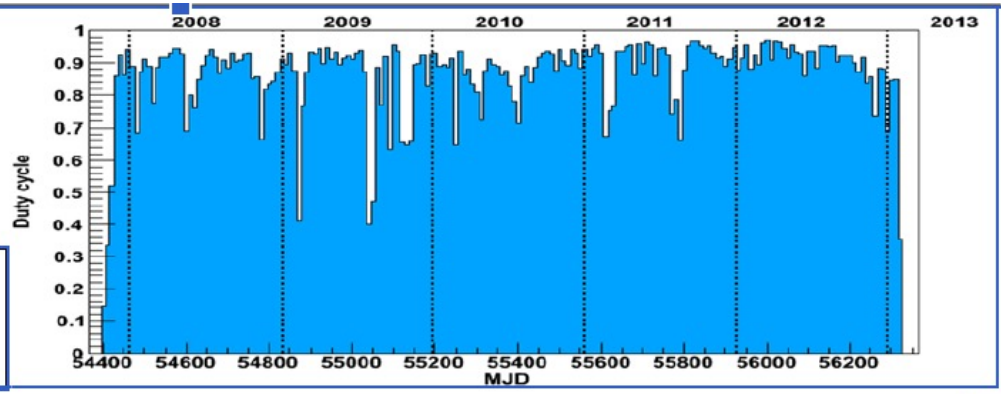

Event Rate ~ 3.5 kHz for N_{hit} >20 - Duty cycle ~ 86% - 10^{11} evts/yr – 100TB/yr

High space/time granularity
+ Full coverage
+ High altitude

detailed study on the EAS space/time structure with unique capabilities

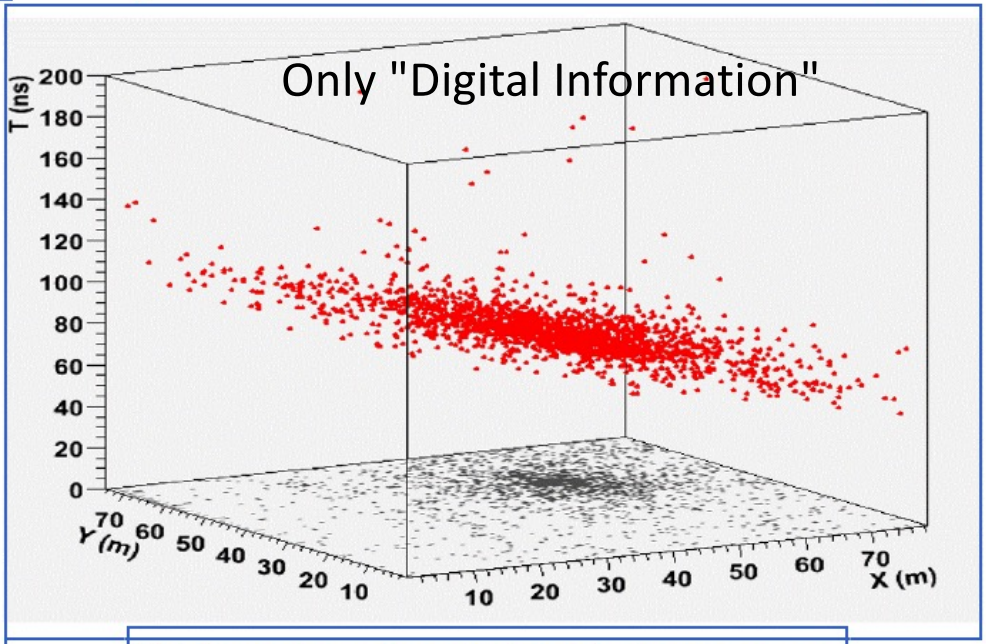

3-D view of a detected shower

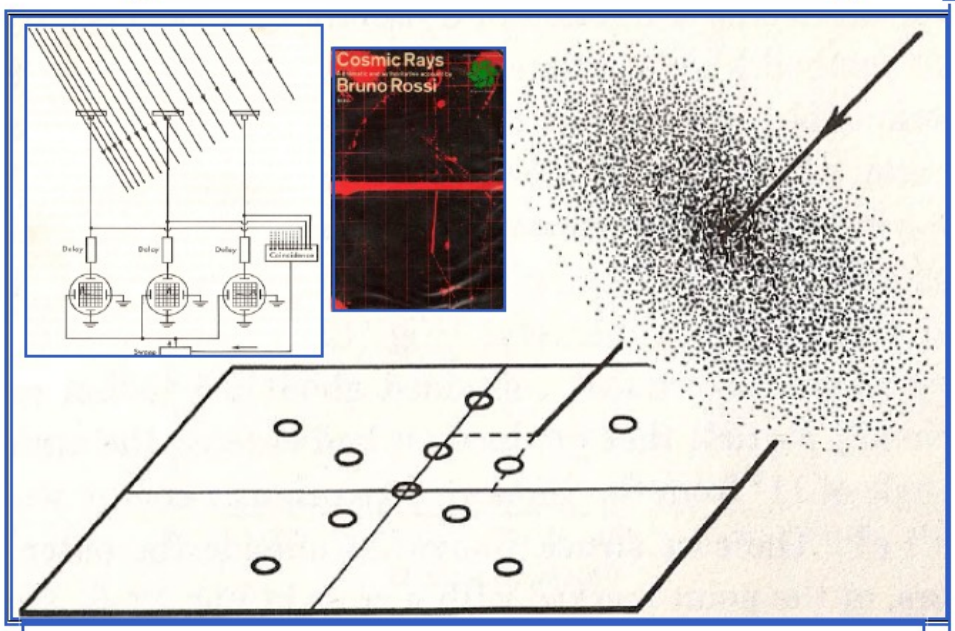

Bruno Rossi conceptual EAS detector

The ARGO-RPC analog readout

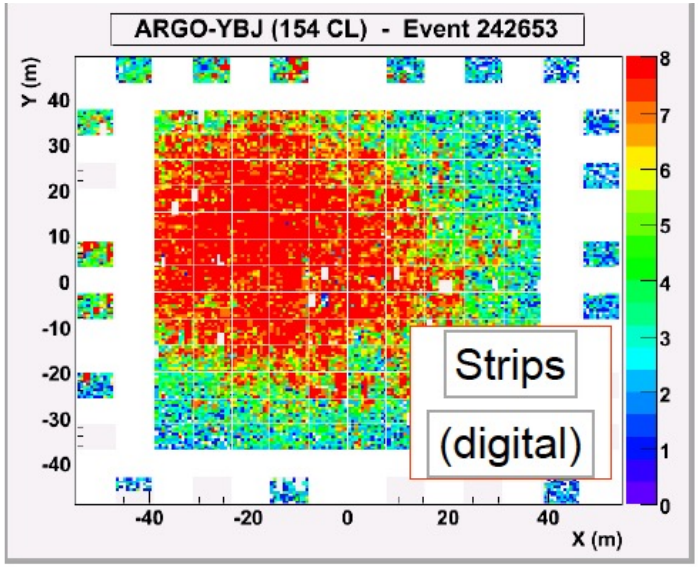

- ✓ Extend the explored energy range
- ✓ Access the LDF down to the shower core
- ✓ Sensitivity to primary mass
- ✓ Info/checks on Hadronic Interactions

Eight different gain scales (G0, G1, ..,G7) ensure a good linearity up to about $2 \cdot 10^4$ particles/m^2.

G7 data overlap the digital-mode linearity range, and have then been used for intercalibration and cross checks.

Real event

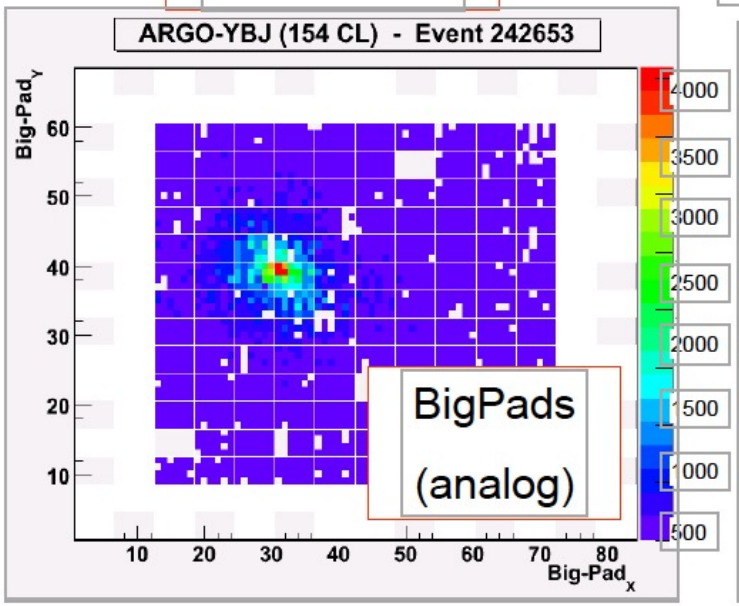

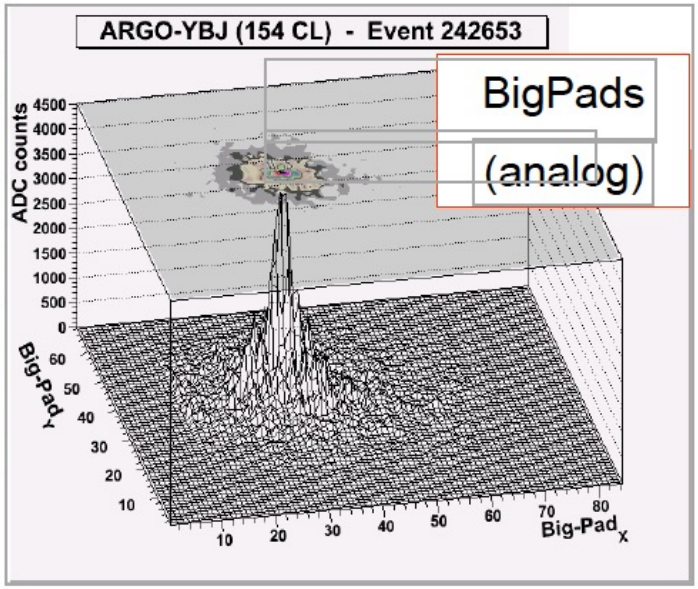

In this study we used data taken with G4 and G1 scales that allow covering the 50TeV – 5PeV energy range with high efficiency and no saturation.

ARGO search for VHE γ point-like sources

THE ASTROPHYSICAL JOURNAL LETTERS, 745:L22 (5pp), 2012 February 1

The Cygnus region

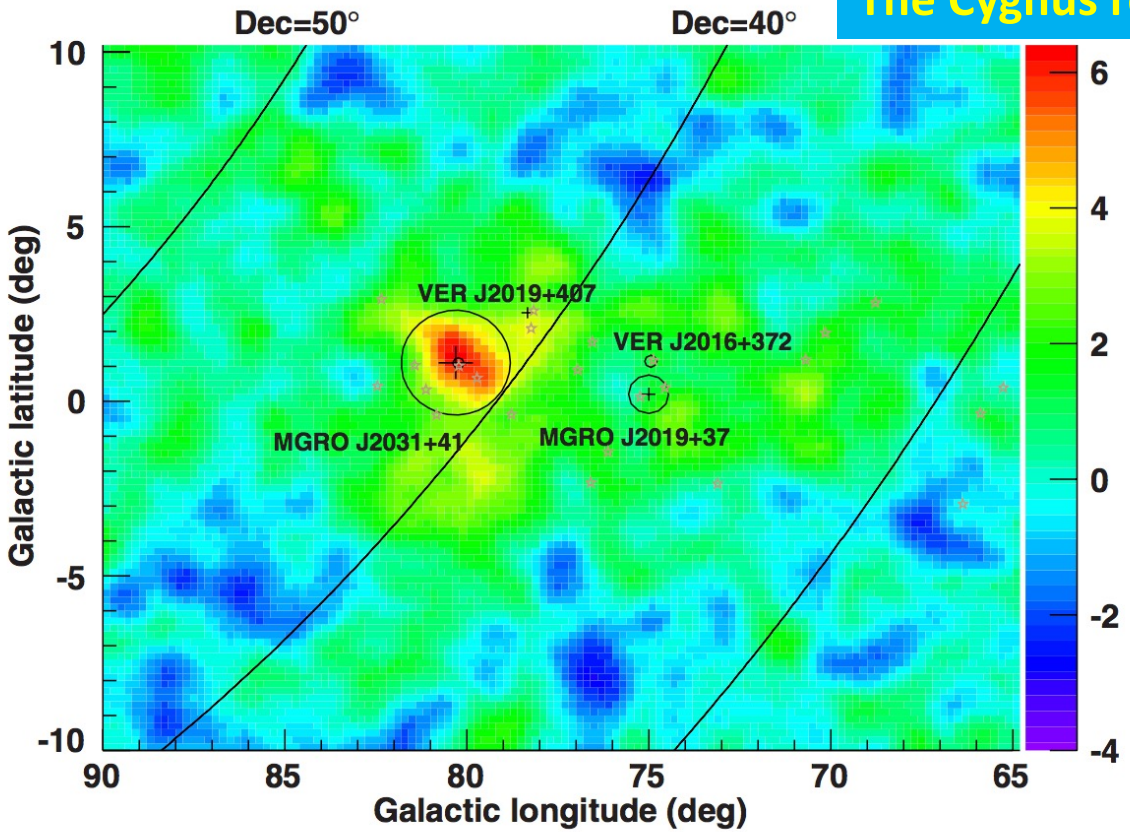

Figure 1. Significance map of the Cygnus Region as observed by the ARGO-YBJ experiment. The four known VHE γ-ray source are reported. The errors on the MGRO source positions are marked with crosses, while the circles indicate their intrinsic sizes (Abdo et al. 2007a, 2007b). The cross for VER J2019+407 indicates its extension (Weinstein 2009). The source VER J2016+372 is marked with small circles without position errors. The small circle within the errors of MGROJ2031+41 indicates position and extension of the source TeV J2032+4130 as estimated by the MAGIC collaboration (Albert et al. 2008). The open stars mark the location of the 24 GeV sources in the second *Fermi*-LAT catalog.

Significance map of the Cygnus region as observed by ARGO-YBJ using events with $N_{pad} > 20$.
For comparison, the 4 known TeV sources and 24 GeV sources in the second *Fermi*-LAT catalog are marked in the figure. An excess is observed over a large part of the Cygnus region, which indicates a possible diffuse γ-ray emission.

ARGO search for VHE γ point-like sources

One example: the source J2032 in the Cygnus region

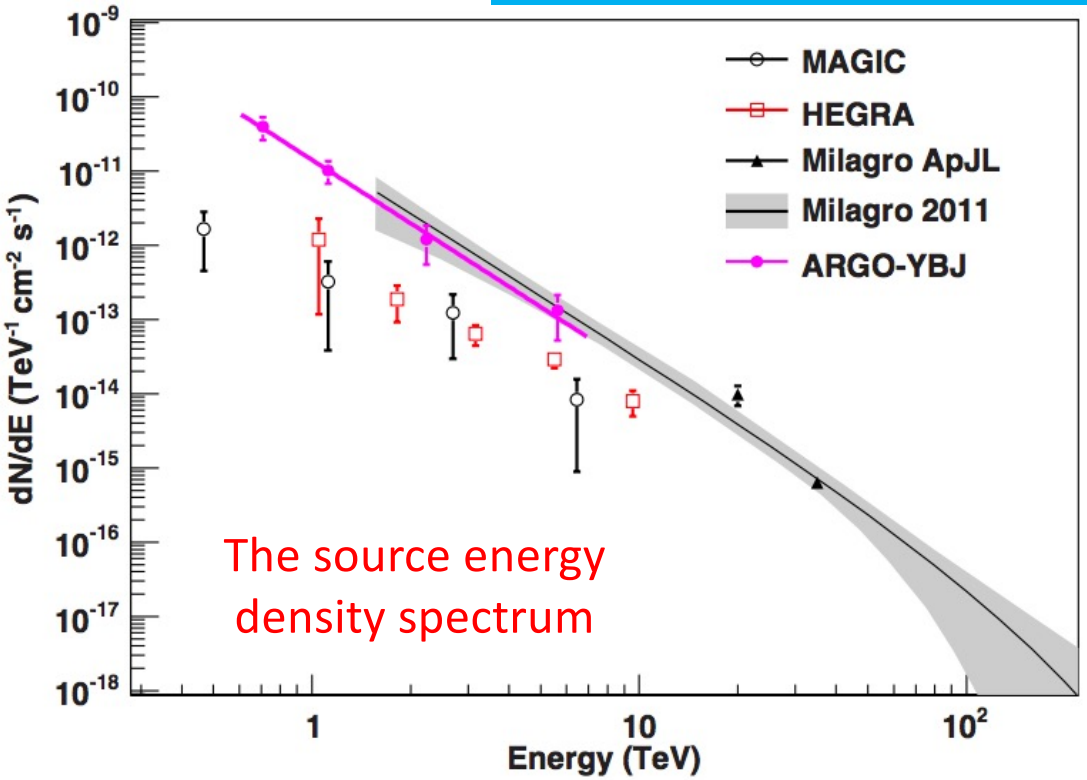

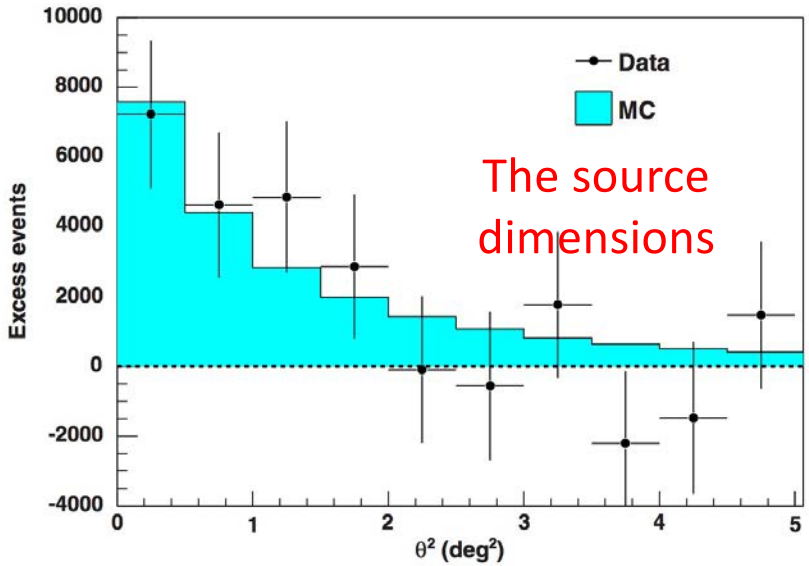

Figure 2. Distribution of θ^2 for the number of excess events around TeV J2032+4130. The filled region is the best fit to simulated data.
(A color version of this figure is available in the online journal.)

Figure 3. Energy density spectrum from TeV J2032+4130/MGRO J2031+41 as measured by the ARGO-YBJ experiment (solid magenta line). The spectral measurements of HEGRA (Aharonian et al. 2005) and MAGIC (Albert et al. 2008) are also reported for comparison. The solid line and shaded area indicate the differential energy spectrum and the 1 s.d. error region as recently determined by the Milagro experiment (Bonamente et al. 2011). The two triangles give the previous flux measurements by Milagro at 20 TeV (Abdo et al. 2007a) and 35 TeV (Abdo et al. 2009).

The source differential flux →

$$\frac{dN}{dEdAdt} = (1.40 \pm 0.34) \times 10^{-11} \left(\frac{E}{1\,\mathrm{TeV}}\right)^{-2.83 \pm 0.37} \quad [\,\mathrm{TeV^{-1}\,cm^{-2}\,s^{-1}}\,]$$

Antimatter in Cosmic Rays and the Moon Shadow

To search for anti-matter in the Universe we could investigate high-energy cosmic rays.
To measure $\overline{p}/p$ ratio in the TeV range, we can exploit the Moon as an effective absorber. Due to the Earth magnetic field, different particles, while travelling toward the Earth, are bent according to their rigidity, following the formula:

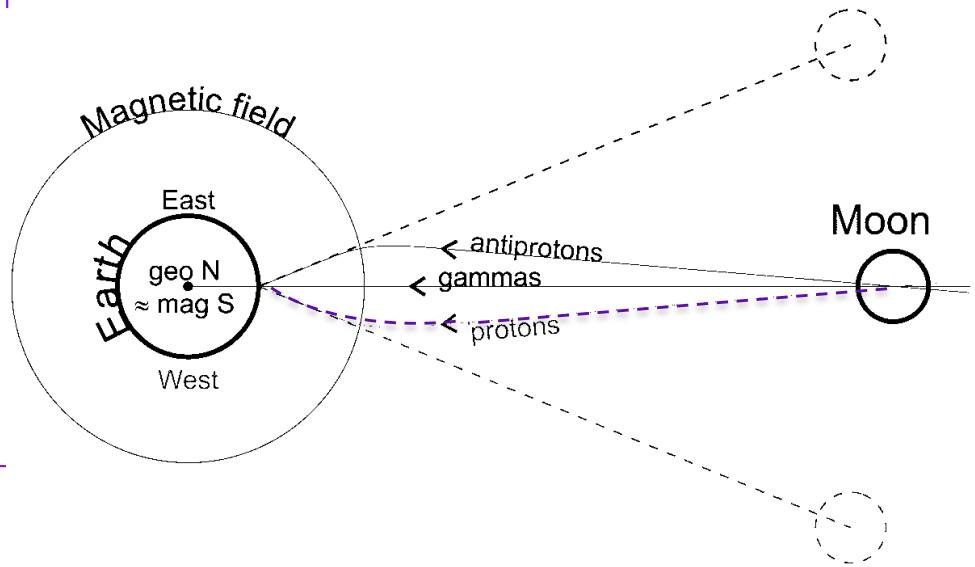

$$\Delta\theta = \frac{0.3\ Z \int_{in}^{out} \vec{B} \cdot d\vec{\ell}}{E} \approx \frac{30\ Z}{E[TeV]} mrad$$

This different bending can be inferred observing the region close to the Moon, as the Moon absorbs the particles and casts a shadow in an otherwise uniformly- bright cosmic ray sky. As can be seen in the picture, protons are deflected eastward, so that the dip in the occurrency frequency of CR due to the Moon absorption is displaced to the West. The opposite occurs to antiprotons, in such a way that one should see three dips: one toward the Moon for the unbent gamma-rays, one toward East for the antiprotons and one toward West for the protons. Even if one does not observe the $\overline{p}$ dip, the mere observation of the p dip puts an upper limit on negative particles flux and, consequently on $\overline{p}$flux. This was done by Tibet ASγ collaboration, that set an upper limit at 10 TeV of 22% on the $\overline{p}/p$ ratio (Amenomori et al., 1999).

The Moon shadow and the ratio $\bar{p}/p$

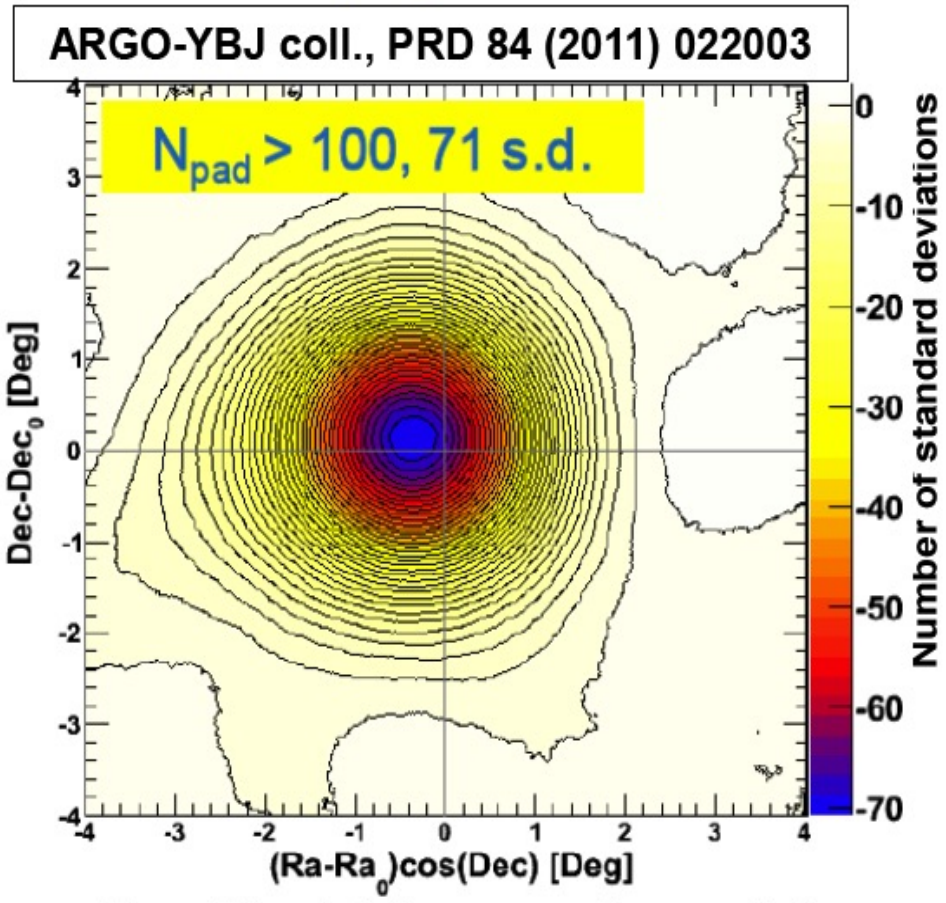

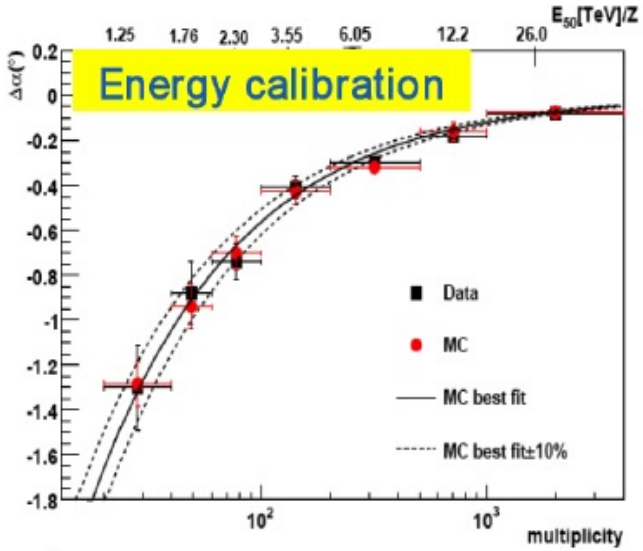

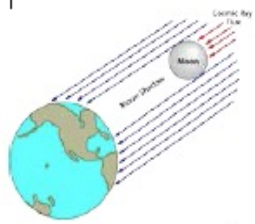

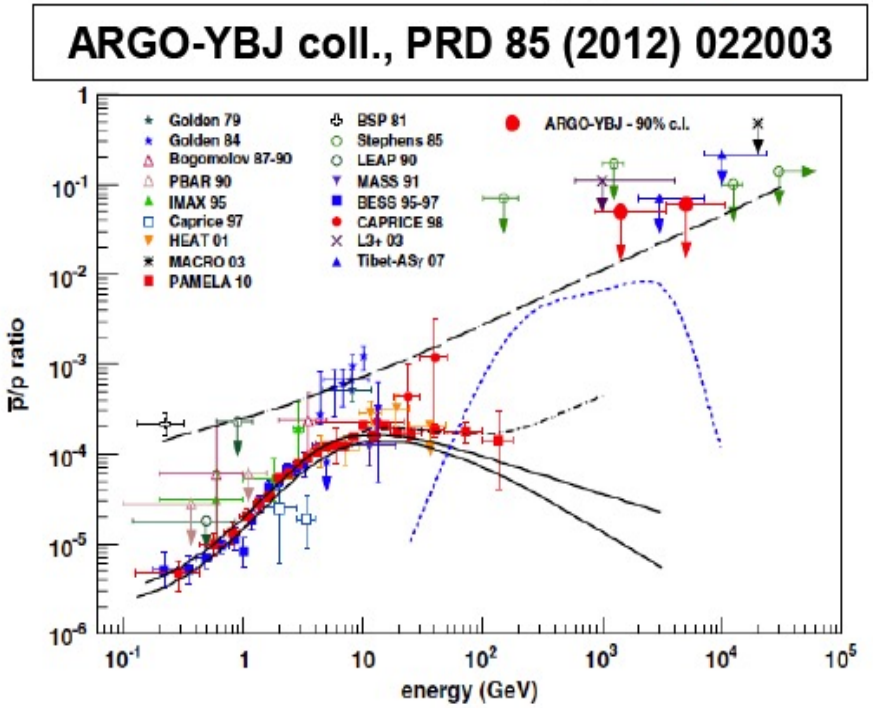

- Size of the deficit ⇒ **angular resolution**
- Position ⇒ **pointing accuracy**
- West displacement ⇒ **Energy calibration** (Geomagnetic bending ≈ 1.57° / E (TeV))
- **Antiprotons** should give a shadow on the opposite side ⇒ **Upper limit**

ARGO: measurement of the p-air cross section

Use the shower frequency vs (secθ -1)

$$I(\theta) = I(0) \cdot e^{-\frac{h_o}{\Lambda}(\sec\theta - 1)}$$

for fixed energy and shower age.

The lenght Λ is connected to the p interaction lenght by the relation $\Lambda = k\,\lambda_{int}$ where k is determined by simulations and depends on:

- **hadronic interactions**
- **detector features and location (atm. depth)**
- **actual set of experimental observables**
- **analysis cuts**
- **energy, ...**

Then: $\sigma_{p\text{-}Air}$ **(mb) = 2.4 10⁴ / λ_{int}(g/cm²)**

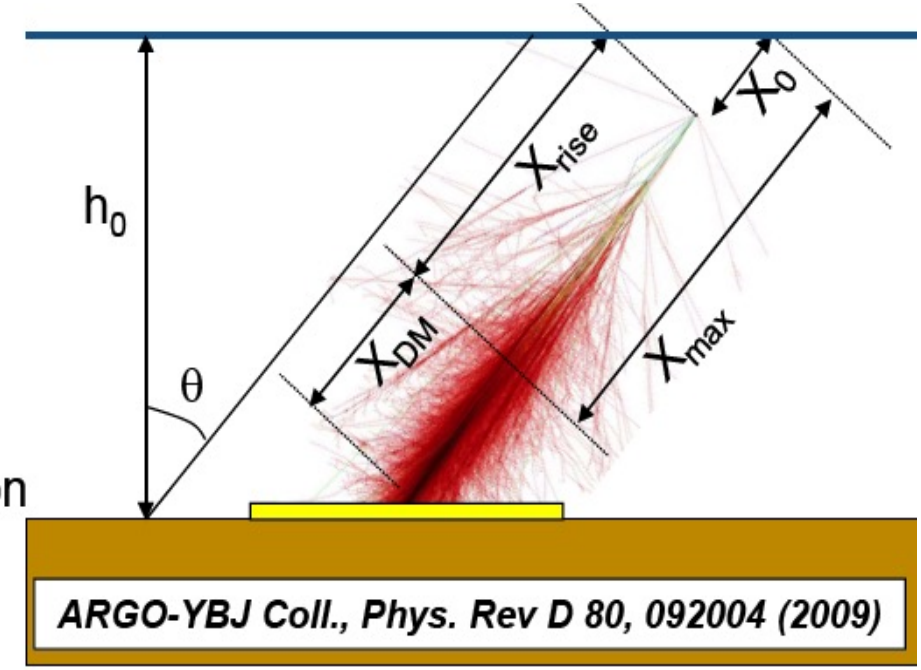

- **Constrain** $X_{DM} = X_{det} - X_{max}$
- **Select** deep showers (large X_{max}, i.e. small X_{DM}) to access exponential tail and reduce shower fluctuations → cut on Rs_{70} (strip concentration parameter)
- **Exploit** detector features (space-time pattern) and location (depth).

ARGO: measurement of the p-air cross section

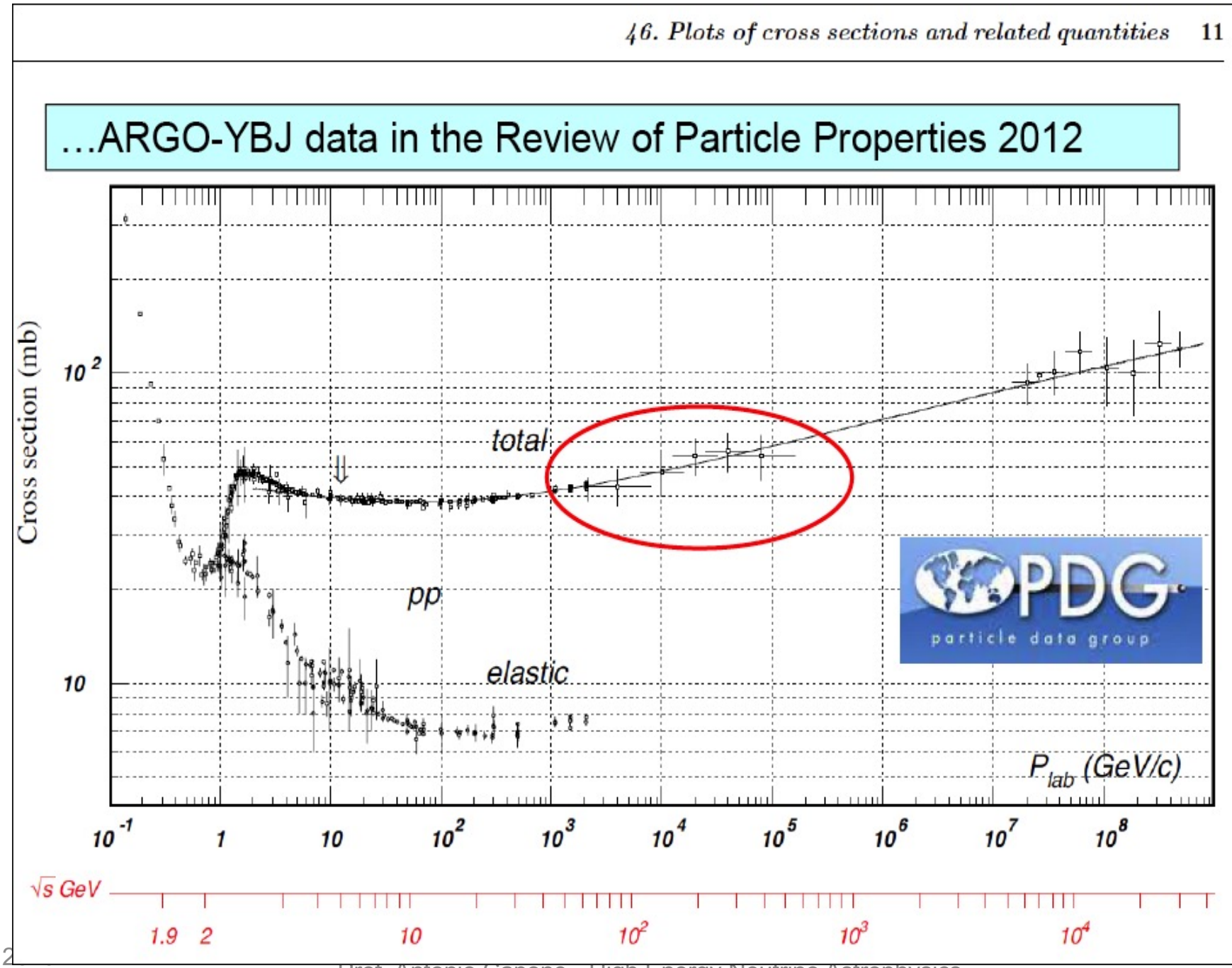

ARGO: measurement of the total p-p cross section

- Energy interval scarcely explored by p-p (and pbar-p) accelerator experiments
- The $\log^2(s)$ asymptotic behaviour is favoured

Milagro - 1

- Milagro was a water Cherenkov detector designed for VHE gamma-ray astronomy
- It was located near Los Alamos, New Mexico, USA, at an elevation of 2630 meters a.s.l.
- It operated from 2000 to 2008

Milagro - 2

Milagro was a water-Cherenkov detector at an altitude of 2650m capable of continuously monitoring the overhead sky. It was composed of a central 60m x 80m pond with a sparse 200m x 200m array of 175 "outrigger" tanks surrounding it. The pond is instrumented with two layers of photomultiplier tubes. The top "air-shower" layer consists of 450 PMTs under 1.4m of purified water while the bottom "muon" layer has 273 PMTs located 5m below the surface. The air-shower layer allows the accurate measurement of shower particle arrival times used for direction reconstruction and triggering. The greater depth of the muon layer is used to detect penetrating muons and hadrons. Simple cuts have been developed to distinguish between gamma-ray– and hadron/muon–induced showers. The outrigger array improves the core location and angular resolution of the detector by providing a longer lever arm with which to reconstruct events. The angular resolution improves from ≈0.75° to ≈0.45° when outriggers are used in the reconstruction.

Milagro's large field of view (~2πsr) and high duty cycle (>90%) allow it to monitor the entire overhead sky continuously, making it well-suited to searching for new TeV sources and scanning known sources at higher energies.

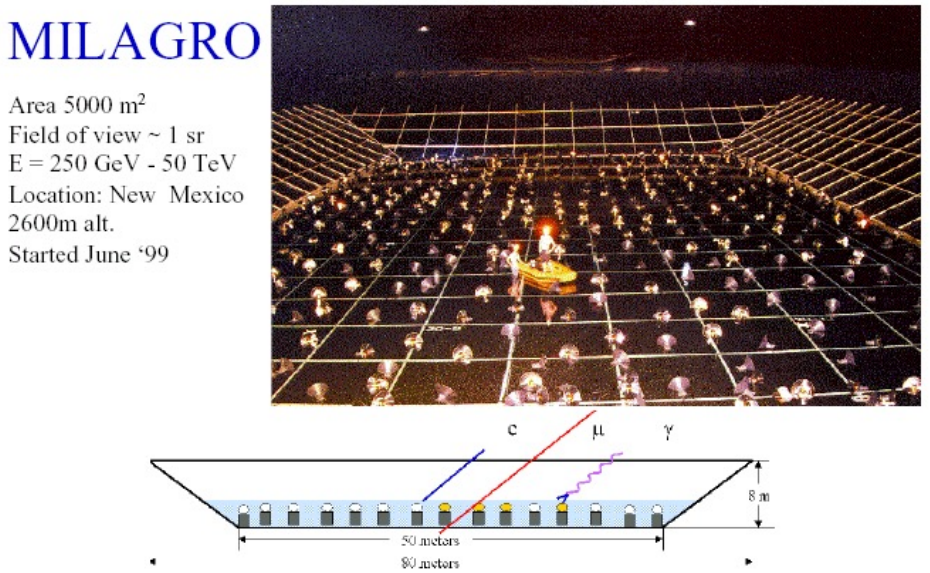

Milagro - 3

- Central 80 m x 60 m x 8 m water reservoir, containing two layers of PMTs:
  450 PMTs at 1.4 m below the surface (top layer)
  273 PMTs at 6 m below the surface (bottom layer)

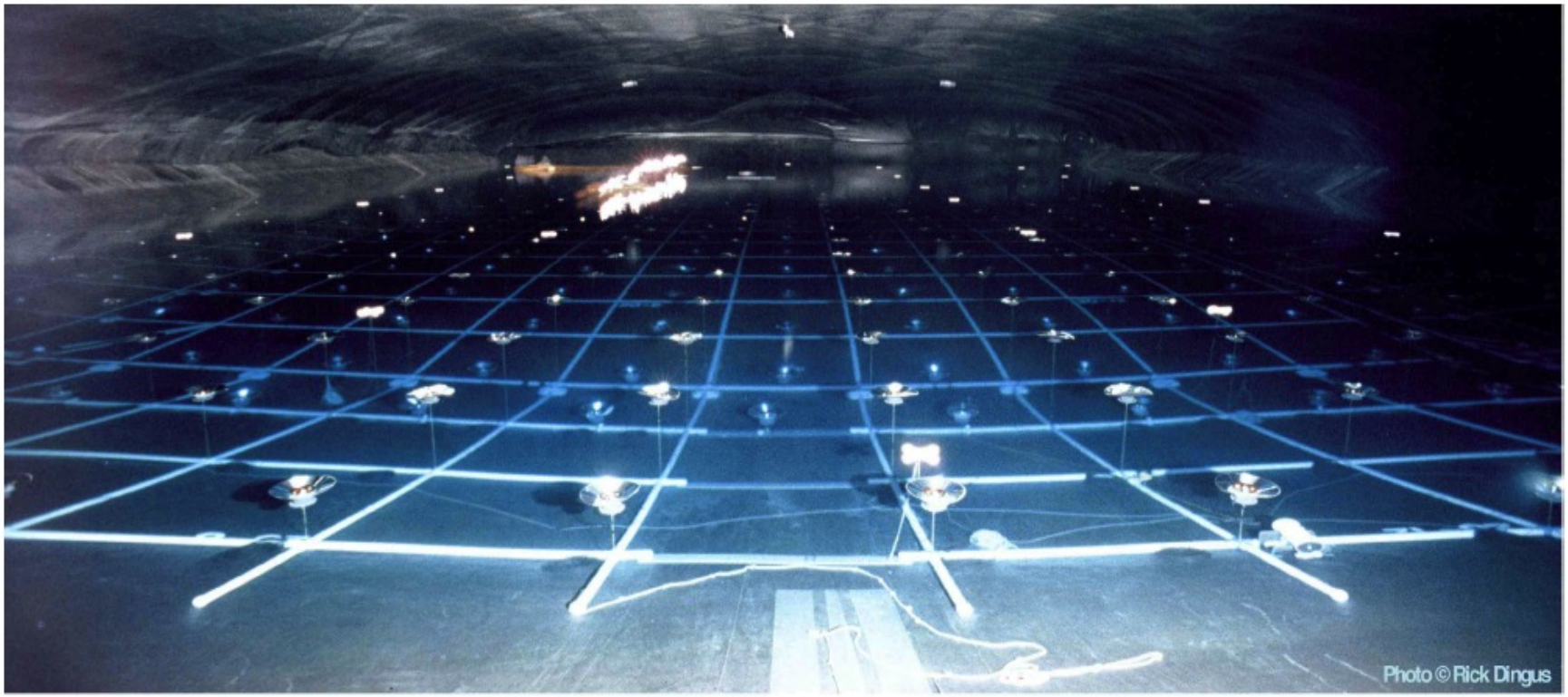

Milagro - 4

- From 2004: Outrigger Array, consisting of 175 tanks filled with water and containing one PMT, distributed on an area of 200 m x 200 m around the central water reservoir.

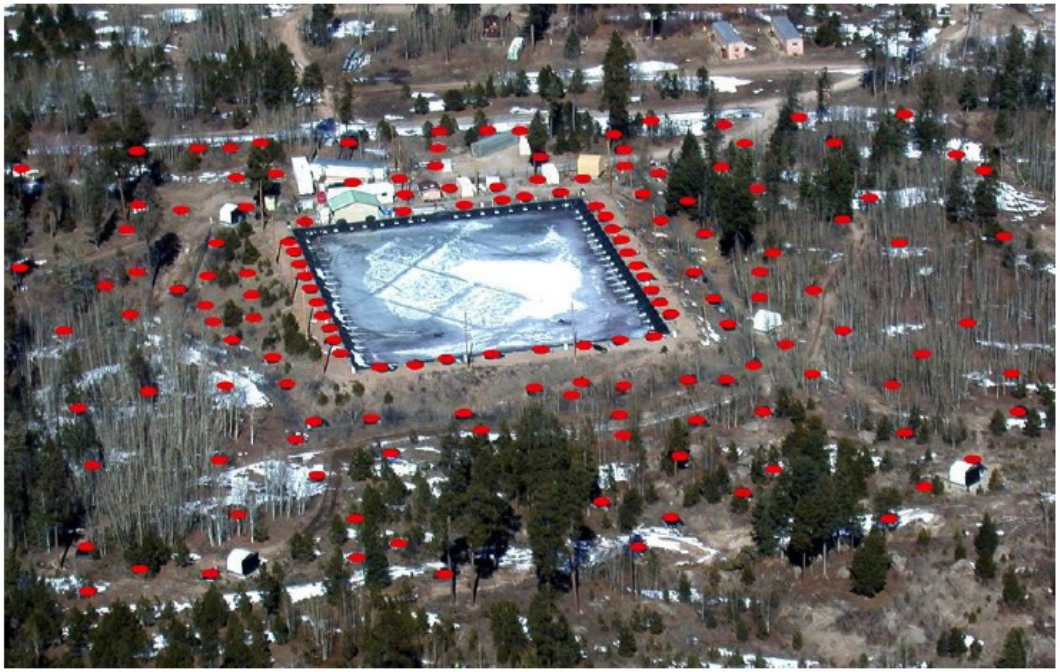

Milagro reached its final configuration in September 2005

- Detector Performances:
  - It operated with a duty cycle $\geq$ 90 %
  - Its field of view was of $\sim$ 2 sr
  - It was sensitive between 100 GeV to 100 TeV

- These characteristics made Milagro well suited to study the VHE emission from
  - Extended sources
  - Transient sources (GRBs, **AGN** flares)
  - Sun

Angular resolution and discovery power

Let's define S(>E) and B(>E) the number of Signal and Background events (with energy >E) obtained as the result of data measurement, selection and analysis. We can qualify our discovery capability in terms of the ratio

$$\frac{S(>E)}{B(>E)} = \frac{number\ of\ signal\ events > E}{\sqrt{number\ of\ signal\ events > E}}$$

The background, usually due to C.R. is isotropic and has flux $\phi_{B(>E)} = K_B E^{-\gamma_B}$
The signal is coming from a point source and has flux $\phi_{S(>E)} = K_S E^{-\gamma_S}$

Then if I collect data with a detector with effective area A_{eff} for the time T integrating in a solid angle around the source direction with aperture $\delta\varphi$ defined by the detector "point spread function", by definition
$S(>E) = K_S E^{-\gamma_S} \cdot T \cdot A_{eff}$ while $B(>E) = K_B E^{-\gamma_B} \cdot T \cdot (\delta\varphi)^2 \pi \cdot A_{eff}$ *and*

$$\frac{S(>E)}{B(>E)} = cost\ E^{(\frac{\gamma_B}{2} - \gamma_S)} \frac{\sqrt{T \cdot A_{eff}}}{\delta\varphi}$$

The discovery potential grows slowly with T and A_{eff} and improves very fast improving the angular resolution (reducing $\delta\varphi$)

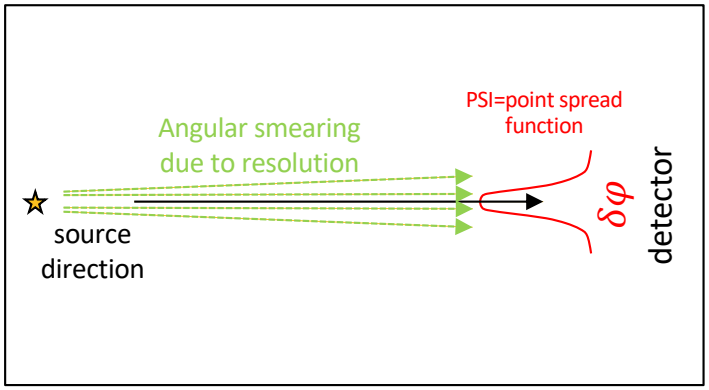

Milagro Cosmic Ray Observations

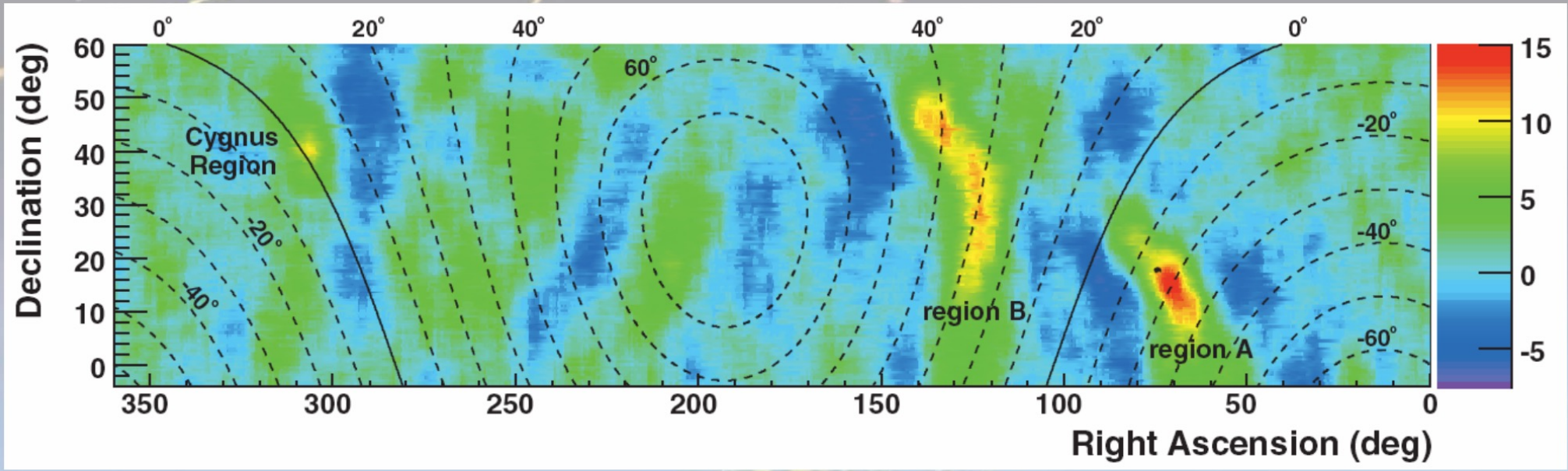

- No weighting or cutting. Map dominated by cosmic rays.
- Background subtraction serves as a high-pass filter.
- 10o smoothing looks for largeish features.
- Two regions of excess 15.0σ and 12.7σ. Fractional excess of 6×10^{-4} (4×10^{-4}) for region A(B).
- Seen also by Tibet ASγ and ARGO-YBJ

MILAGRO survey of the Galactic Plane

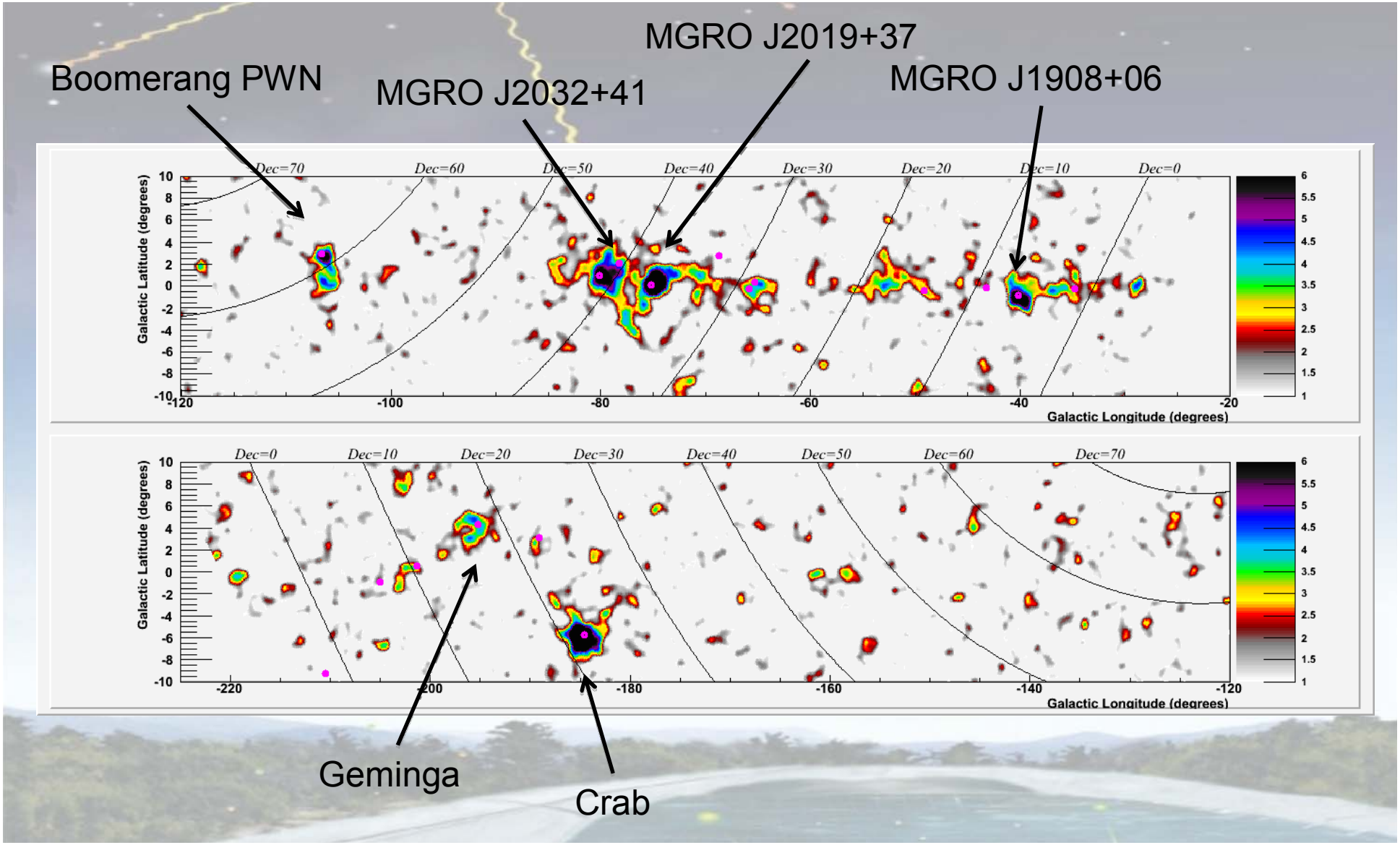

Fermi and MILAGRO

the MeV – TeV connection for γ-rays Sources

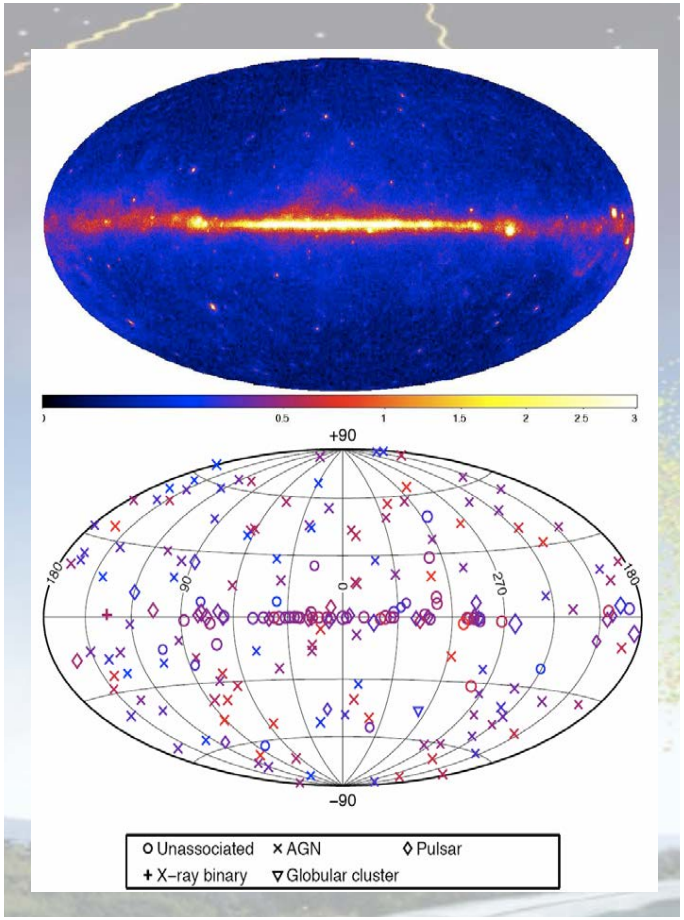

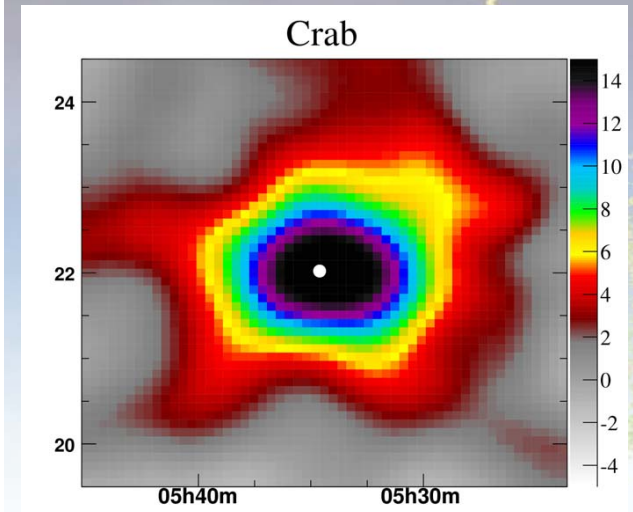

- Milagro's strongest sources are very likely TeV PWN. Typical TeV source is a PWN.
- TeV emission is quite commonly associated with MeV-GeV Pulsars.
- Spectrum to connect Milagro measurements to Fermi measurements are universally softer than 2.3.

MILAGRO searches for point like sources: Markarian 421

Light curve above 300 GeV

- Observation period:

  From September 21, 2005 to March 15, 2008

- Significance: $\sim 7.1\ \sigma$

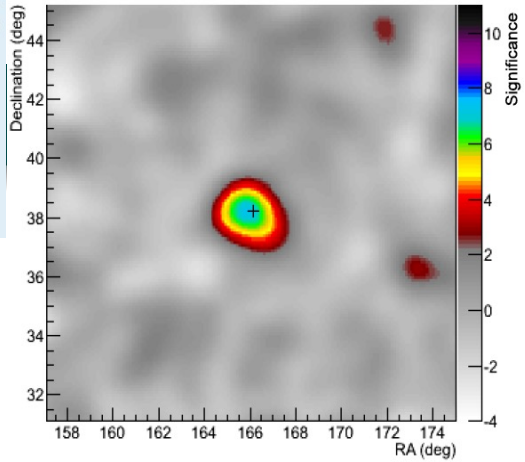

Comparison with Whipple, VERITAS and MAGIC (Acciari et al. 2011, Aleksíc et al. 2010)

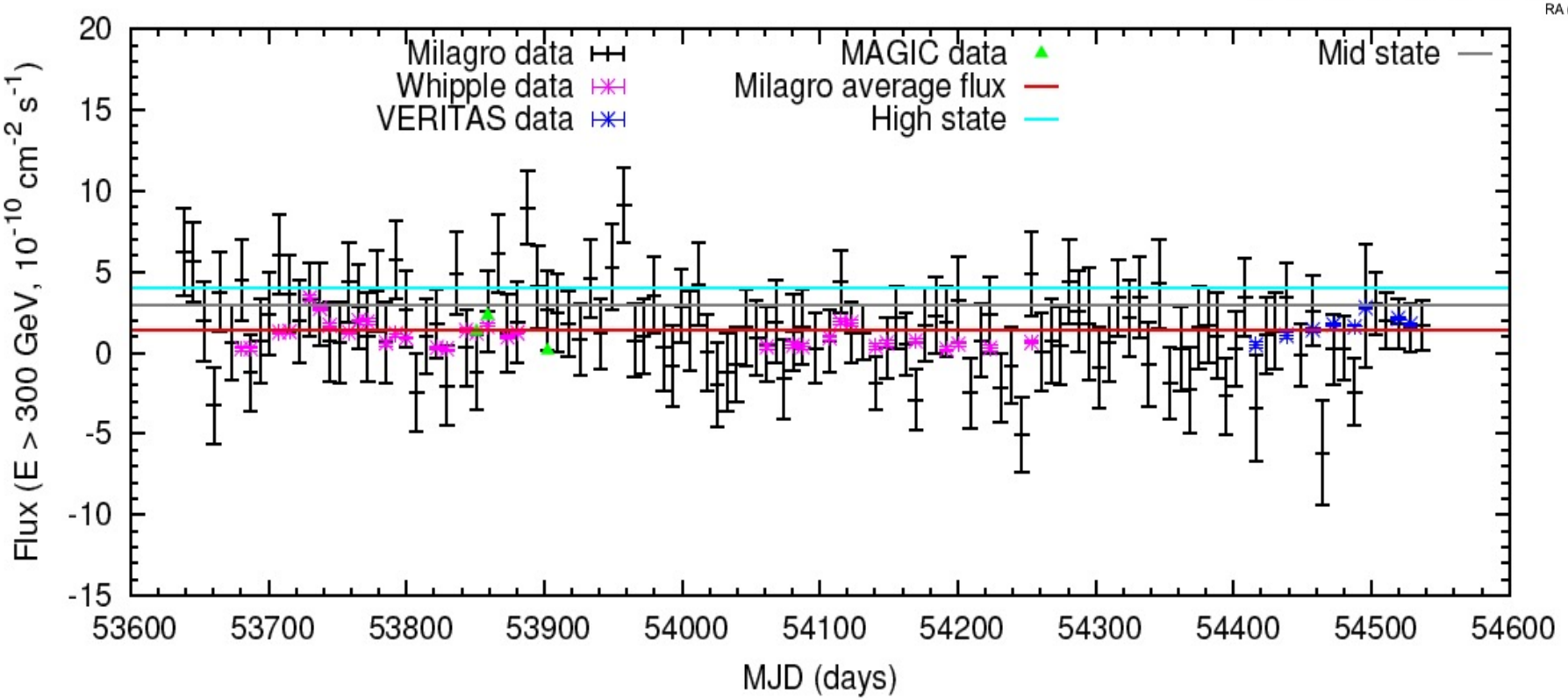

The evolution of MILAGRO experiment

The Instruments: HAWC

HAWC is located on the flanks of the Sierra Negra volcano near Puebla, Mexico at an altitude of 4100 meters

Energy range: ~300 GeV - 100 TeV
Angular resolution: ~0.1°
Field of view: ~2 sr
High duty cycle
>3 years of full array operation

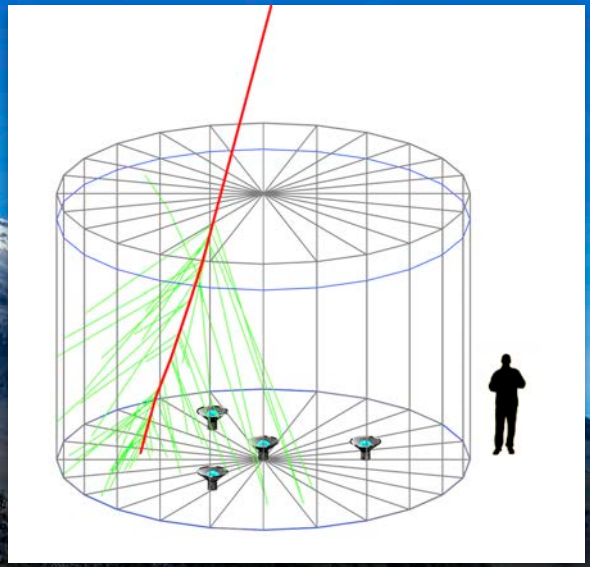

HAWC consists of an array of 300 water Cherenkov detectors (WCDs) covering an area of 22,000 m^2. Each WCD is equipped with four photomultiplier tubes (PMTs) to detect Cherenkov light

HAWC sensitivity to gamma flux

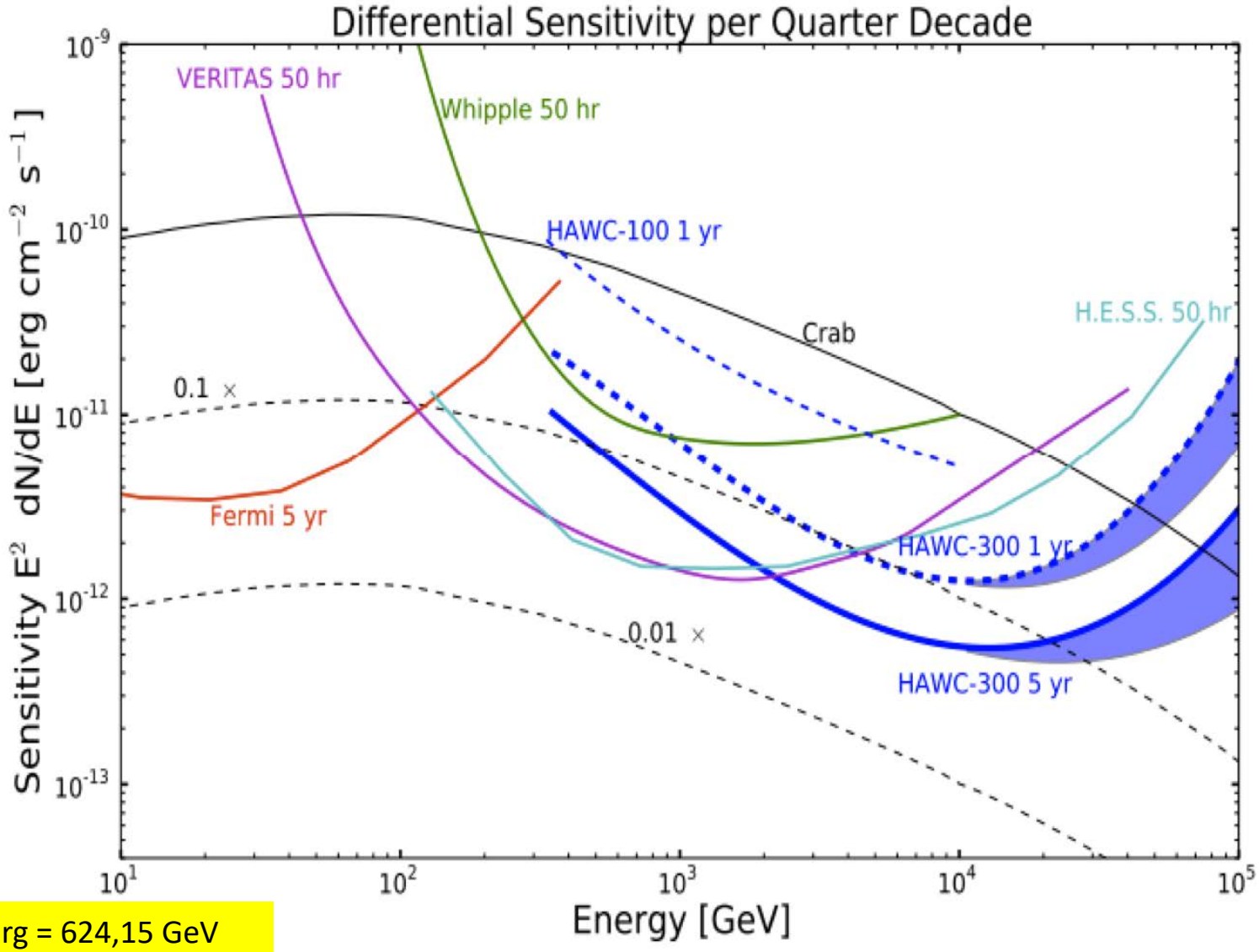

1 erg = 624,15 GeV

Coverage over a broad energy range, differing sensitivities

HAWC and TeV γ sources in the Galactic Plane

HAWC 3 year Galactic Plane Survey

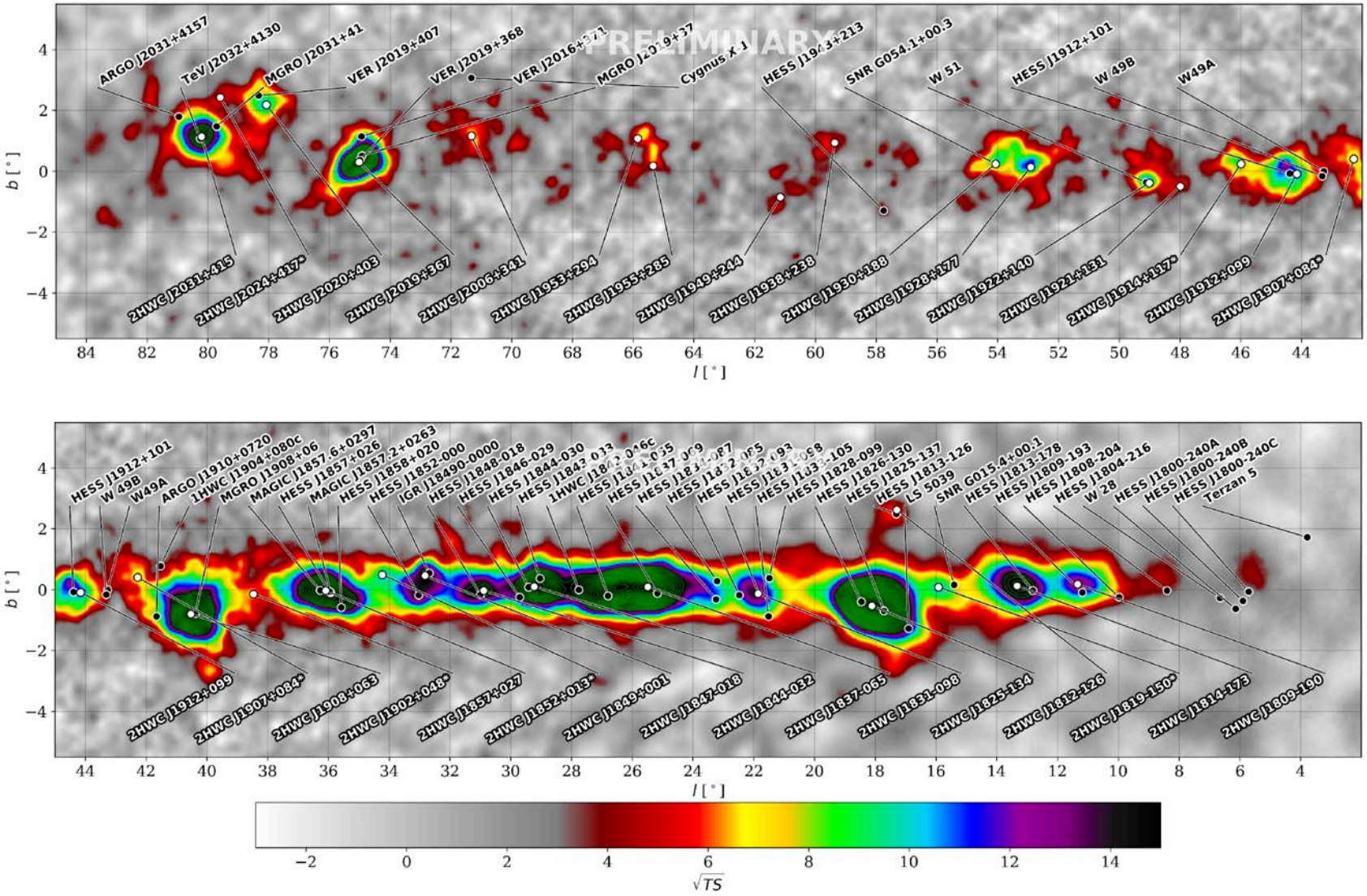

HAWC and IACT complementarity

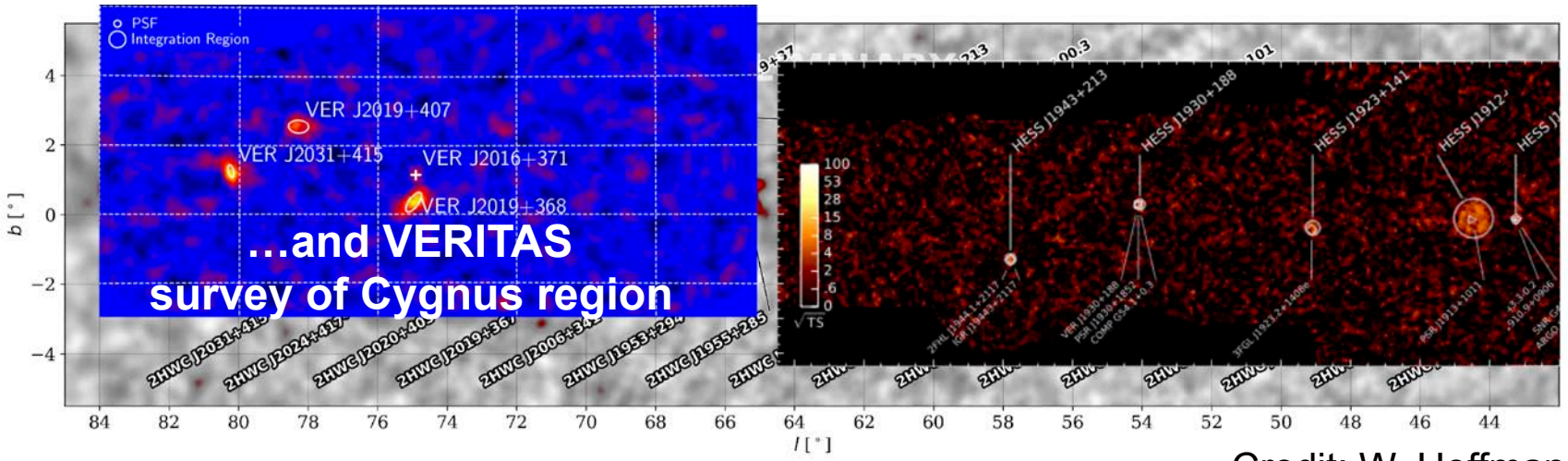

Credit: W. Hoffman

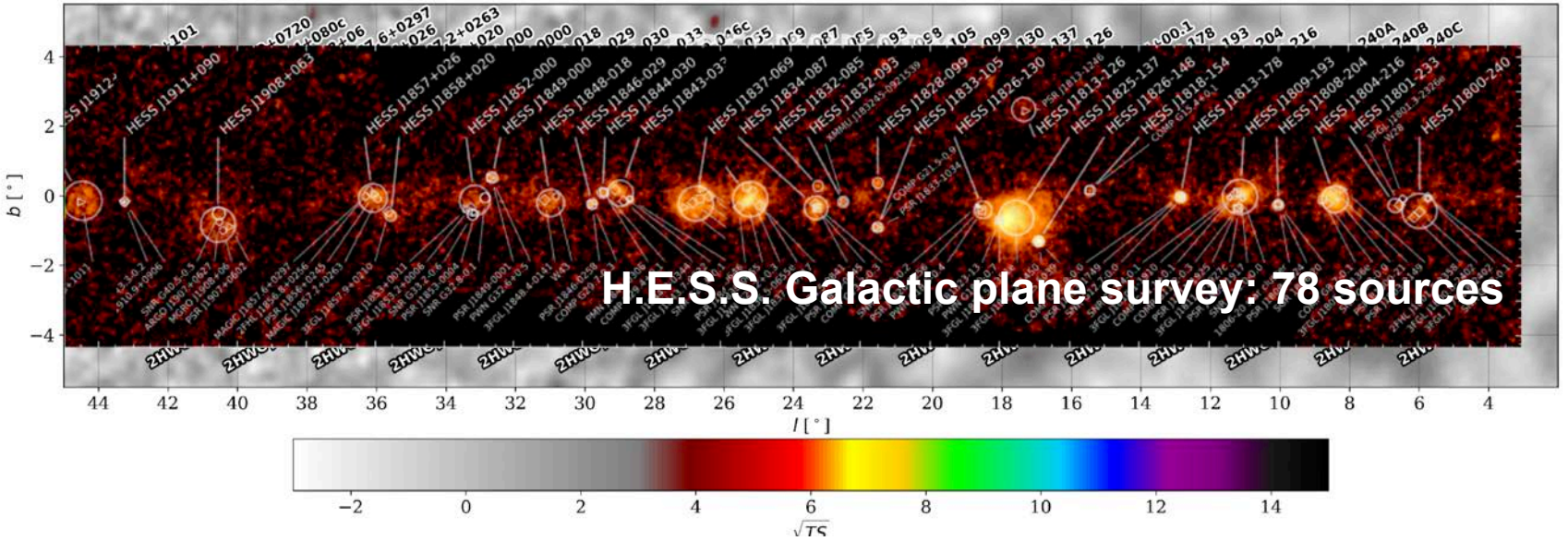

Prospective: Cherenkov Telescope Array

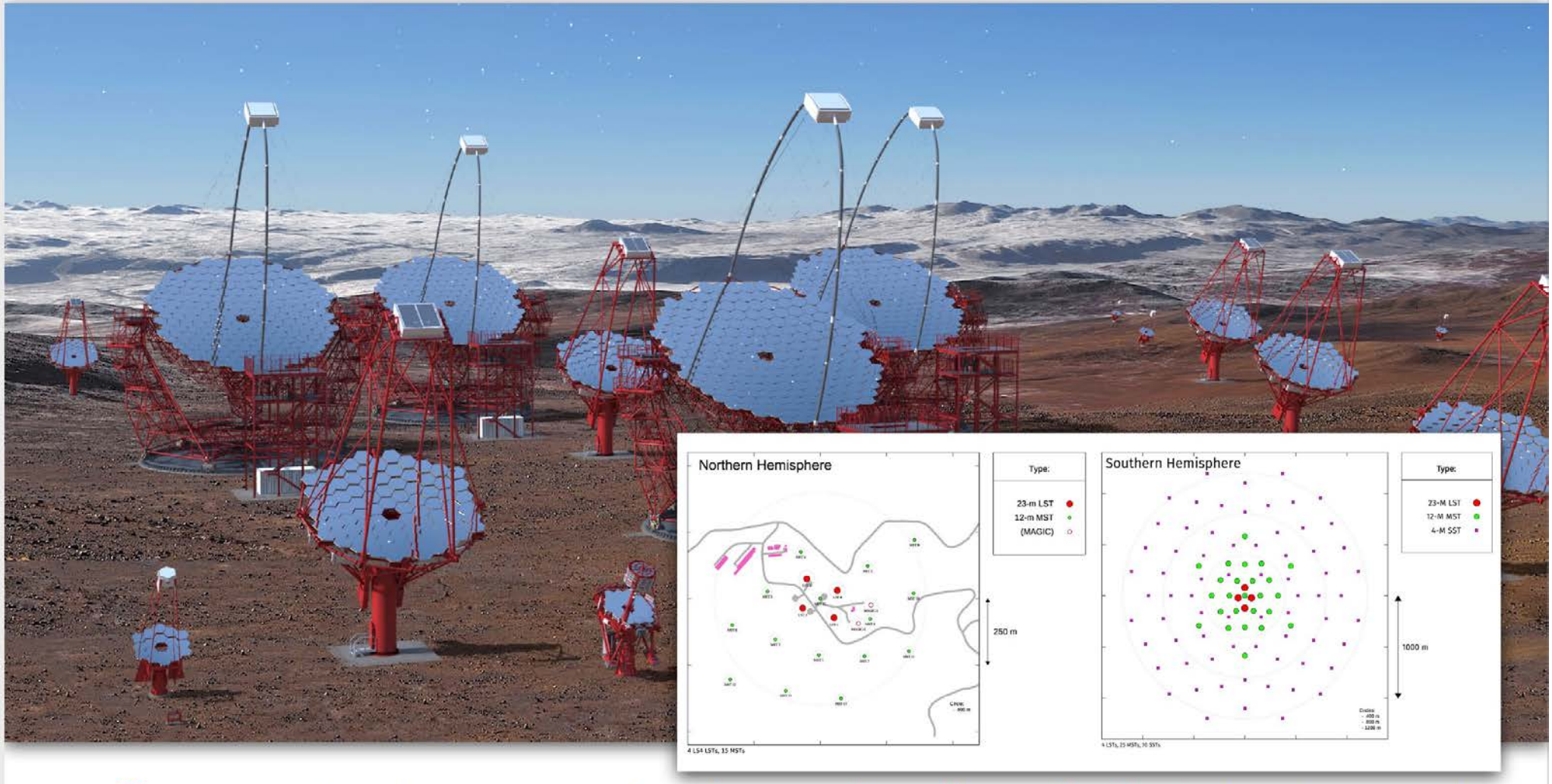

- Two arrays for observations of northern and southern sky (La Palma & Paranal)
- Three telescope sizes for broad energy coverage
  - 4 LSTs (23 m diameter dish), 25 MSTs (12 m), 70 SSTs (4 m)

CTA – the future IACT detector

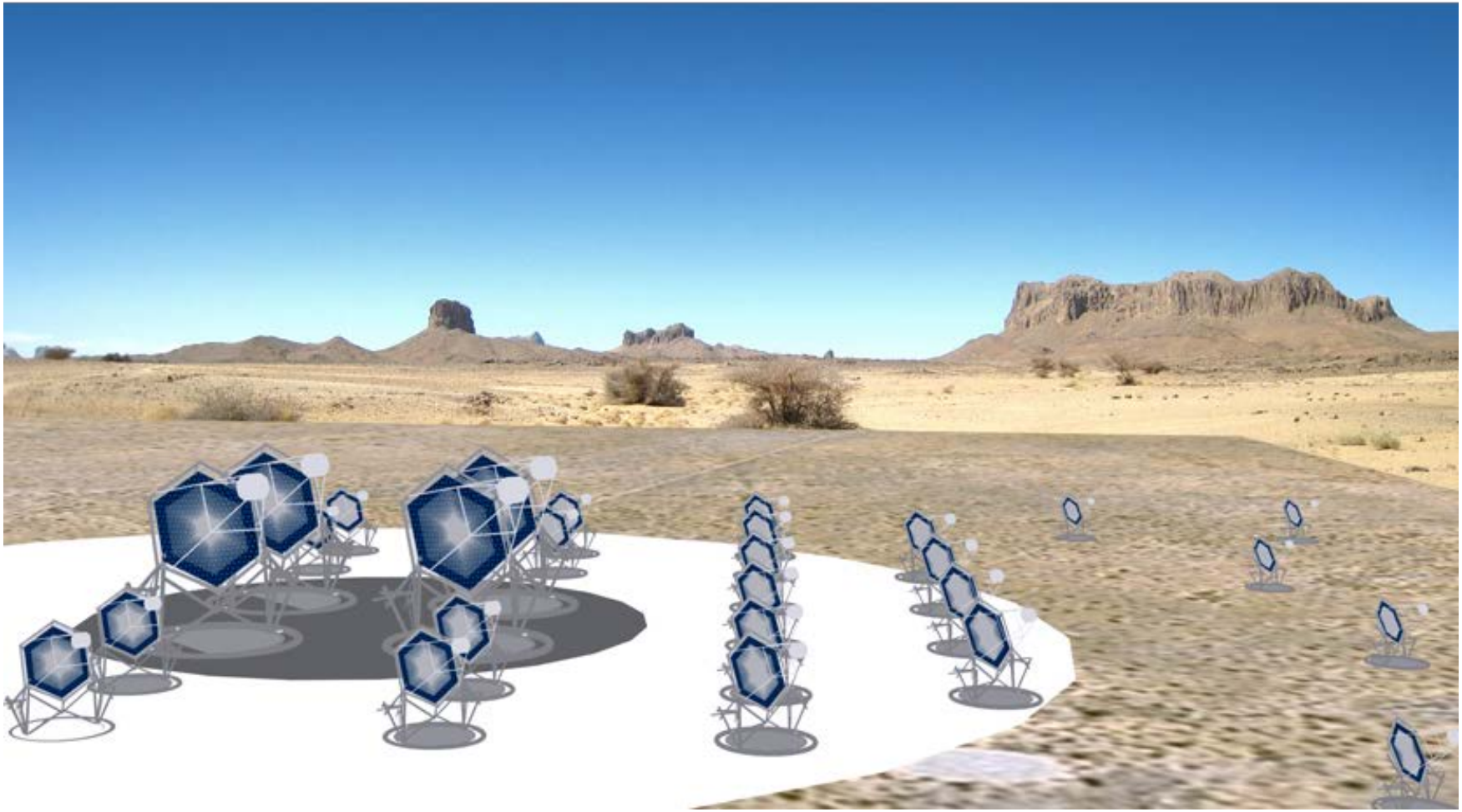

IACT technique provides the best performance in the TeV energy range:

- high-efficiency of detection and identification of electromagnetic showers
- good accuracy of reconstruction of the direction and the energy of the primary γ-ray photon
- large γ-ray photon statistics, allow angular resolution $\delta\theta \approx$ 1-2 arcminutes, and flux sensitivity at the level of 10^{-13} erg/cm^2 s

CTA Potential

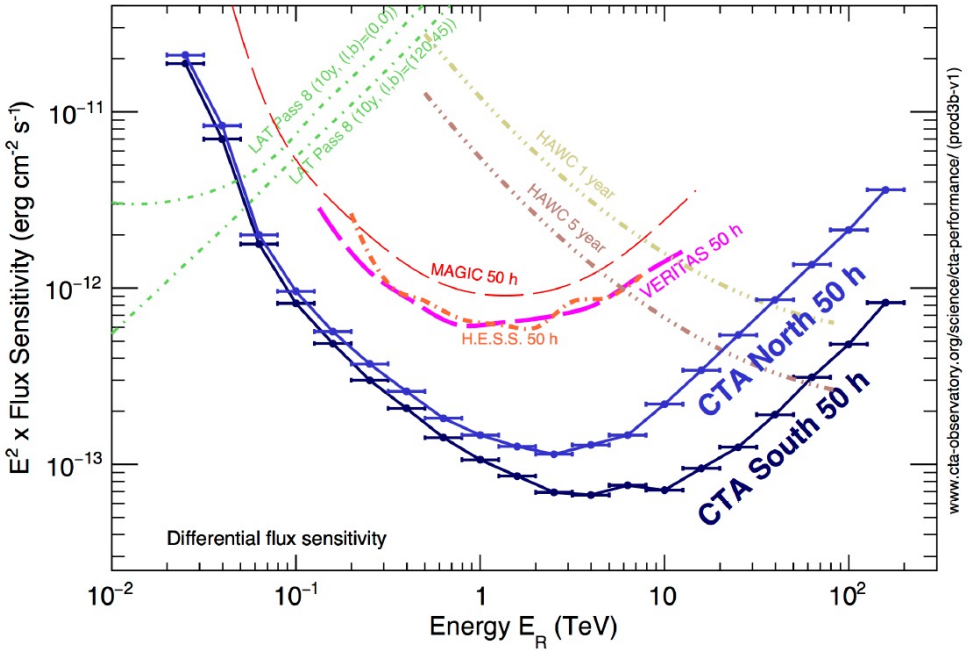

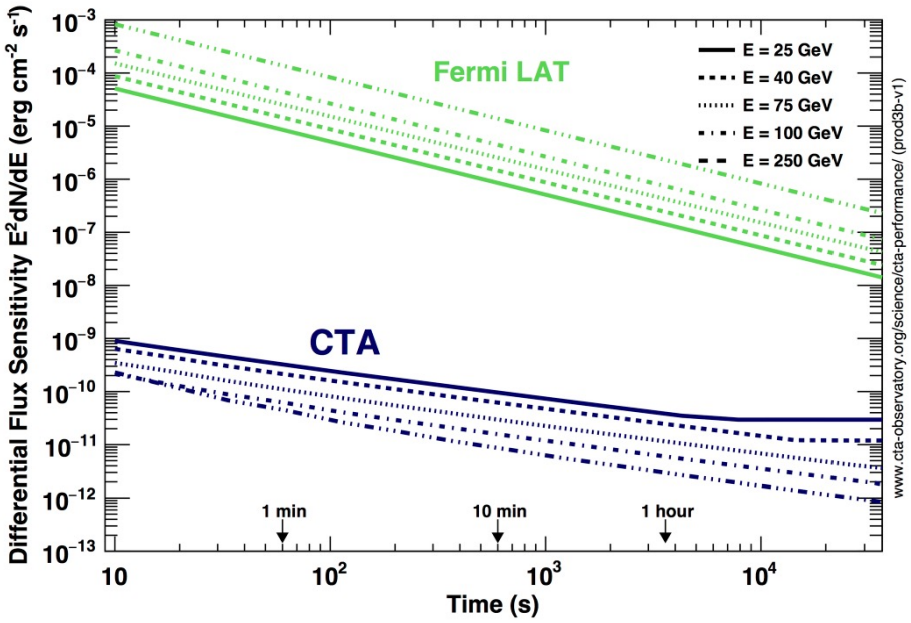

- 5 - 20x improvement in flux sensitivity, broader energy coverage
- Improved angular and energy resolution (5-10x better)
  - Source morphology, characterization of energy spectra
- Substantial gains in sensitivity to transients
  - Alert follow-ups
- Large array: operation in survey mode
  - Unbiased survey of TeV emitters

Prototyping and Construction

- Prototypes well-advanced for all telescope types
- “First light” and calibration studies
- Construction timeline
  - 2020 Pre-production telescopes on site
  - 2022 Start of “science” observations
  - 2025 Construction complete

CTA – the future IACT detector

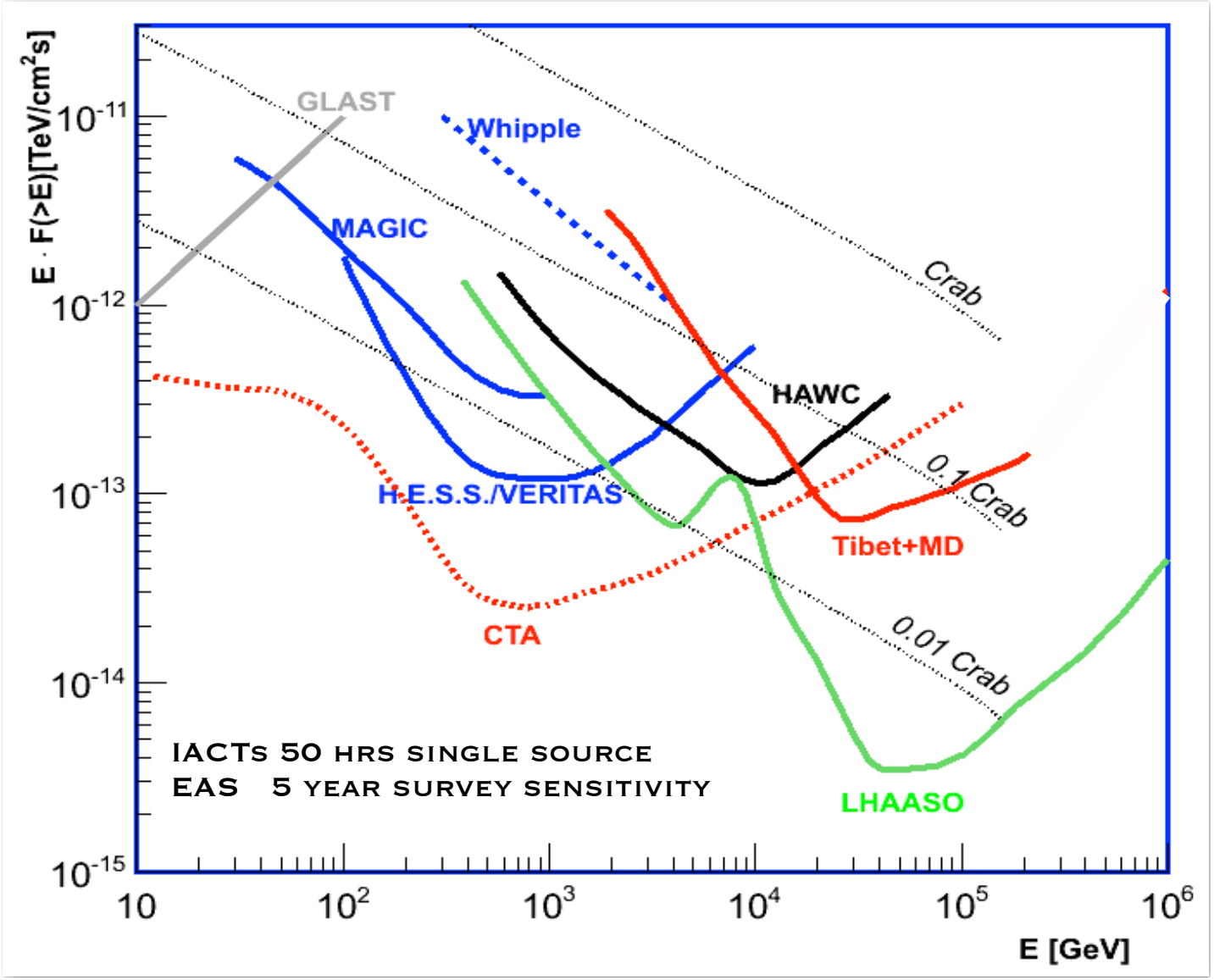

The energy-flux sensitivities of the current and future ground-based detectors, the IACT and EAS arrays in the energy range 10^{10} to 10^{16} eV.

LHAASO: high altitude Atmospheric Showers detector in construction: main components

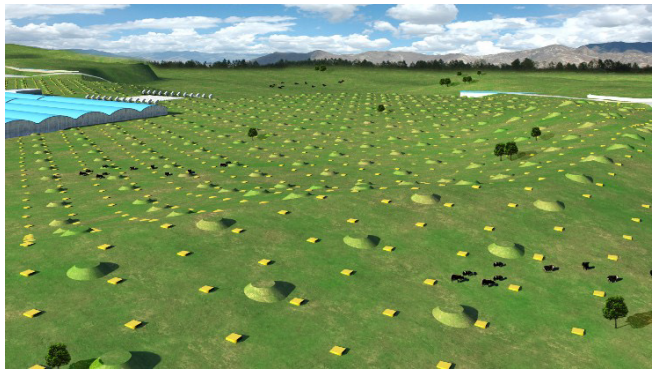

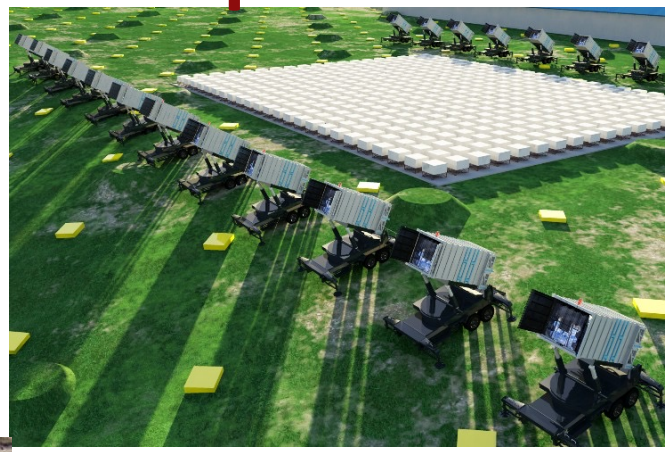

1 KM2A:
5635 EDs
1221 MDs

WFCTA:
24 telescopes
1024 pixels each

WCDA:
3600 cells
90,000 m^2

SCDA:
452 detectors

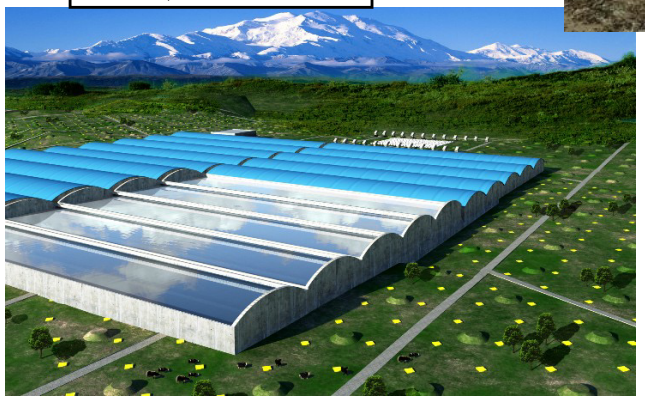

Coverage area: 1.3 km^2

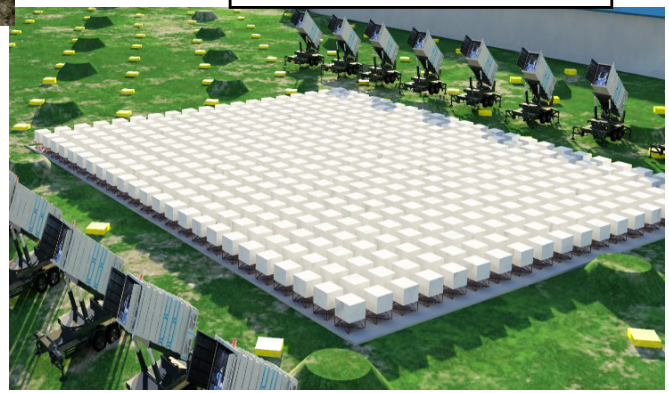

Detection of Very High Energy (~100TeV) charged C.R.

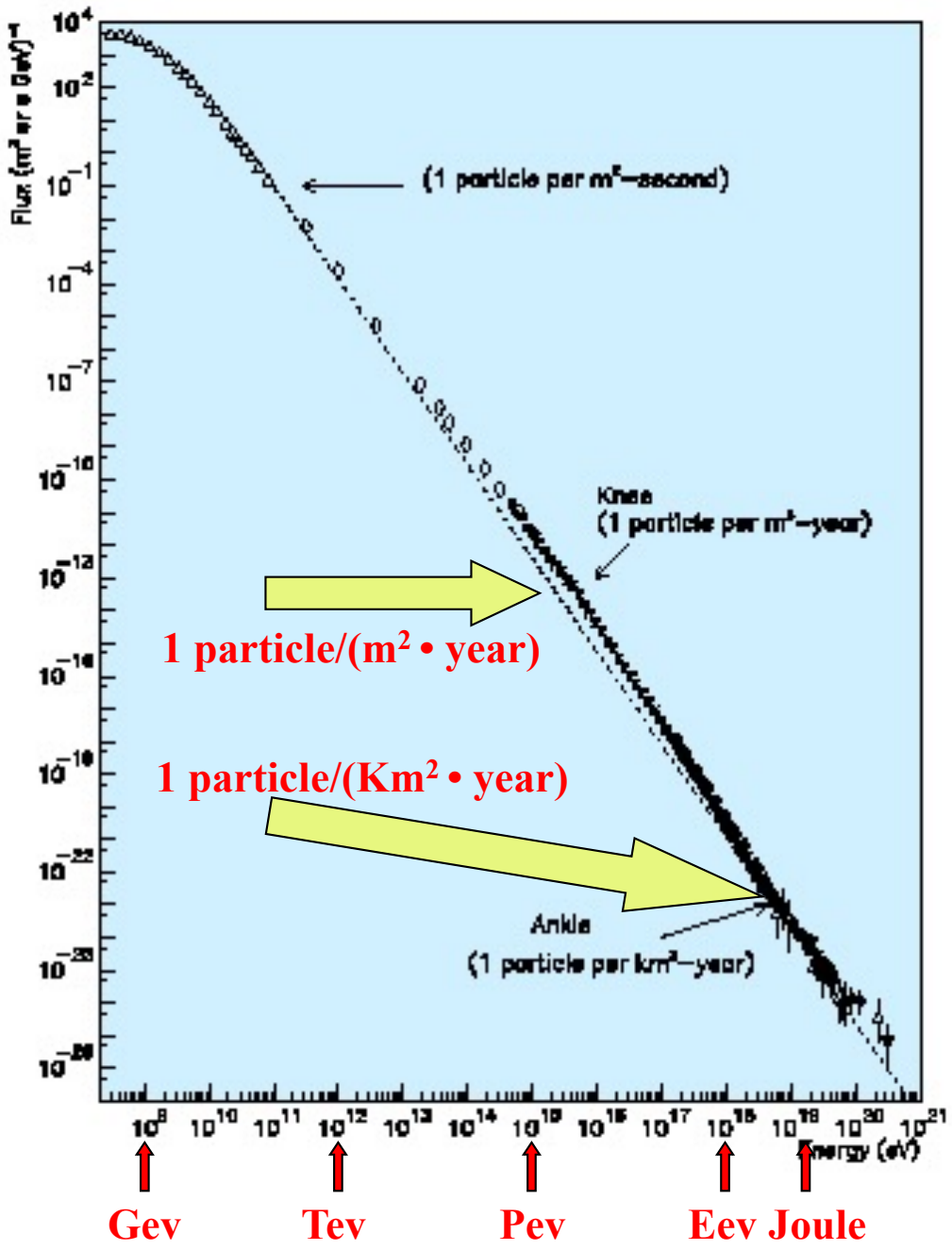

The study of cosmic rays with E ≥ 100TeV requires:

- ➔ **large equipment (scintillator apparatus, Cherenkov light, tracers, ...)**
- ➔ **on the earth's surface**
- ➔ **Studied the "results" of the interactions of the primary cosmic rays with the atmosphere**
- ➔ **From these measurements go back to E, direction, nature of the "primary"**

Aa example: the KASKADE detector for C.R.s

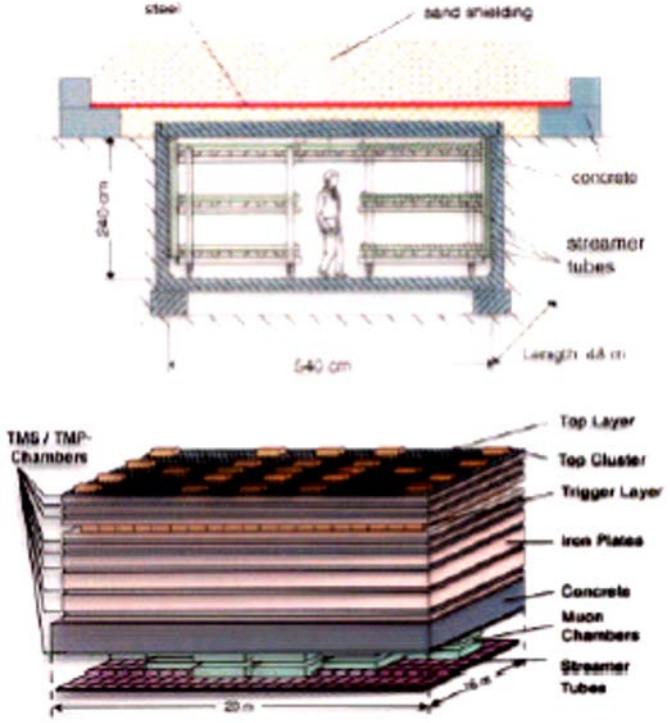

Atmospheric showers induced by charged C.R.

Atmospheric Thickness:

1035 g/cm²

≈ 11 λ_I (hadr. interact. lengths)

≈ 27 X_0 (radiation lengths)

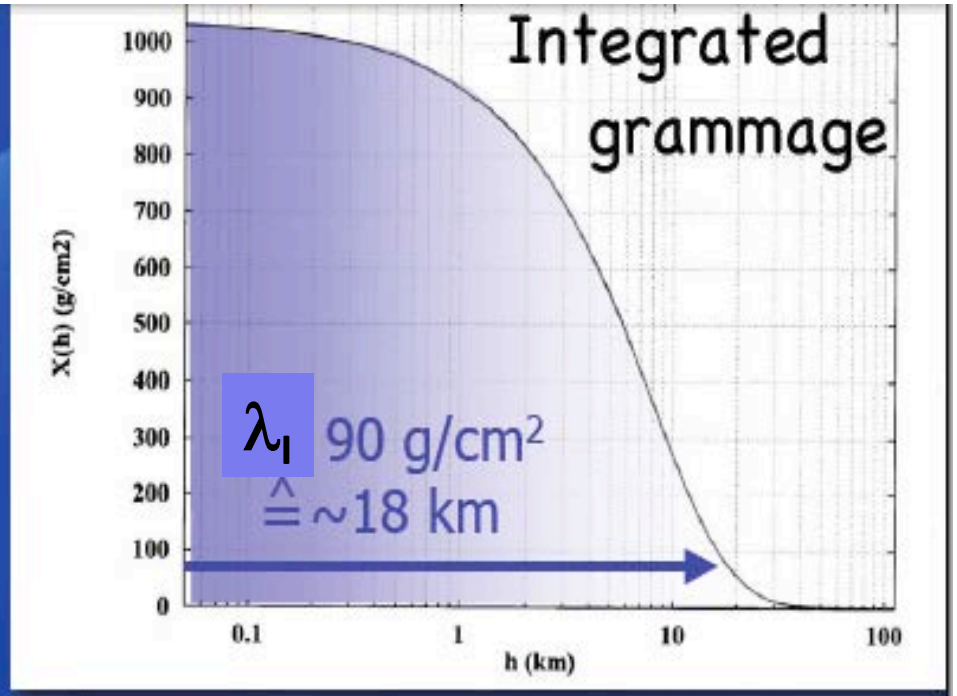

Some basics...

$$\lambda_I = \frac{1}{n \cdot \sigma} \cong 90 \text{ g/cm}^2 \text{ (p-Air)}$$

(*n*: density of absorber nuclei;
σ: total inelastic X-section)

X_0 defined by energy loss of high-energy electrons in media:

$$\langle E_e \rangle \propto e^{-\frac{X}{X_0}}$$

In air: X_0 = 36.66 g/cm²

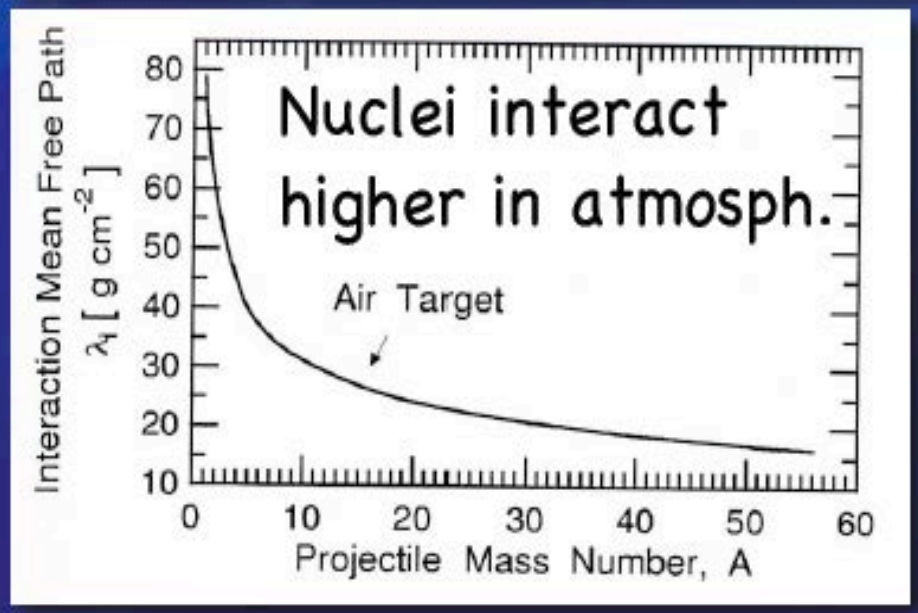

If the primary C.R. is a proton: p-air interaction

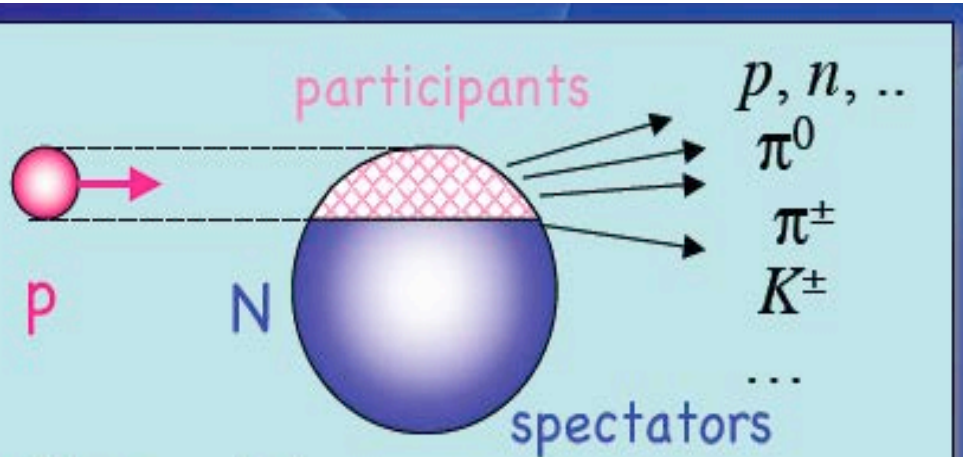

after ~ 1 λ_I

projectile looses ~ 40-60% of its initial energy (inelasticity)

Consequences:

pions are the most abundant hadrons in showers;

μ's are integrative; decay into e± of no relevance

$\pi^0 \rightarrow \gamma\gamma \quad (\tau_0 = 0.8 \cdot 10^{-16}\,\mathrm{s})$

$\pi^\pm \rightarrow \mu^\pm + \nu_\mu \quad (\tau_0 = 26\,\mathrm{ns})$

decay of $\pi^\pm$:

$$R_\pi = \gamma \cdot v \cdot \tau_0 \simeq \frac{E_\pi^{tot}}{m_0 c^2} \cdot c \cdot \tau_0$$

≈7.8 m

e.g.: E_π=14 GeV → R_π =780 m

≈ 1 λ_i at 5 km height

consequence:

in early shower, the hadronic interaction of $\pi^\pm$ is more probable than decay into μ and vice versa in late showers

p vs Fe induced EAS at the same total energy

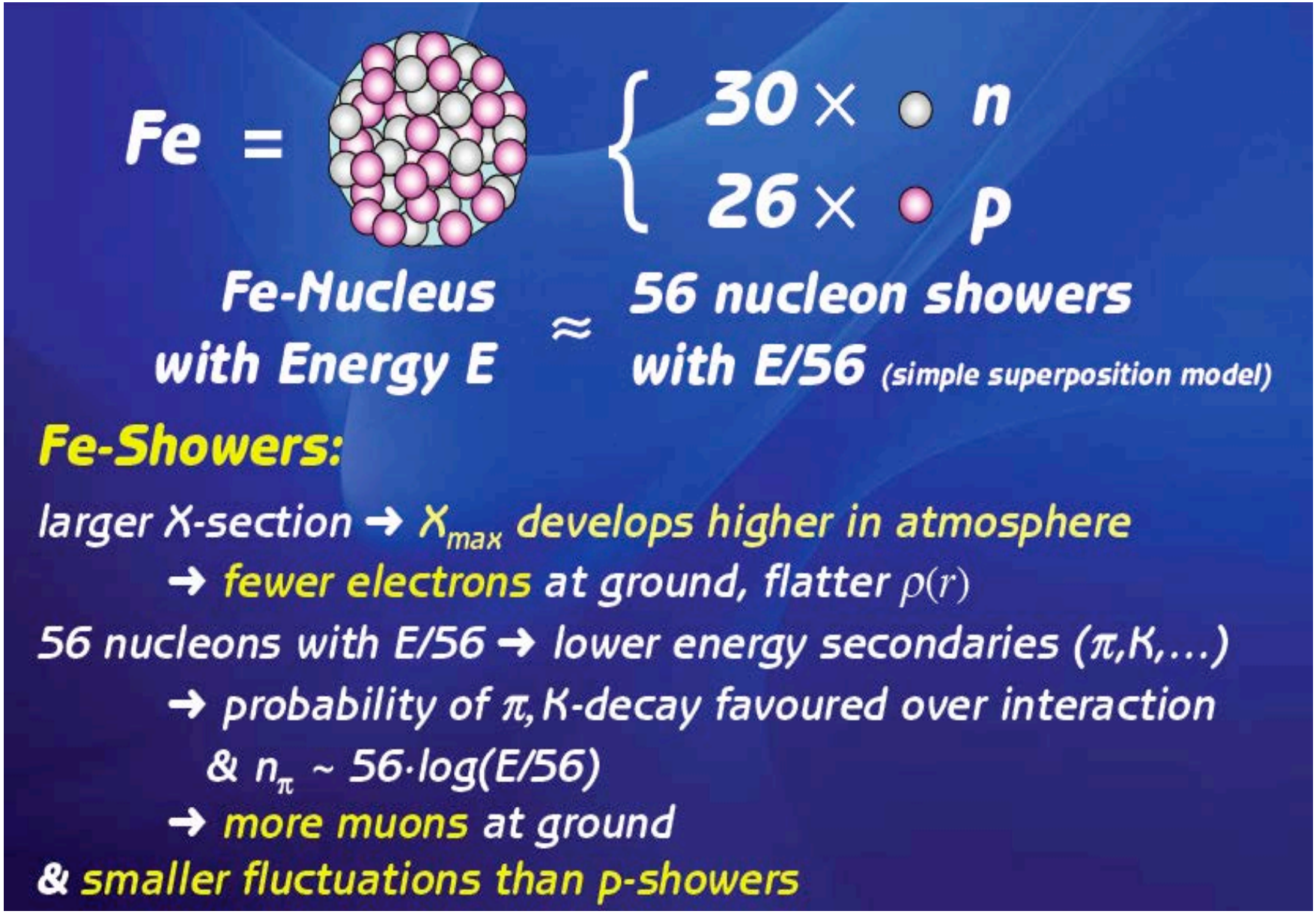

Development of hadronic showers in the atmosphere. C.R. composition: measure of A

A detector for atmospheric air showers is realized with an apparatus, usually composed of different parts, capable of measuring with good resolution the arrival times of the incident particles, in which it is possible to define the "coincidence" time between the signals on different parts of the apparatus itself. A nucleus of mass A and total energy E_0 can be treated as A set of A nucleons each with energy $E = E_0 / A$

The shower induced by a nucleus with mass A and energy is E similar to A showers induced by protons with E/A energy but:

- For protons $x_{max} \sim \lambda \cdot \ln (E/E_C)/\ln(2)$

- for nuclei A $x_{max} \sim \lambda \cdot \ln (E/AE_C)/ \ln(2)$

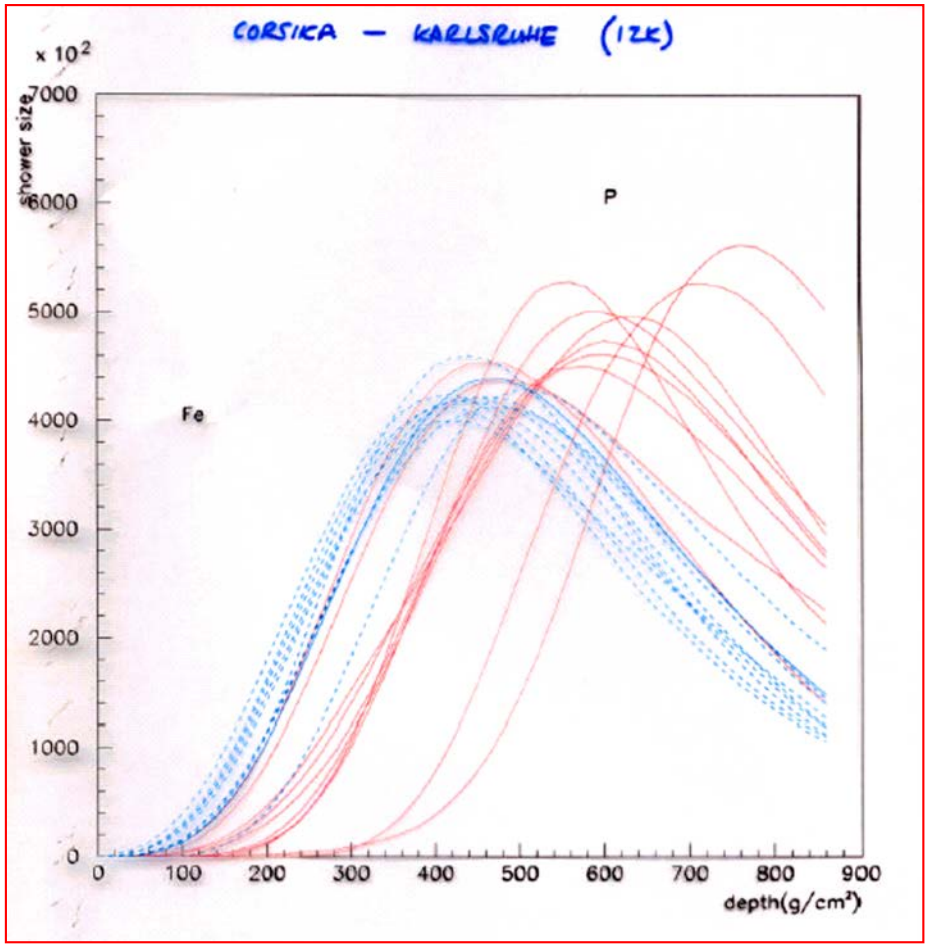

Proton and Iron induced showers (MC simulation)

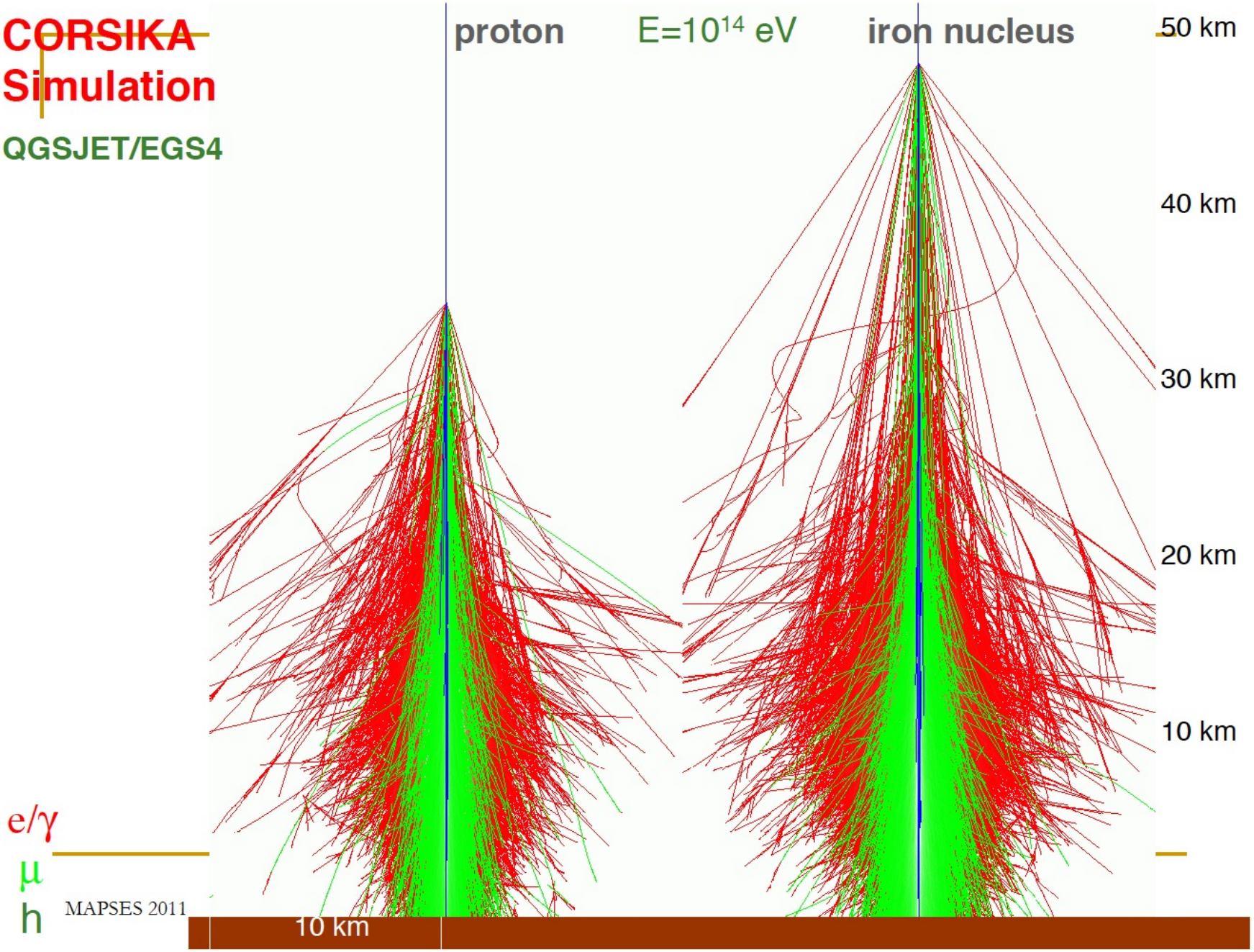

Shower Longitudinal Development

Individual components @ 10^{15} eV
for different prim. masses

$N(t) \sim t^{\alpha} \cdot e^{-\beta t}$

$(t = x/X_0)$

position of X_{max}
changes logarithm. with E

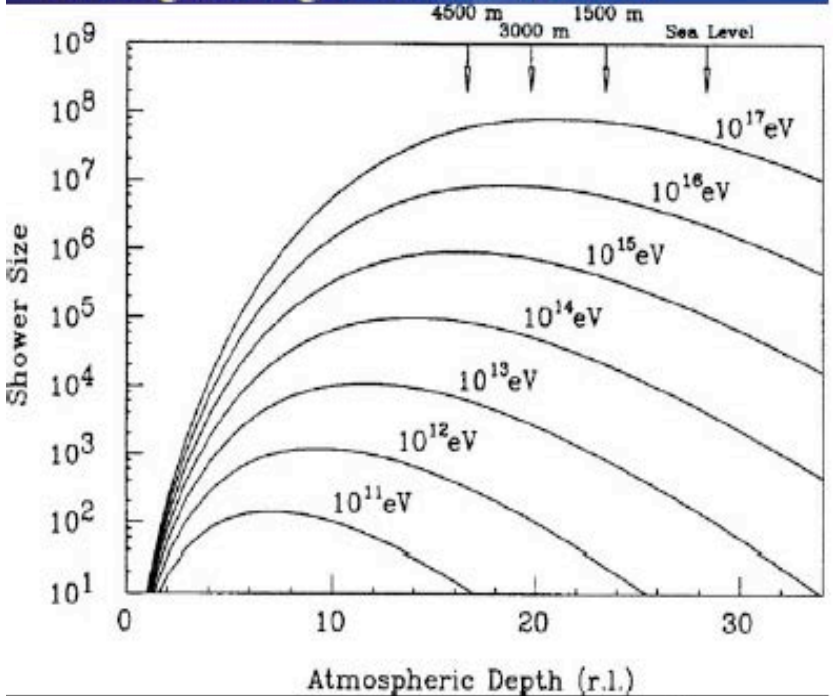

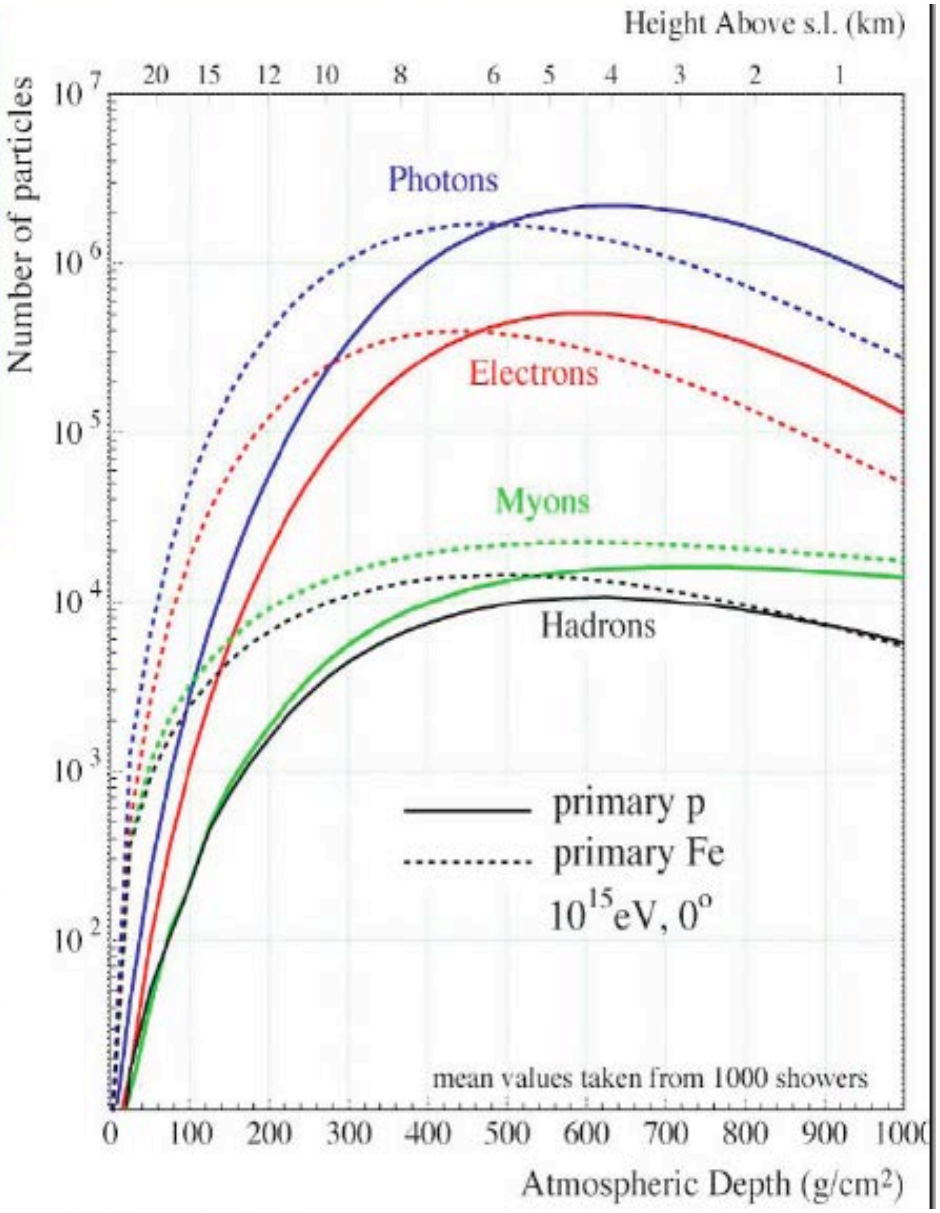

Energy deposition for muons (stopping power)

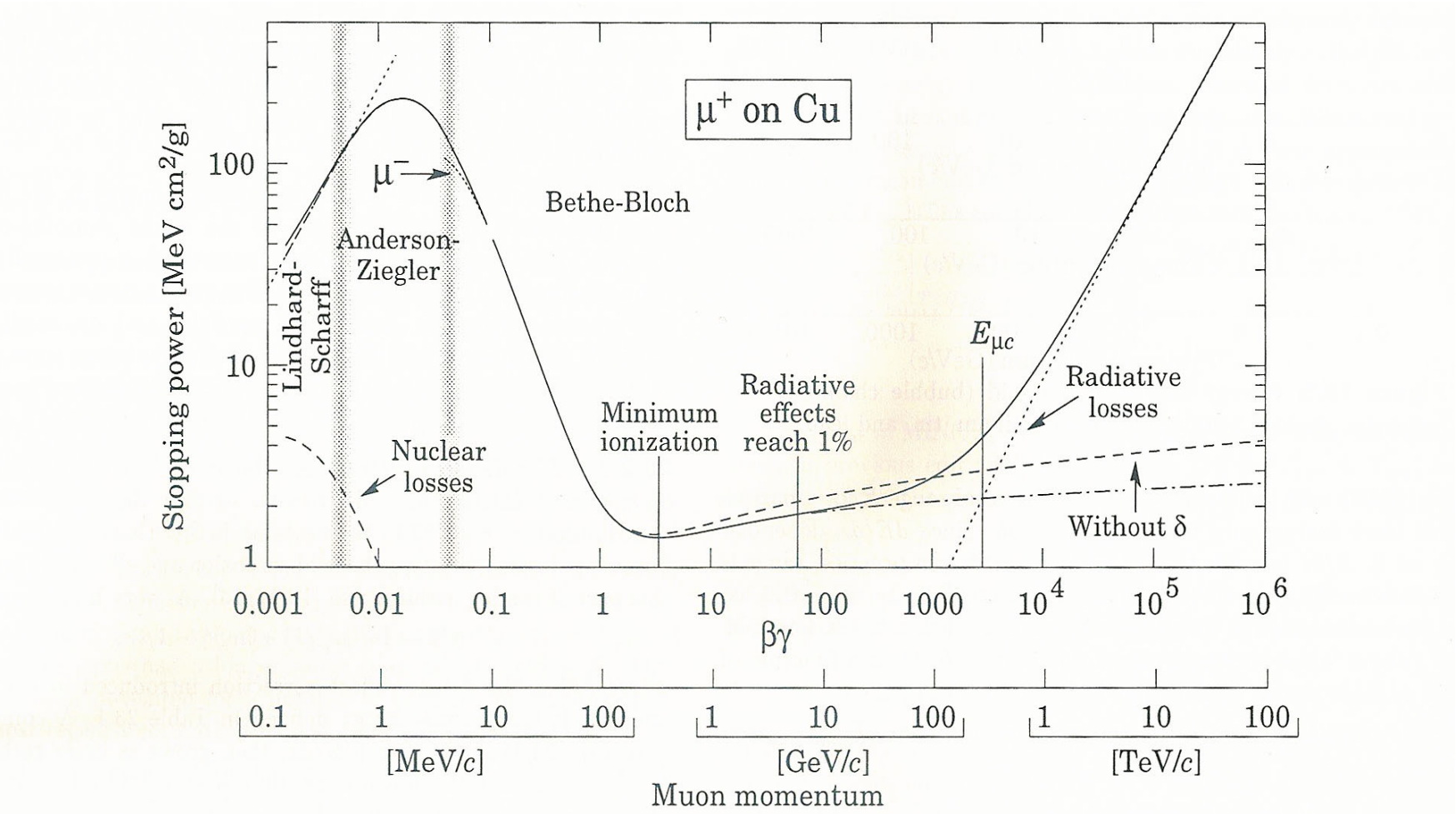

Fig. 23.1: Stopping power ($= \langle -dE/dx \rangle$) for positive muons in copper as a function of $\beta\gamma = p/Mc$ over nine orders of magnitude in momentum (12 orders of magnitude in kinetic energy) [1]. Solid curves indicate the total stopping power. Data below the break at $\beta\gamma \approx 0.1$ are taken from ICRU 49 [2], and data at higher energies are from Ref. 1. Vertical bands indicate boundaries between different approximations discussed in the text. The short dotted lines labeled "μ^-" illustrate the "Barkas effect," the dependence of stopping power on projectile charge at very low energies [3].

2 TeV Proton induced EAS

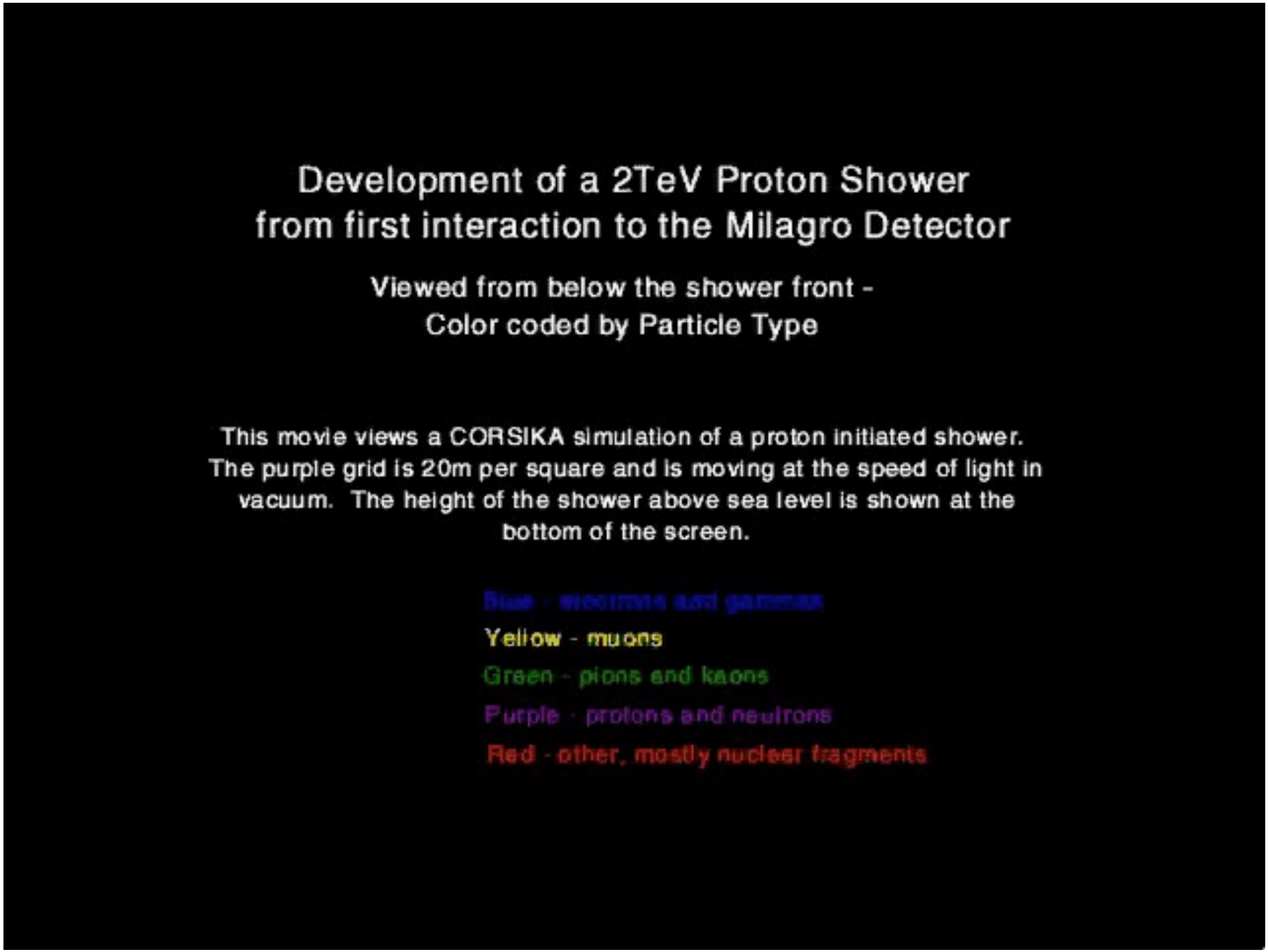

2 TeV Photon induced EAS

KASKADE experiment

Karlsruhe **S**hower **C**ore and **A**rray **DE**tector -Grande is an extensive air shower experiment array to study the cosmic ray primary composition and the hadronic interactions in the energy range $E_0=10^{16}$-10^{18}eV.

The experiment was situated near Karlsuhe (Germany) at 110m a.s.l, corresponding to an average atmospheric depth of 1022g/cm^2.

It measures simultaneously the electromagnetic, muonic and hadronic components of extensive air showers of cosmic rays.
As an extension of the former KASCADE experiment running successfully since 1996, KASCADE-Grande was built by reassembling 37 stations of the former EAS-TOP experiment -basically the electromagnetic detectors- running between 1987 and 2000 at Campo Imperatore, Grand Sasso Laboratories, Italy.

One of the main results obtained by these two experiments is a picture of increasingly heavier composition above the 'knee' caused by a break in the spectrum of the light components. Conventional acceleration models predict a change of the composition towards heavier components. The discovery of the knee in the heavy components, represented by iron, would be a convincing verification of these theories. From the observed rigidity dependent breaks of the spectra of different lighter primaries observed between 10^{14} and 10^{16}eV, the iron 'knee' is expected around $E_0=10^{17}$eV.

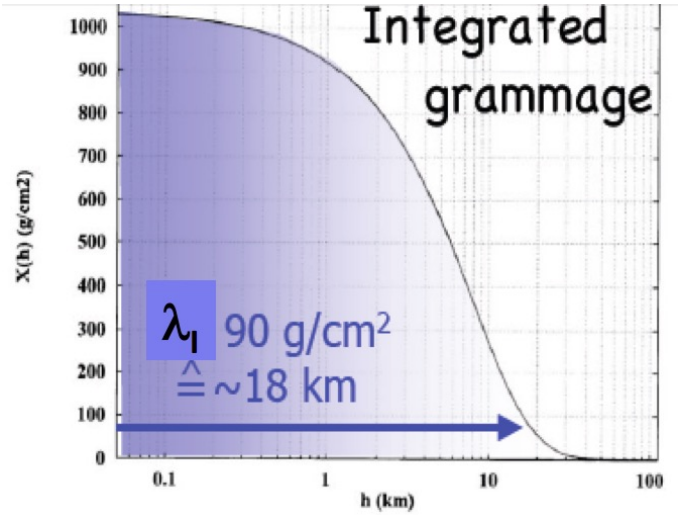

KASKADE experiment

The field array (200m x 200m) consists of 252 detector stations arranged on a rectangular grid with a distance of 13 meters to each other. 16 (resp. 15) of the stations form a so-called cluster with an electronics container in the centre and which act as an independent shower experiment. In the middle of the array one can see the building with the KASCADE central detector

The original KASCADE Array is a Scintillator Array which measures the electrons, photons and muons of extensive air showers outside the core region in 252 detector stations on a rectangular grid of 13 m spacing, hence forming an array of 200 x 200 m².

T.Antoni et al. NIM A513 (2003) 490

- **Energy range 100TeV – 80PeV**
- **Since 1995**
- **Large number of observables: electrons, muons@4 thresholds, hadr**

Andreas Haungs – KASCADE-Grande Collaboration

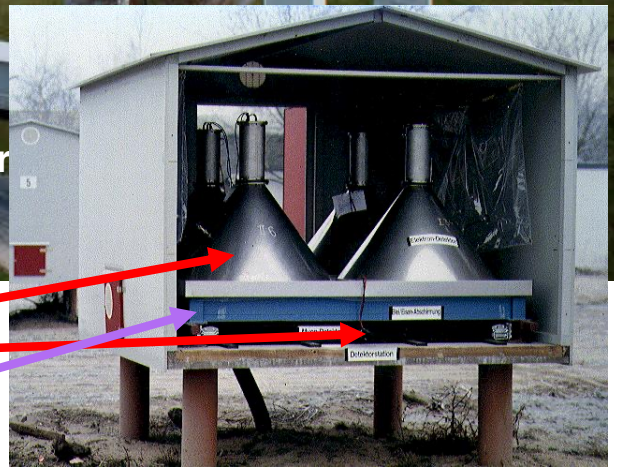

In each station there are up to four electron-gamma detectors and one muon-detector
under a iron-lead-absorber of about 20 attenuation lengths.

KASCADE: the central detector

Tunnel with muon detector (streamer tubes)

Central Detector: iron sampling calorimeter

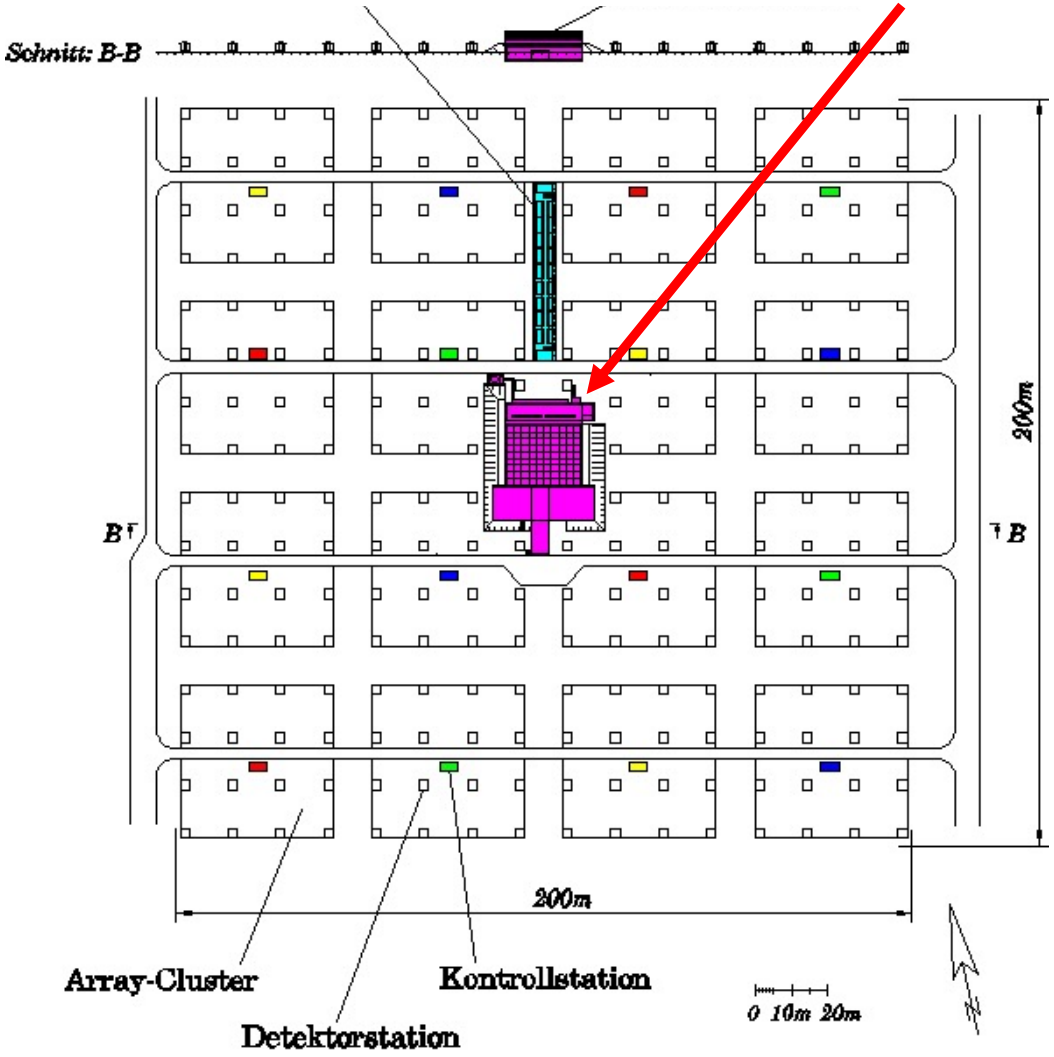

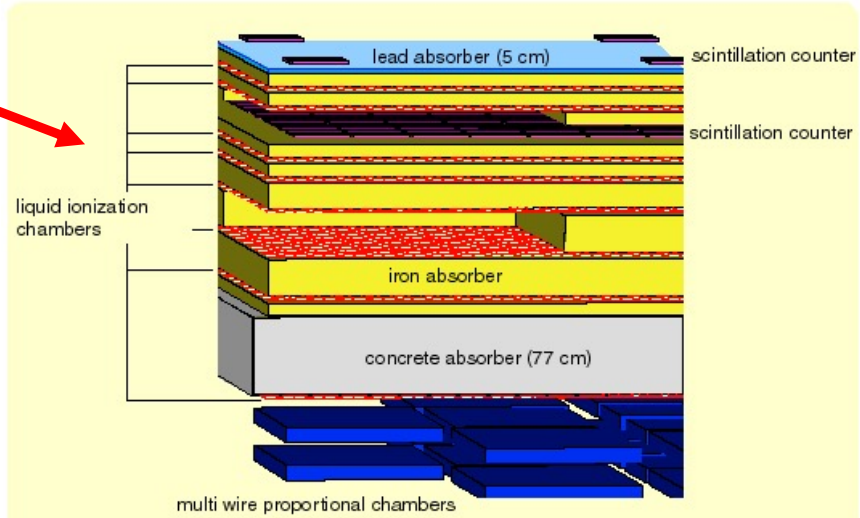

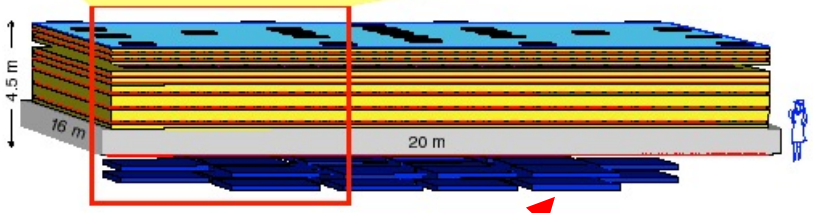

Multiwire proportional chambers to detect muons below the iron-sampling calorimeter

KASCADE: the central detector

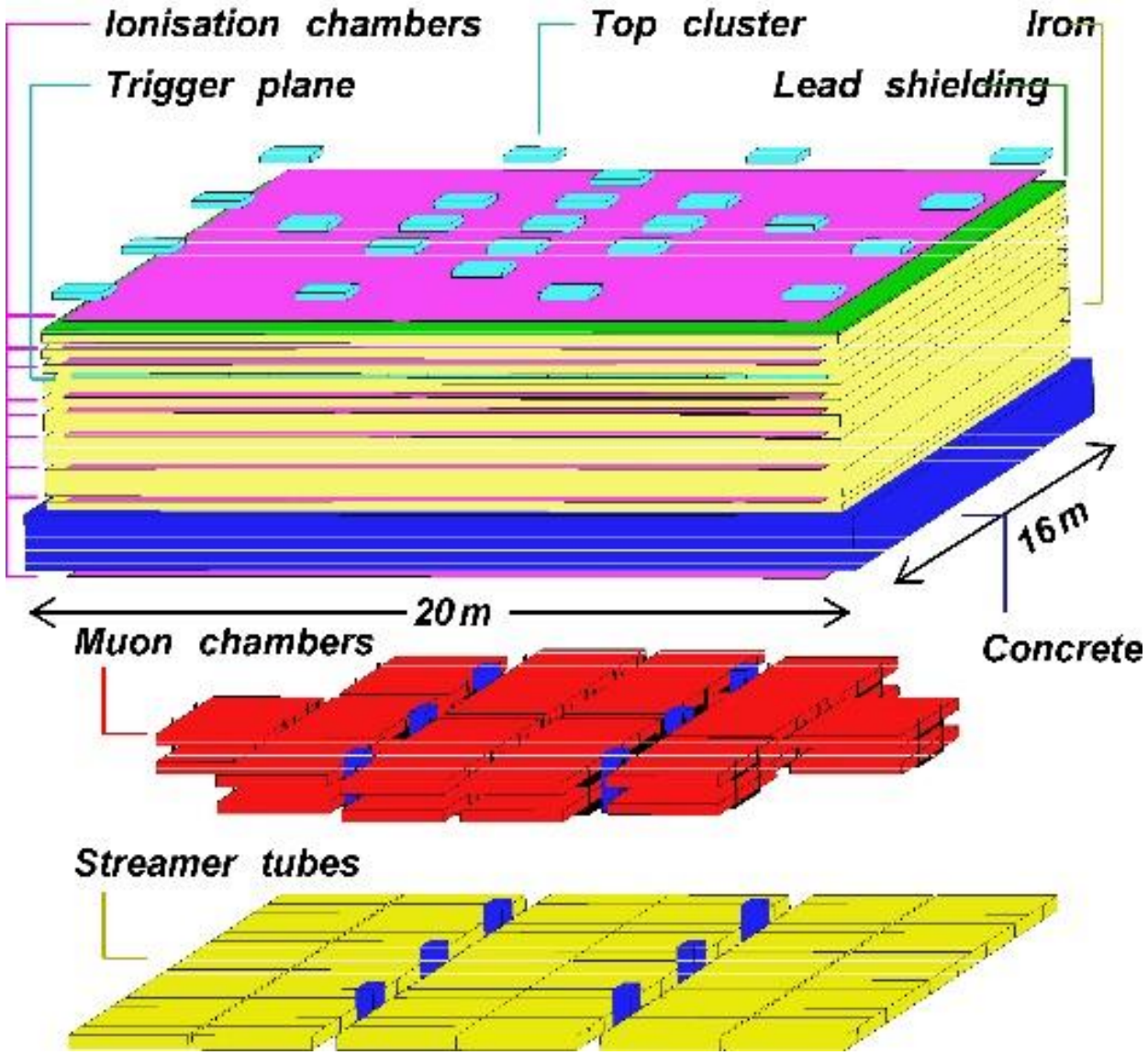

KASKADE-GRANDE experiment

KASCADE-Grande is an extensive air shower experiment array to study the cosmic ray primary composition and the hadronic interactions in the energy range $E_0=10^{16}$-10^{18}eV.

KASCADE-Grande

The **KASCADE-Grande Detector Array** has been realized by means of 37 stations at a mutual distance of about 130 m covering an area of 0.5 km^2 next to the KASCADE site in order to operate jointly with the KASCADE detector components.

KASCADE-Grande was realized to expand the energy range for cosmic ray studies from 10^{14}-10^{17} eV primary energy range up to **10^{18} eV.** This is performed by extending the area covered by the KASCADE electromagnetic array from 200×200m^2 to **700×700m^2** by means of 37 scintillator detector stations of 10 m^2 active area each. This new array is named Grande and provides measurements of the all-charged particle component of extensive air showers, while the original KASCADE array particularly provides information on the muon content. Additional dense compact detector set-ups being sensitive to energetic hadrons and muons are used for data consistency checks and calibration purposes.

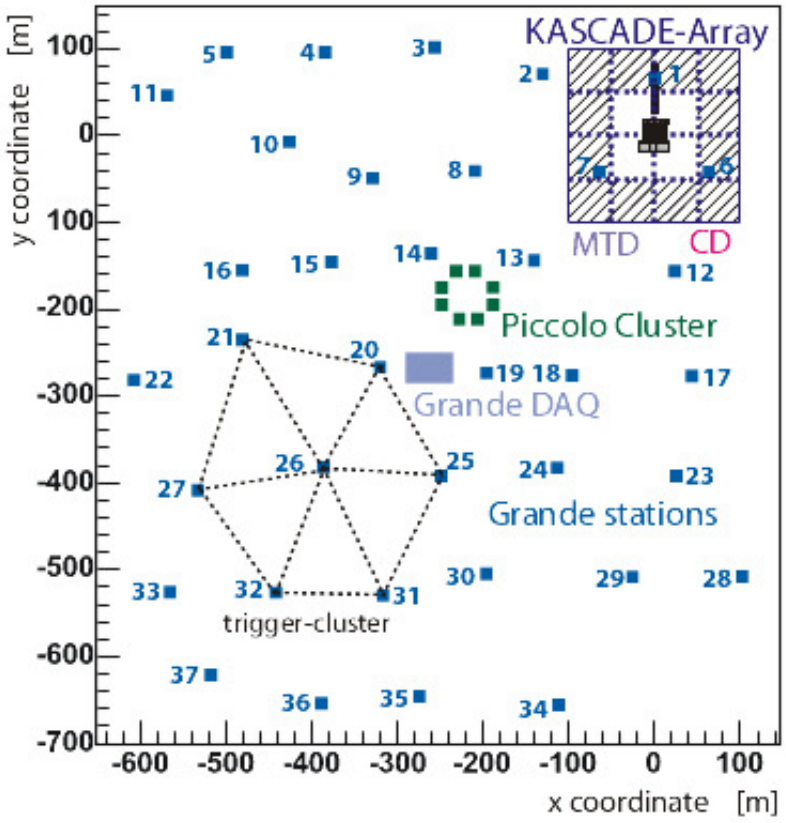

The **KASCADE-Piccolo Trigger Array** consists of an array of 8 stations equipped with 10m^2 of plastic scintillator each and is placed towards the centre of the Grande array. The main aim of piccolo is to provide an external trigger to Grande and to KASCADE for coincidence events.

KASCADE-Grande detectors & observables

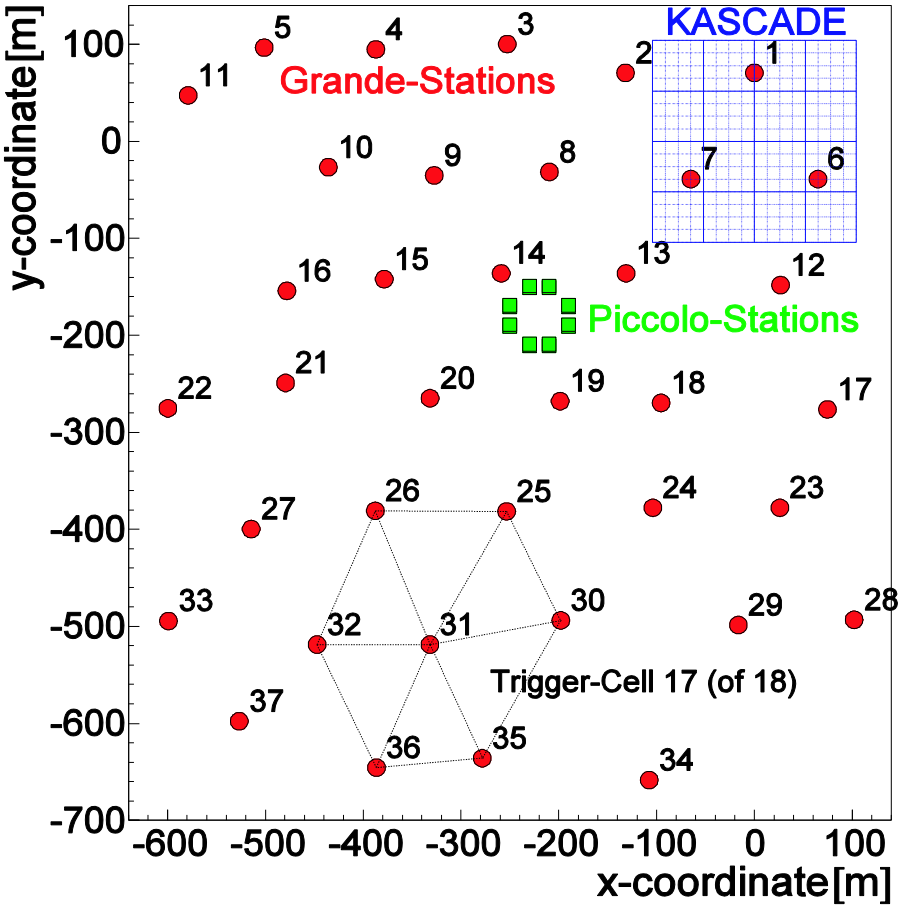

Grande array → cover an area of 0.5 km², detecting EAS with high resolution

Detector	Detected EAS component	Detection Technique	Detector area (m^2)
Grande	Charged particles	Plastic Scintillators	37x10
KASCADE array e/γ	Electrons, γ	Liquid Scintillators	490
KASCADE array μ	Muons ($E\mu^{th}$=230 MeV)	Plastic Scintillators	622
MTD	Muons (Tracking) ($E\mu^{th}$=800 MeV)	Streamer Tubes	4x128

- Shower core and arrival direction
- Shower Size (N_{ch} number of charged particles)
  - Grande array

- μ Size (E_μ>230 MeV)
  - KASCADE array μ detectors
- μ density & direction (E_μ>800 MeV)
  - Streamer Tubes

*Flux*E*$^{2.5}$ for charged primary Cosmic Rays around the knee

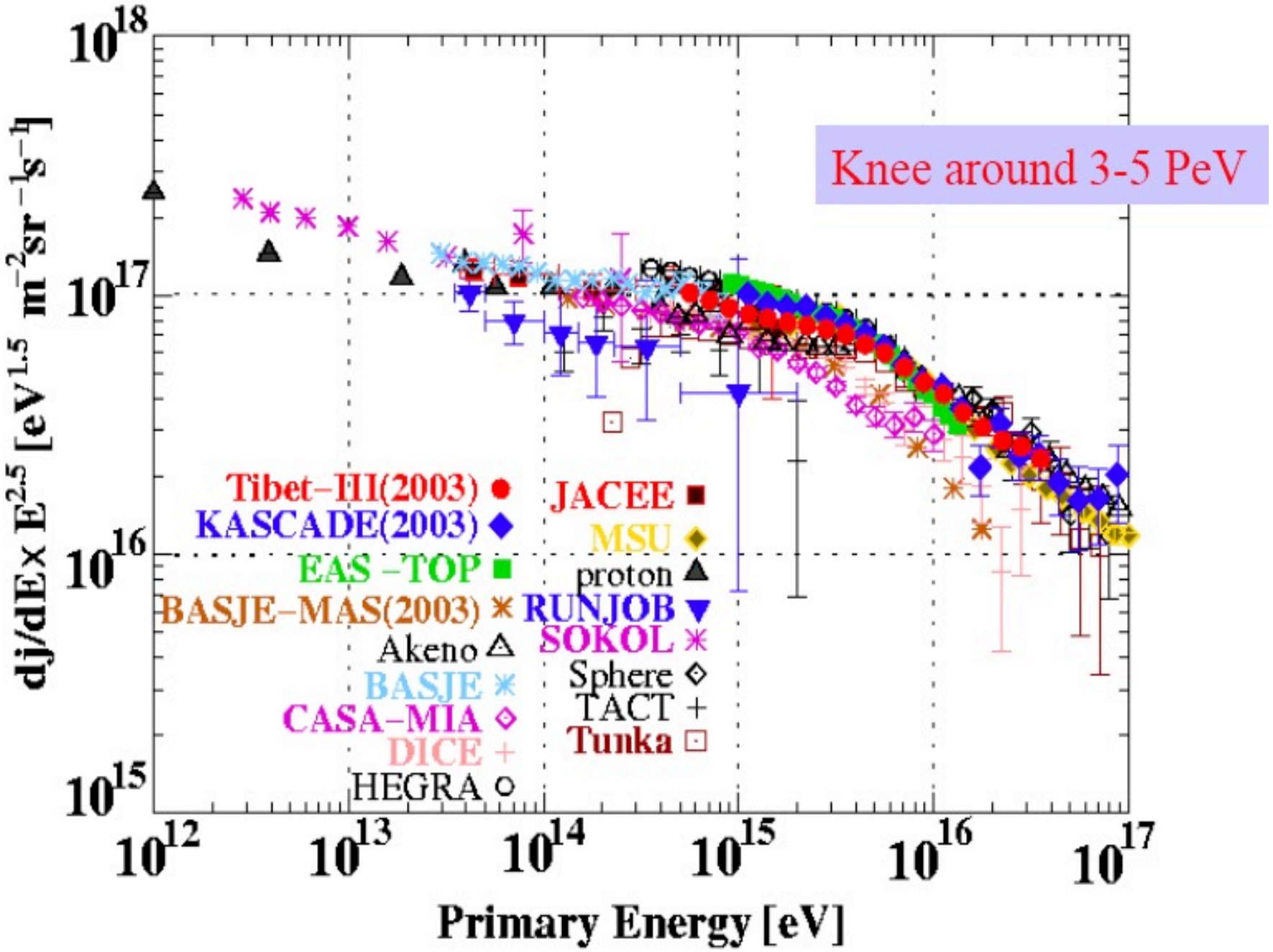

The "Knee" of primary Charged Cosmic Rays spectrum

- Knee is due to the light component of cosmic rays
- Change of slope of the heavy component observed at 8×10^{16} eV
- Knee interpretation either by acceleration limit in galactic sources or by propagation effects
- Not yet identified the transition to extragalactic primaries

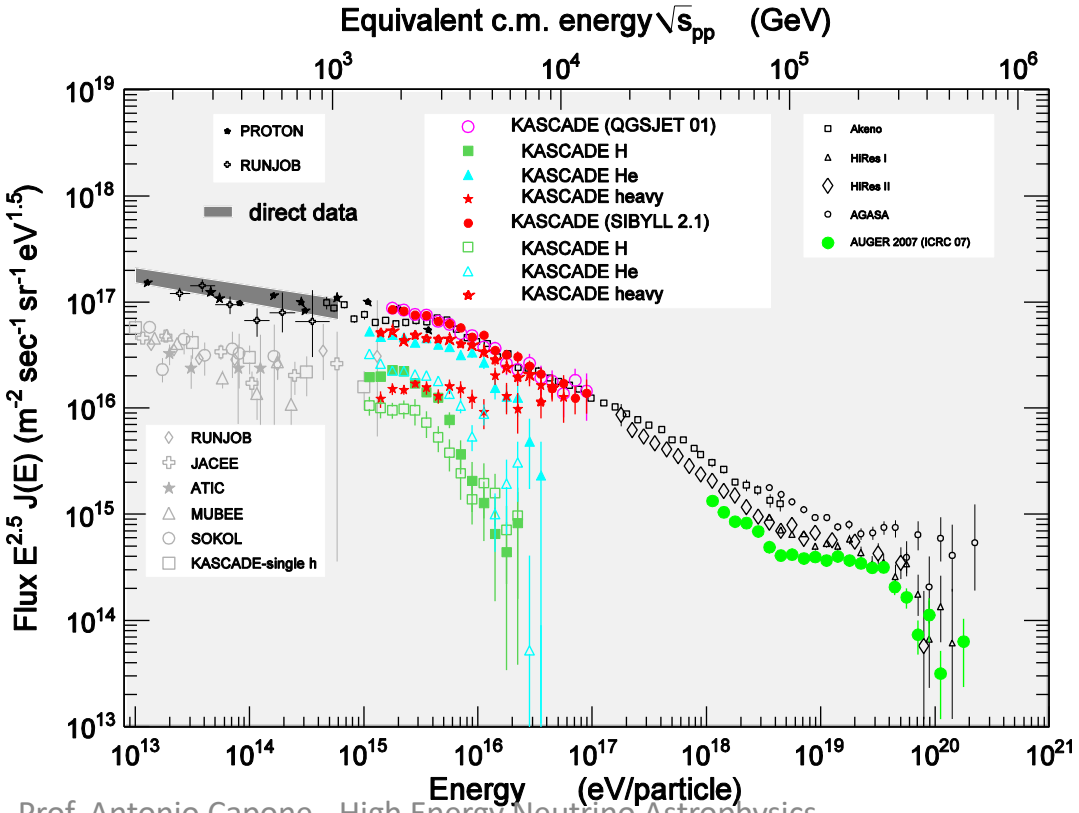

All particle energy spectrum

- Combination of N_{ch} and N_{μ}
- Five different angular bins

$$k = \frac{\log_{10}\left(N_{ch}/N_{\mu}\right) - \log_{10}\left(N_{ch}/N_{\mu}\right)_{H}}{\log_{10}\left(N_{ch}/N_{\mu}\right)_{Fe} - \log_{10}\left(N_{ch}/N_{\mu}\right)_{H}}$$

- k parameter evaluates chemical composition, used as a weight in the expression correlating N_{ch} and E

$$\log_{10} E = \left[a_H + \left(a_{Fe} - a_H\right)\cdot k\right]\cdot \log_{10} N_{ch} + b_H + \left(b_{Fe} - b_H\right)\cdot k$$

- Based on QGSJet II-02

Astroparticle Physics 36, (2012) 183

KASCADE and the N_{ch}/N_{μ} ratio

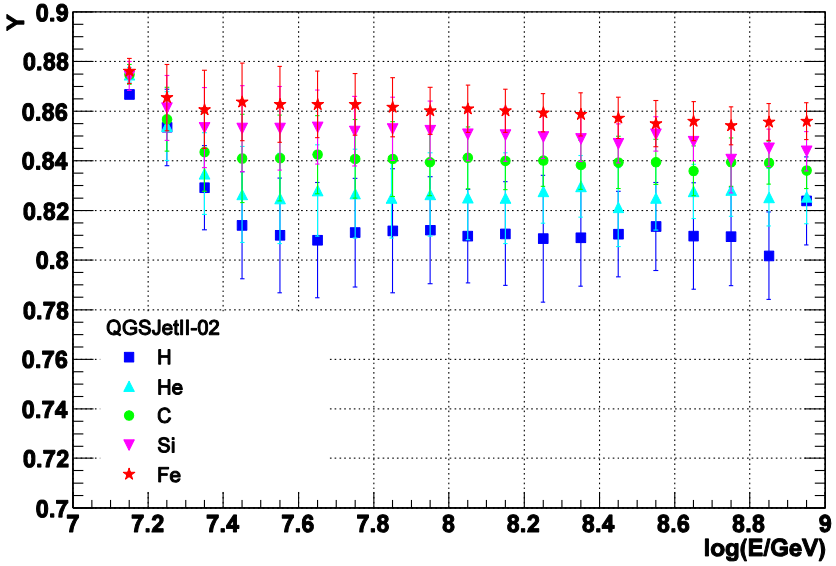

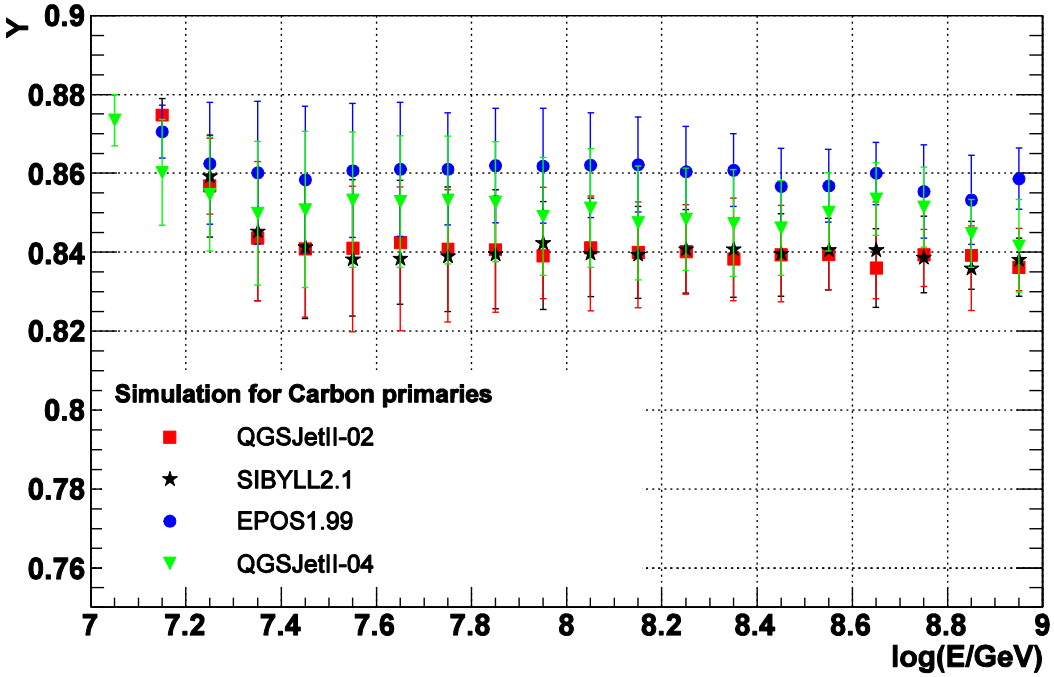

Y_{CIC} is constant with E
(E > full efficiency)

For a specific hadronic interaction model
Y_{CIC} increases with primary mass
choice of Y_{CIC} → choice of a primary mass

$$Y_{CIC} = \frac{\ln N_{\mu}\left(\vartheta_{ref}\right)}{\ln N_{ch}\left(\vartheta_{ref}\right)}$$

For a particular primary element
Y_{CIC} increases when calculated by a model generating EAS with higher N_{μ}
→ for the same primary mass the choice of Y_{CIC} is shifted

KASCADE

Event by event separation in two mass groups by N_{ch}/N_{μ} ratio

Two different ways of taking into account the EAS attenuation in atmosphere

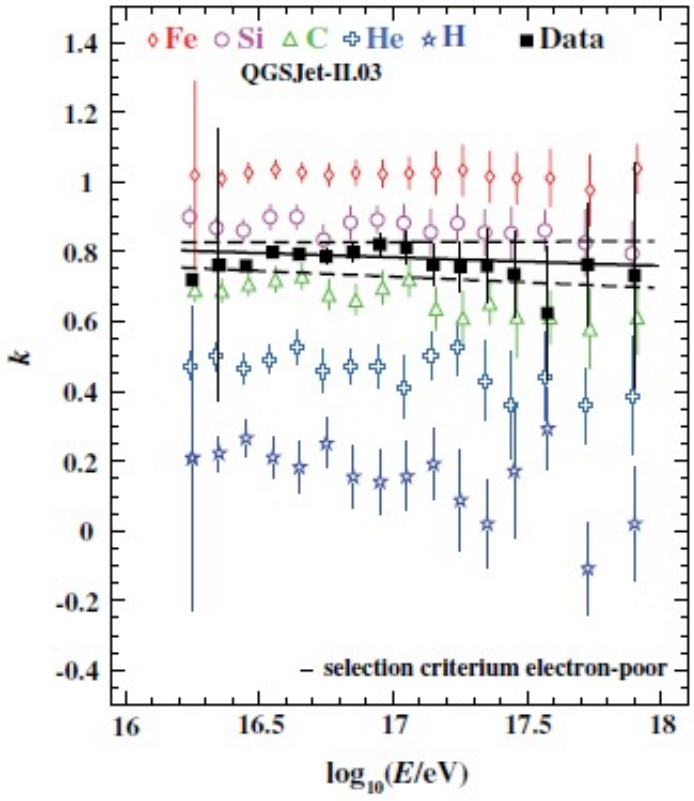

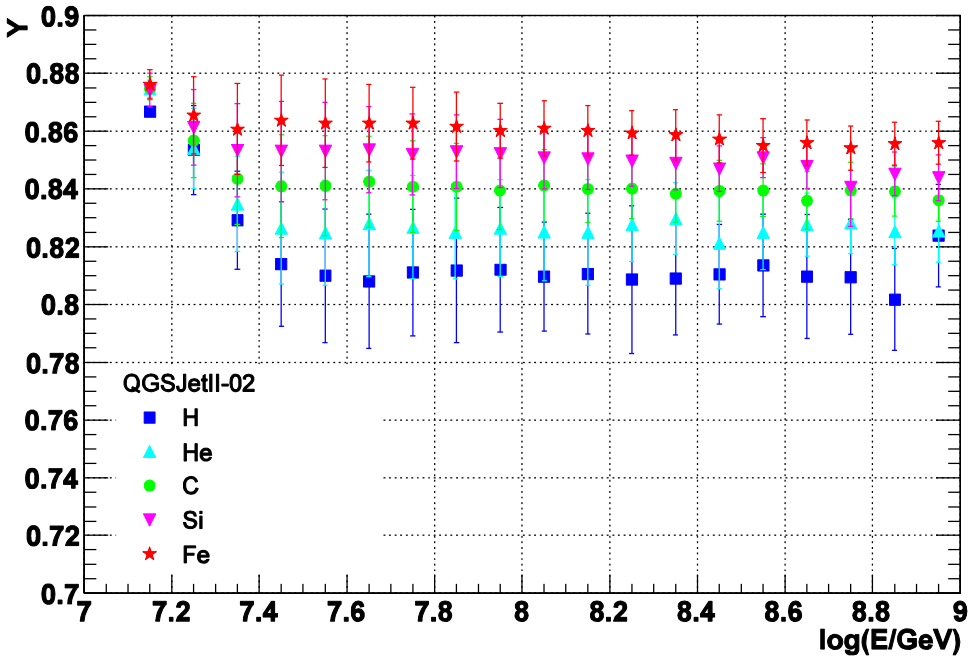

$$k = \frac{\log_{10}\left(N_{ch}/N_{\mu}\right) - \log_{10}\left(N_{ch}/N_{\mu}\right)_{H}}{\log_{10}\left(N_{ch}/N_{\mu}\right)_{Fe} - \log_{10}\left(N_{ch}/N_{\mu}\right)_{H}}$$

$$Y_{CIC} = \frac{\ln N_{\mu}\left(\vartheta_{ref}\right)}{\ln N_{ch}\left(\vartheta_{ref}\right)}$$

Approach to Chemical Composition

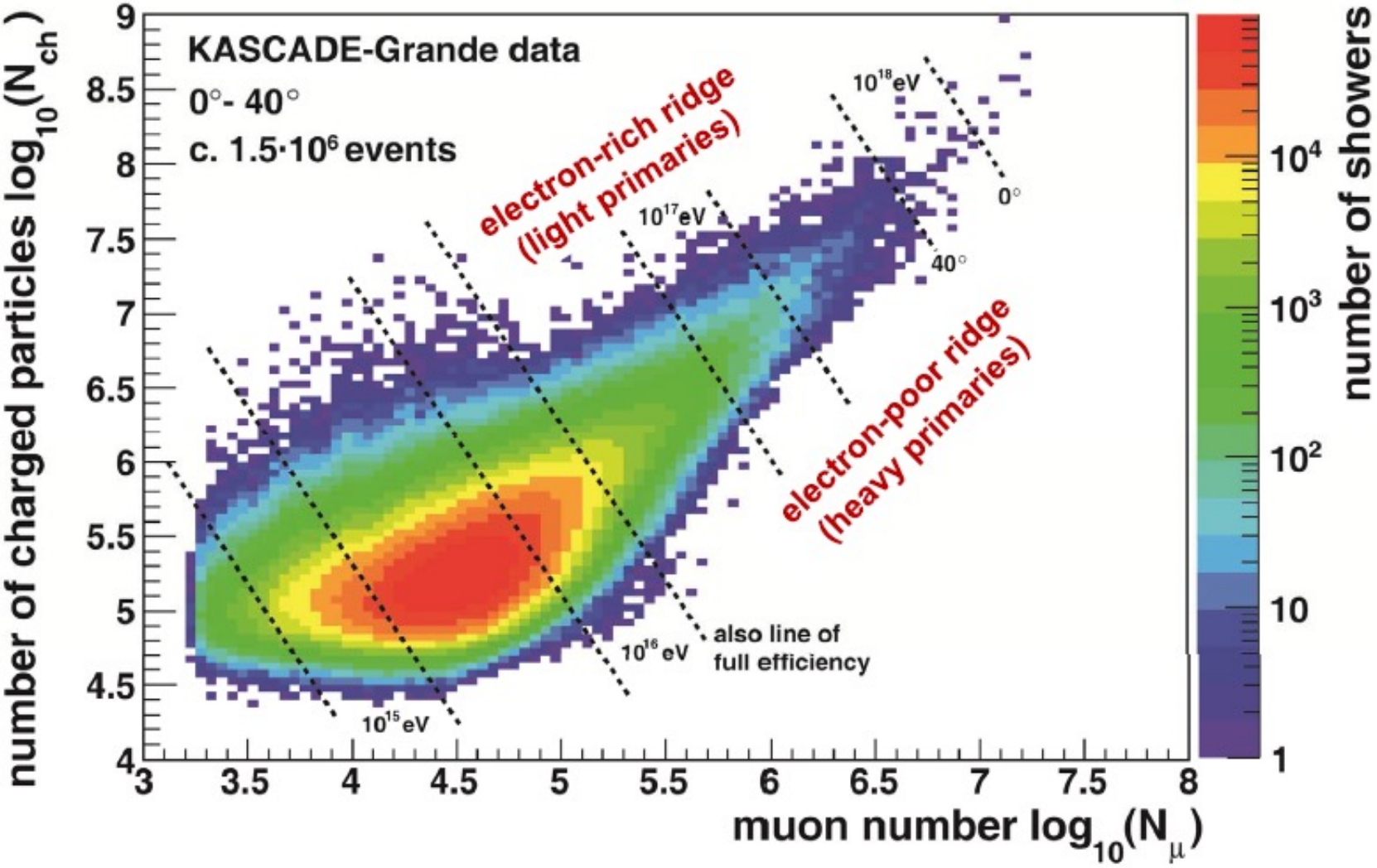

KASCADE Energy spectra

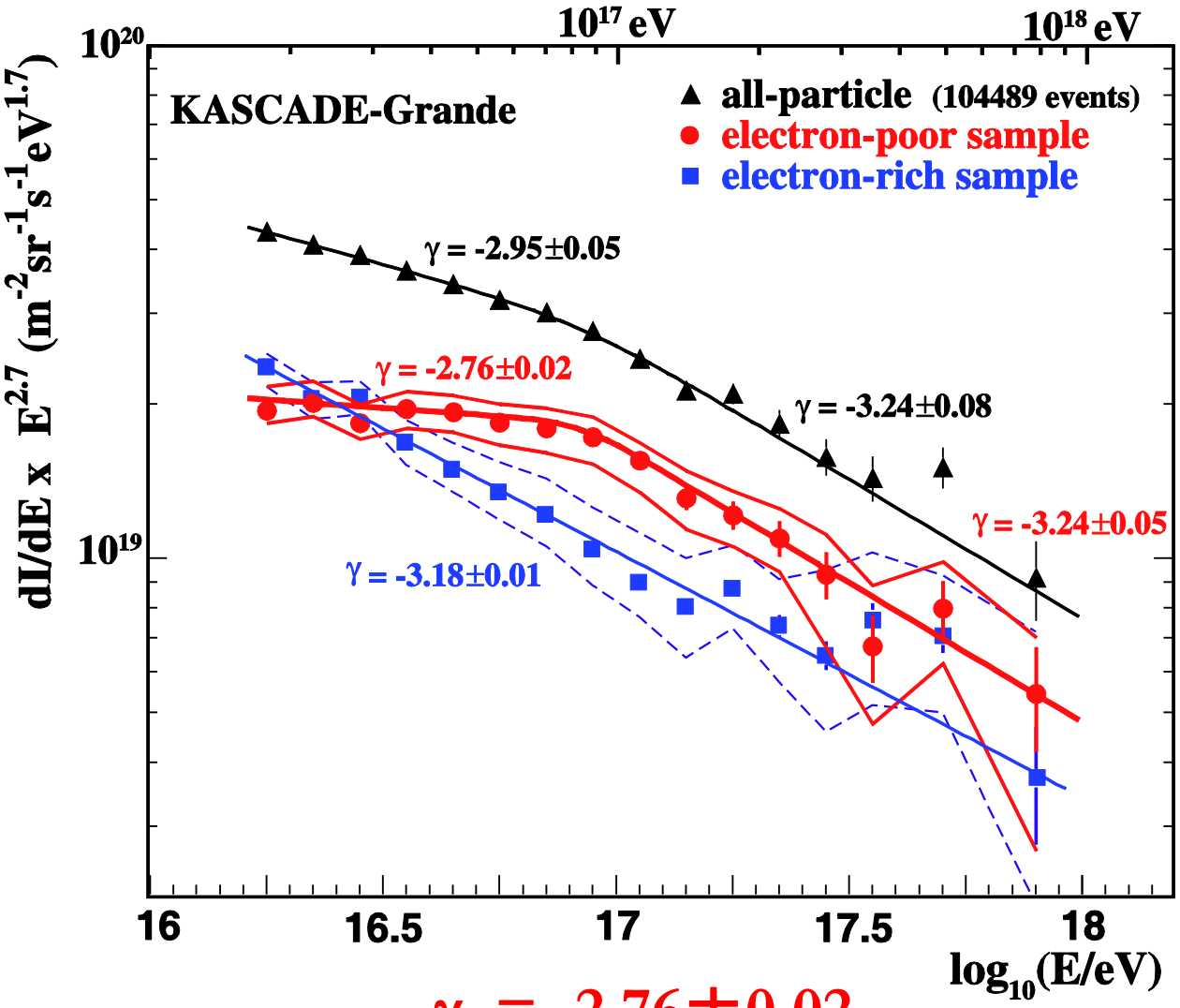

$\gamma_1 = -2.76 \pm 0.02$

$\gamma_2 = -3.24 \pm 0.05$

$E_b = 10^{16.92 \pm 0.04}$

- Energy spectra of the samples obtained by an event selection based on the k parameter

- Spectrum of the electron poor sample → $k > (k_C + k_{Si})/2$ → steepening observed with increased significance → 3.5σ

- Spectrum of electron rich events → can be described by a single power law → hints of a hardening above 10^{17} eV

Phys. Rev. Lett. 107 (2011) 171104

KASCADE summary

KASCADE-Grande
energy spectra of individual mass groups

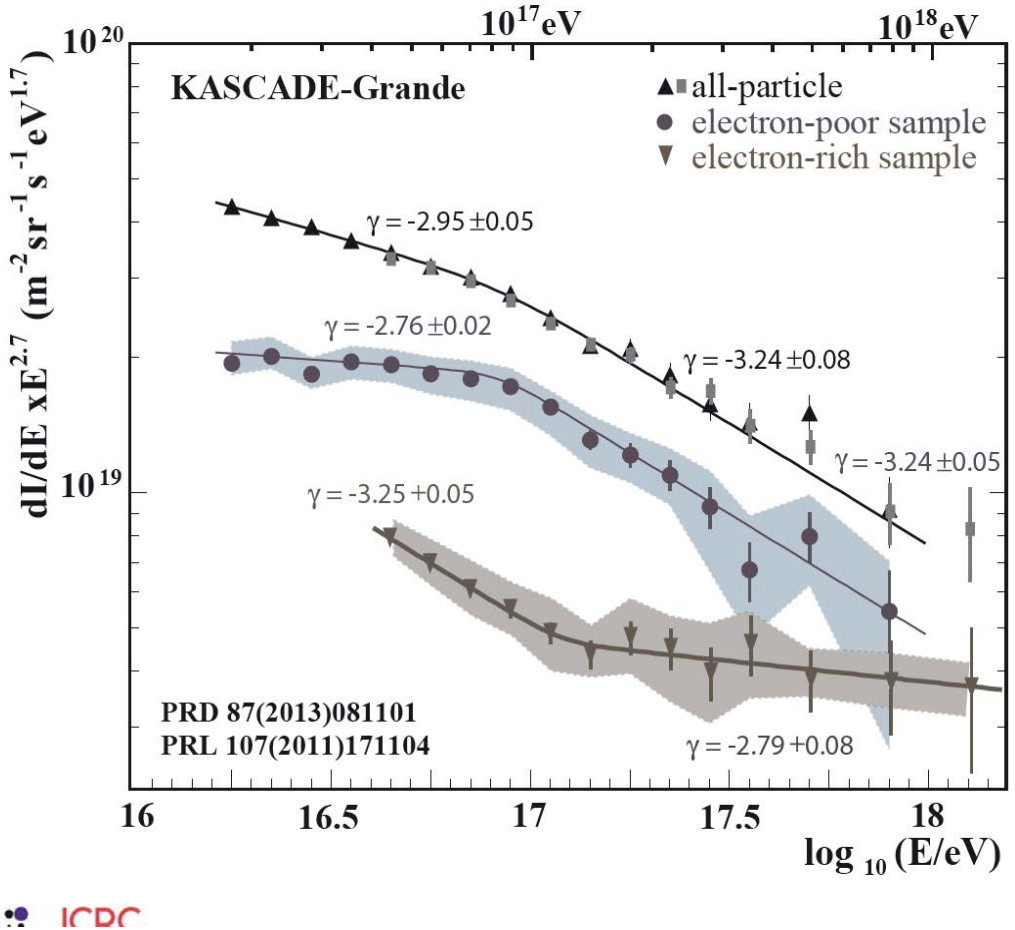

- **steepening due to heavy primaries (3.5σ)**
- **hardening at $10^{17.08}$ eV (5.8σ) in light spectrum**
- **slope change from γ = -3.25 to γ = -2.79!**

Phys.Rev.Lett. 107 (2011) 171104
Phys.Rev.D (R) 87 (2013) 081101

M.Bertaina (KASCADE-Grande) PoS(ICRC2015)???
J.C. Arteaga (KASCADE-Grande) PoS(ICRC2015)314

Development of new detection techniques: electromagnetic signals in radio wavelengths (1)

LOPES

LOPES collaboration:
-) KASCADE-Grande
-) U Nijmegen, NL
-) MPIfR Bonn, D
-) Astron, NL
-) IPE, FZK, D

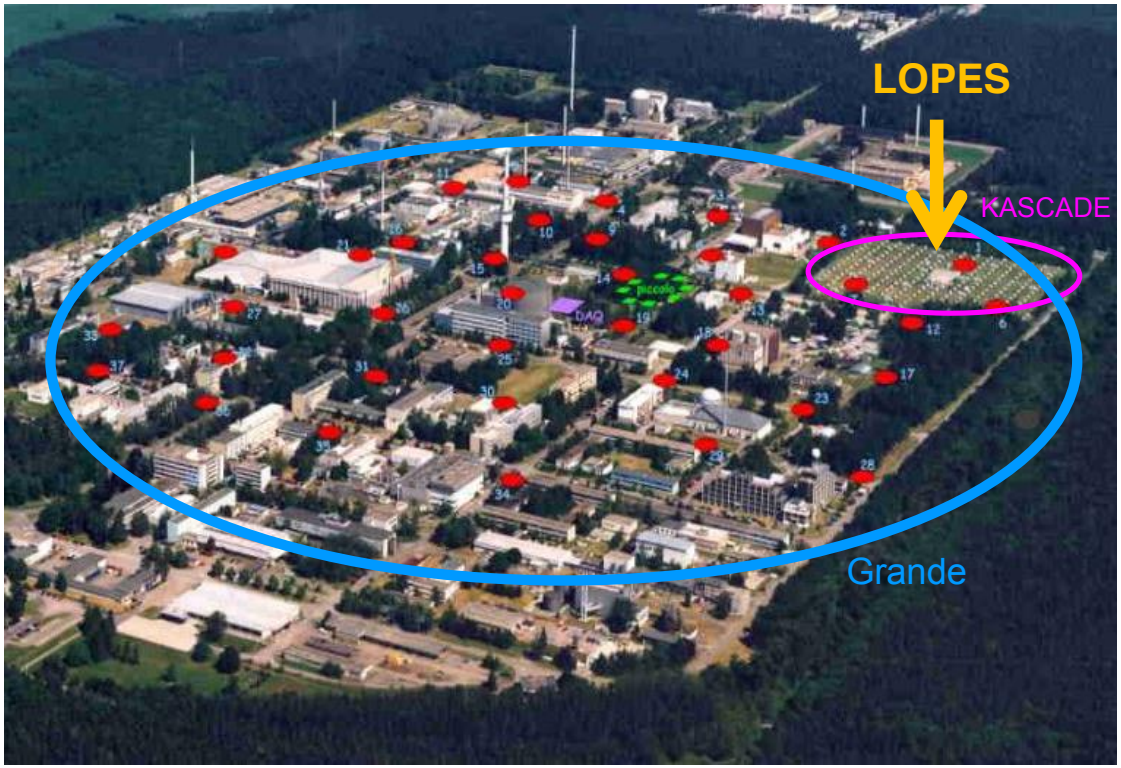

➔Development of a new detection technique!

Development of new detection techniques: electromagnetic signals in radio wavelengths (2)

2. Radio data analysis

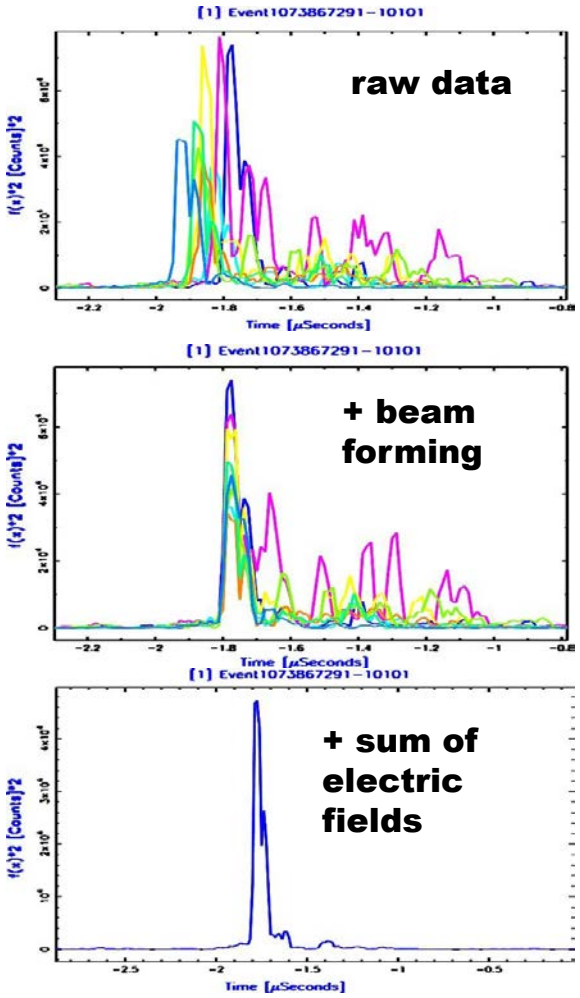

LOPES:
Proof of principle

1. KASCADE measurement

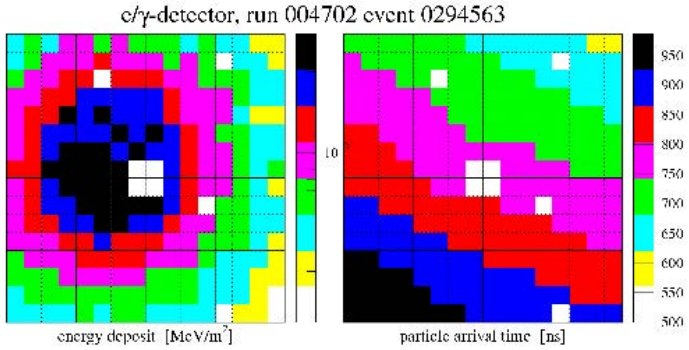

3. Skymapping

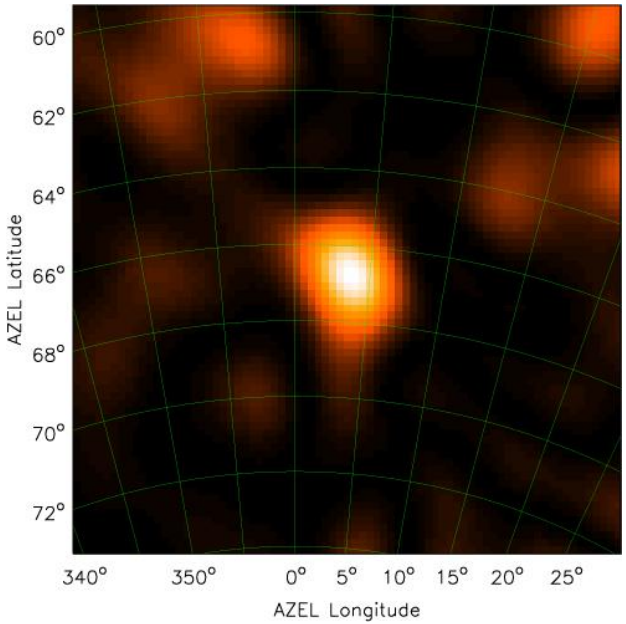

4. Many events

meanwhile >500 events

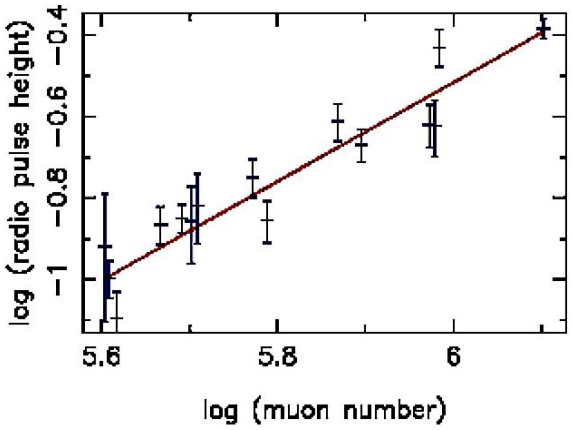

Development of new detection techniques: electromagnetic signals in radio wavelengths (3)

Composition measurements by LOPES

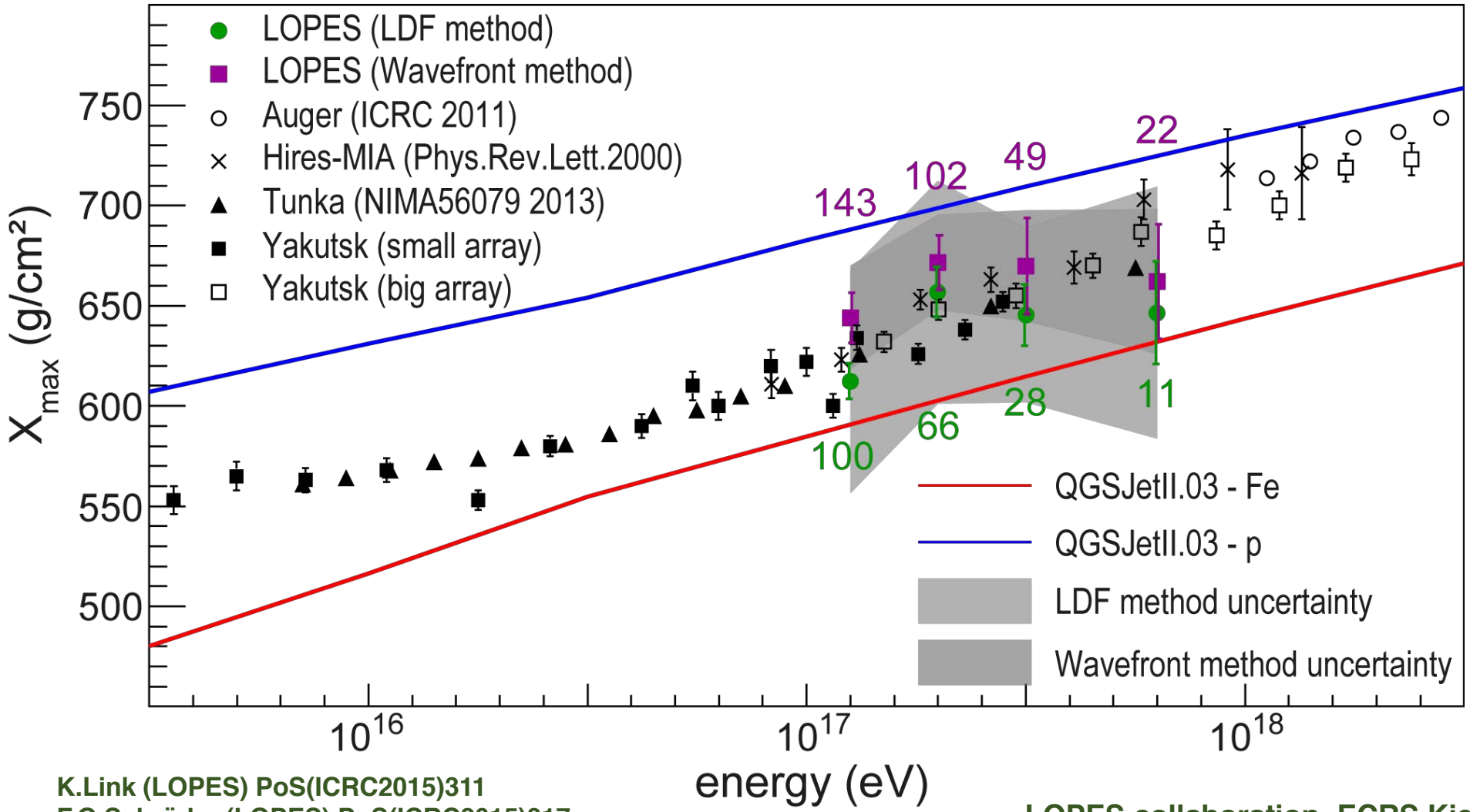

K.Link (LOPES) PoS(ICRC2015)311
F.G.Schröder (LOPES) PoS(ICRC2015)317

LOPES collaboration, ECRS Kiel, 2014

CASA-MIA Particle detector Array

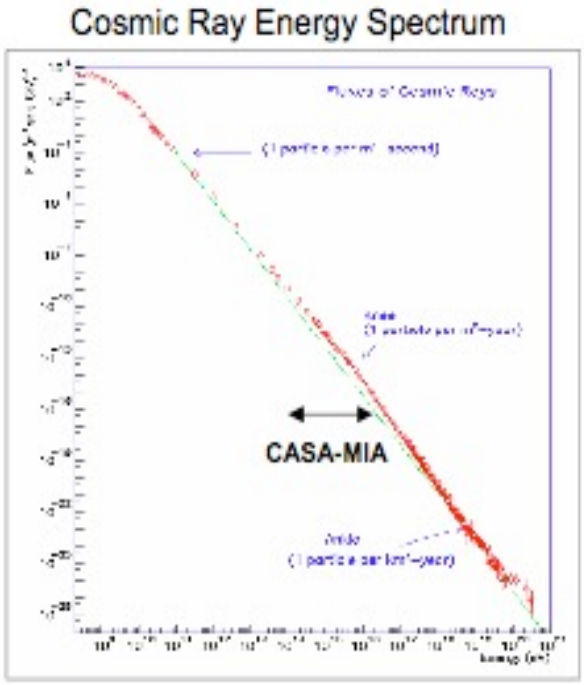

Radius of curvature

$$\rho(m) = \frac{3.3 \times 10^{-6}\, P(eV)}{Z\, B(gauss)}$$

For $P = 10^{18}$ eV

$B = 10^{-6}$ gauss

$\rho = 3.3 \times 10^{18}$ m $\simeq$ 1 pc

For $P < 10^{19}$ eV

$\rho \simeq 10$ kpc (size of galaxy)

No convincing evidence of anisotropy

(but very few events!)

Proposed by J. Cronin in 1985, built in 1987-1997 to reveal C.R. showers with energy less than 10^{17} eV. For this energy the charged particles are deflected by the galactic magnetic field. Only neutral particles can give "astronomical" information.

CASA-MIA: a detector for air shower - (USA, Utah)

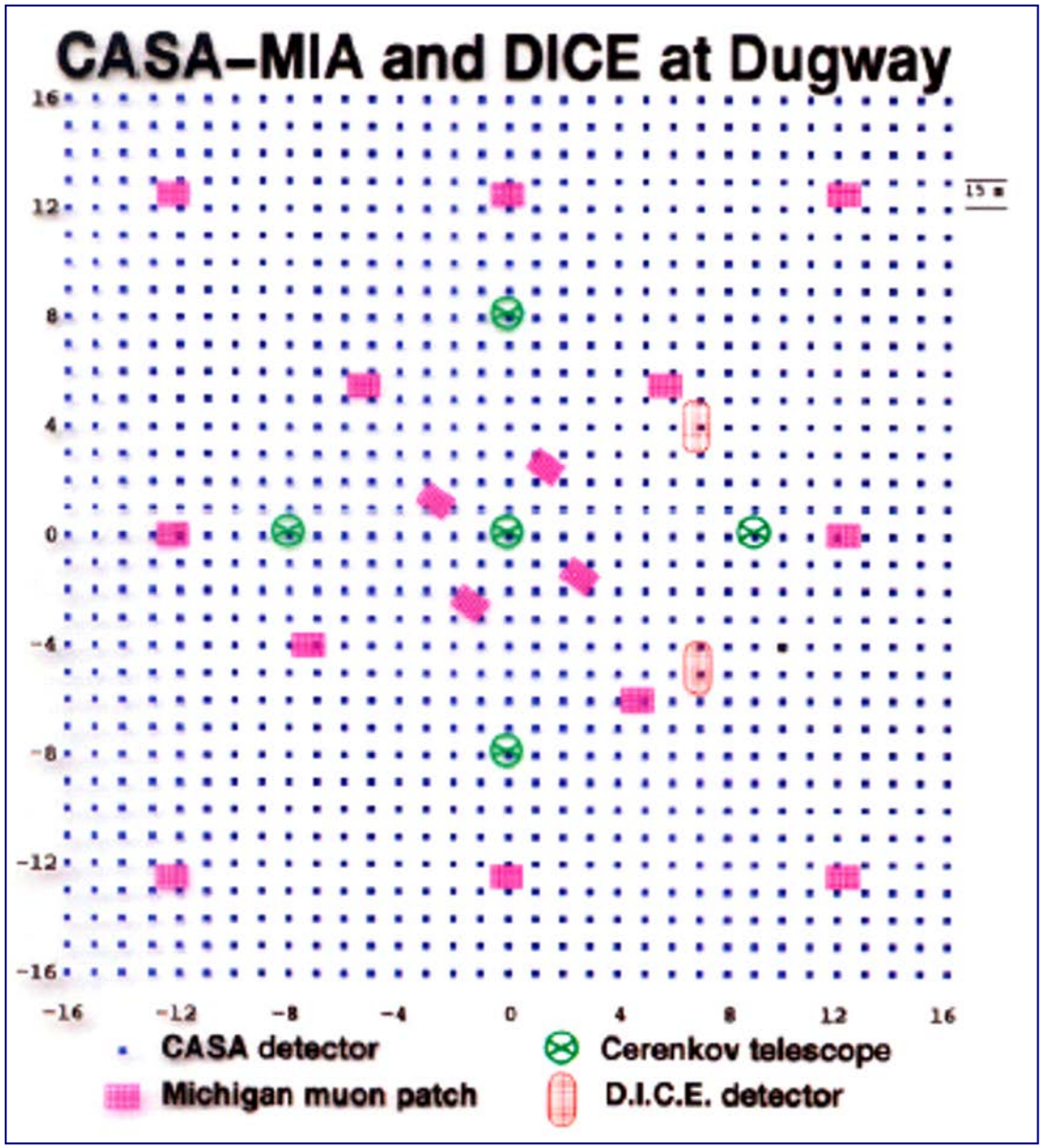

Chicago Air Shower Array: operated 1990 - 1999.

Chicago Air Shower Array: sensitive to showers induced by CR with energies >10^{14}eV. Composed of 1089 "modules" arranged on a lattice with a 15m pitch over a total area of 500m · 500m.
MIchigan Anti: 2500m^2 of underground counters arranged in 16 modules, used to detect the muonic component of the shower (allows to reject 90% of showers of hadron origin)
DICE: two telescopes for Cherenkov light (distant ~ 100m) made with spherical mirrors that project the images into focal planes formed by 256 PMT. You get pixels from 1^o and a total field of view of 16^o x 13.5^o centred around the vertical

CASA-MIA: a detector for air shower - (USA, Utah)

... sensitive to showers with energy E~10^{14} – 10^{17} eV
The average energy of "photons" events observed
<E_γ> ~ 100TeV, angular resolution ~ 0.7°

- **Point Sources:** The primary scientific goal of CASA-MIA was to detect point sources of ultra high energy gamma rays. In this regard, nature was not kind and no clear detections were made by CASA-MIA. However, strong limits were set on the emission from the most interesting sources, such as X-ray binaries (Cygnus X-3 and Hercules X-1) [6], the Crab Nebula [14], and active galactic nuclei [13]. Searches for transient and periodic emission from a number of sources were also carried out, along with a general survey of the overhead sky [12].

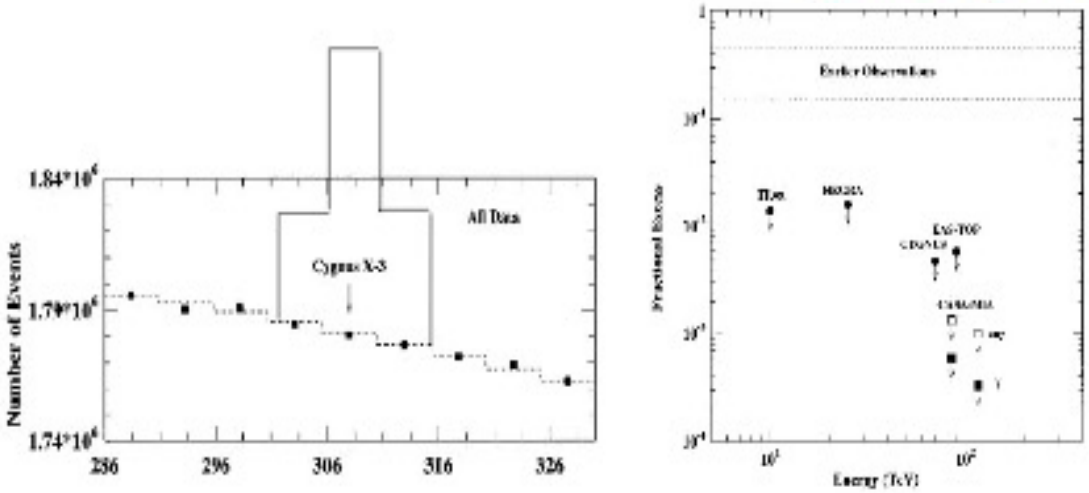

Figure 5: *Results from CASA-MIA on steady emission from the X-ray binary system Cygnus X-3. Left: scan in right ascension across a strip in declination that contains Cygnus X-3. The points correspond to the detected numbers of CASA-MIA events, the dotted curve corresponds to the background estimation, and the solid histogram corresponds to the expected numbers of events assuming the flux measured by the Kiel experiment [4]. Right: limits from several experiments on the flux of ultra high energy gamma rays from Cygnus X-3 as a function of energy. For the CASA-MIA results, the open squares indicate the limits for any neutral particle and the solid squares indicate the limits for gamma rays.*

Detection of U.H.E. Cosmic Rays (E>> 100 PeV)

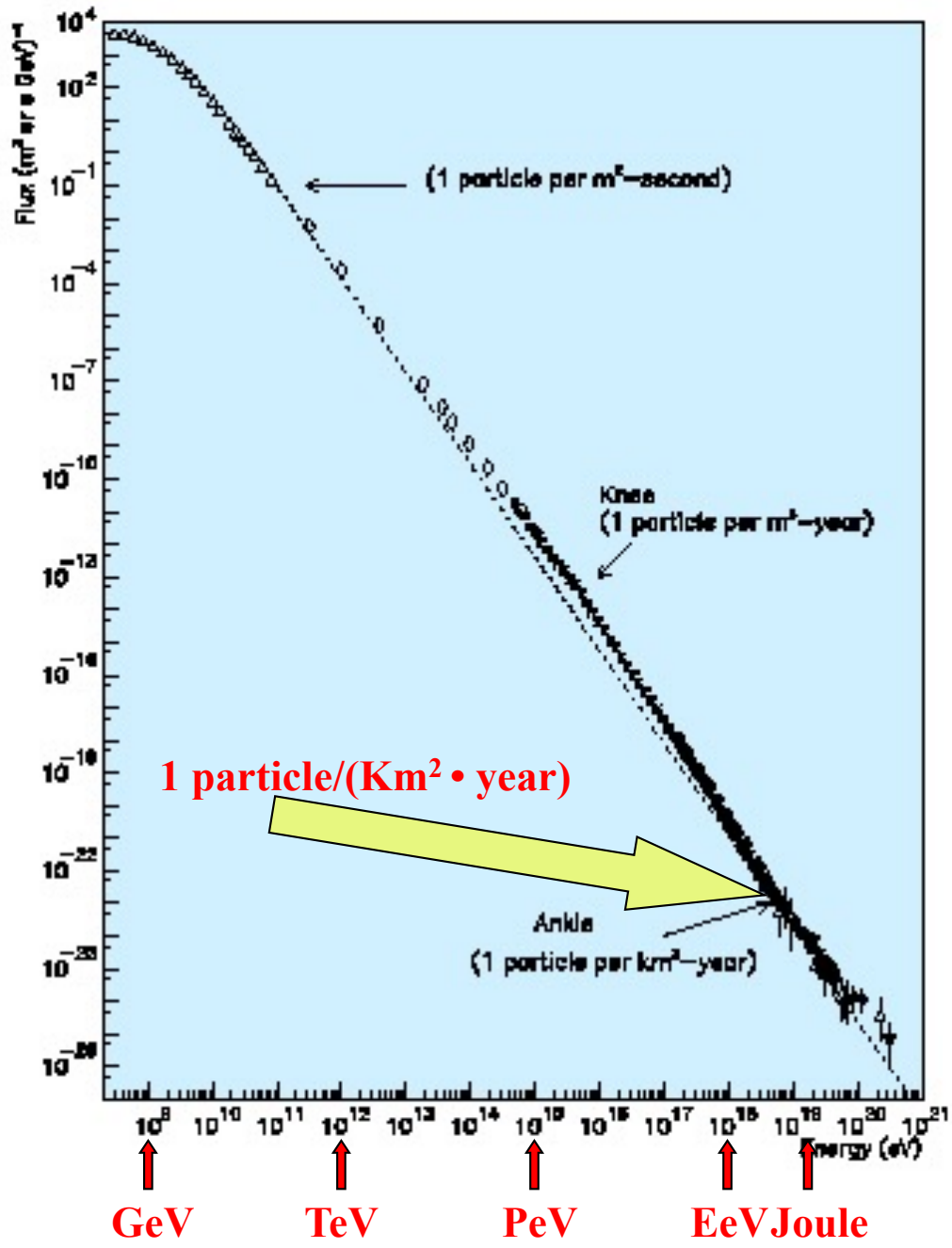

The study of cosmic rays with E >> 100 PeV requires:

⇒ large equipment (sampling, fluorescence detection in the atmosphere, ...)

⇒ on the earth's surface or in space

Ad esempio Akeno Giant Air Shower Array

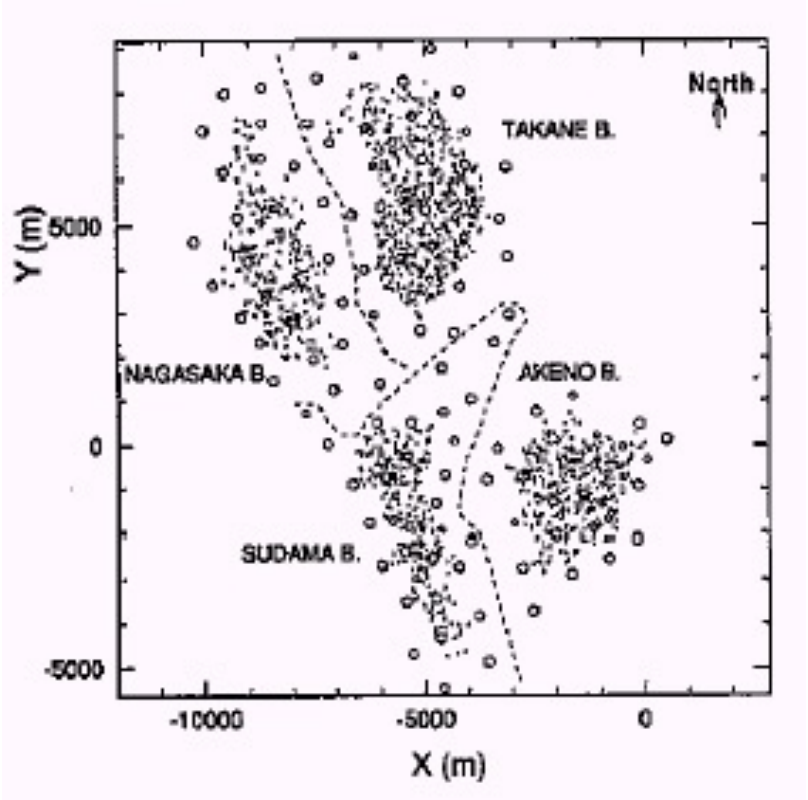

AGASA: the first observations of CR with $E_{shower} > 10^{20}$ eV

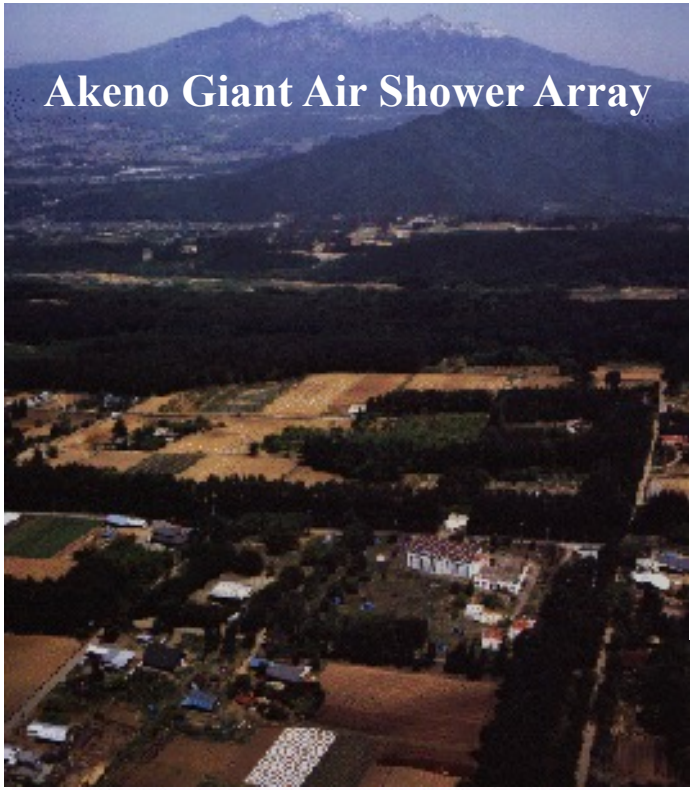

The apparatus, entered into operation in 1990 to observe C.R. with energy> EeV = 10^{18}eV) consists of 111 surface modules (plastic scintillators 2.2 m^2 spaced about 1km to cover a total area of ~ 100 km^2) and 27 buried modules (proportional counters inter-spaced with PB or Fe absorbers or concrete) used as muon detectors.

It is divided into 4 sectors: Akeno, Sudama, Takane, Nagasaka. The AKENO sector (operates since 1984) consists of a region "densely populated" of scintillators and a region with more "dispersed" counters.

Shower parameters: energy reconstructed through the "particle density" 600m away from the "core" of the shower. The measurement of this density requires knowledge of the lateral distribution of the swarm:

AKENO-20 -> centre of the shower

AKENO -1 -> measures the density

$$\rho(R) = C\left(\frac{R}{R_M}\right)^{-1.2}\left(1+\frac{R}{R_M}\right)^{-(\eta-1.2)}$$

Density as a function of the distance
R_M=Moliere radius = 91.6m in Akeno

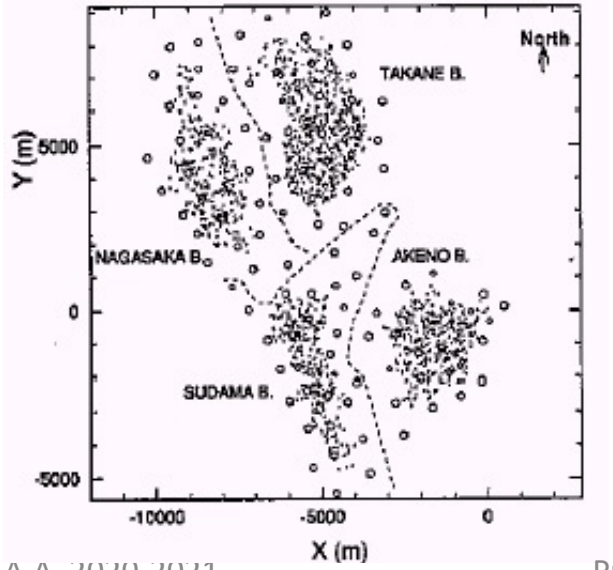

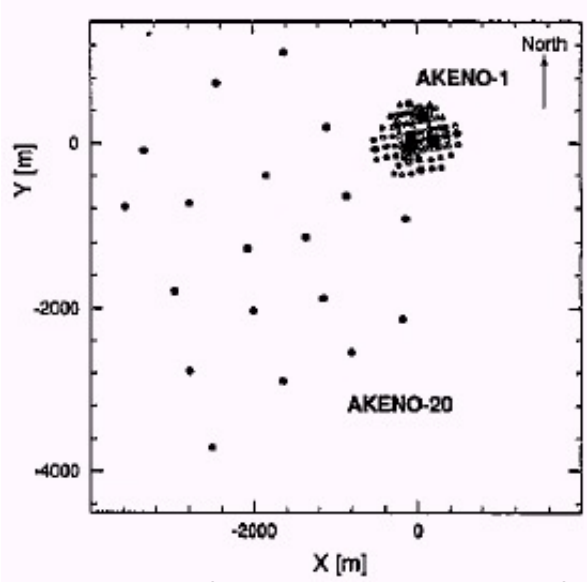

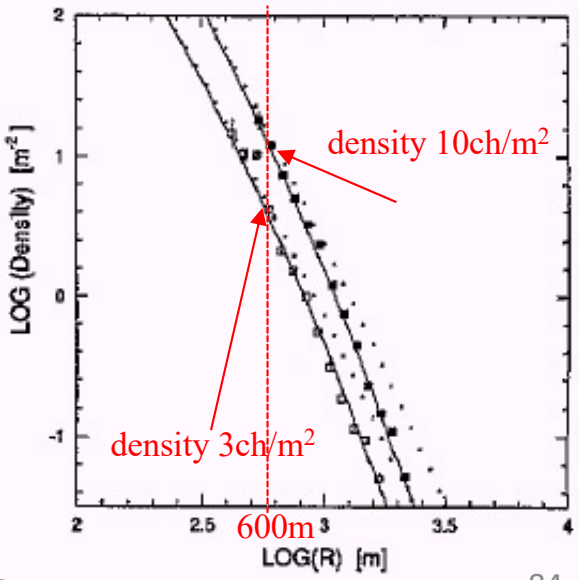

AKENO

"Sampled" surface ~ 100 km^2
111 scintillation counters with area 2.2 m^2
Active until January 2004

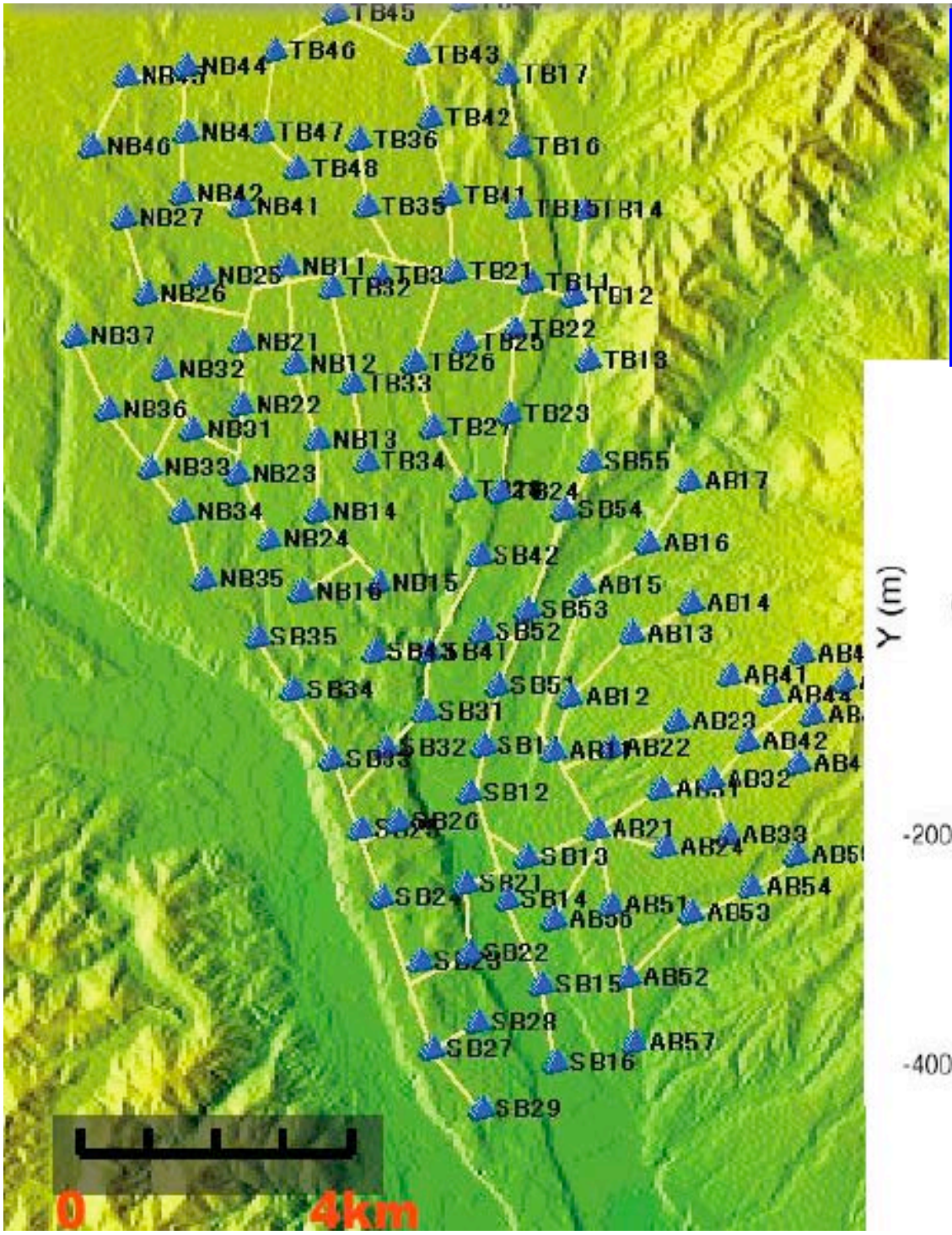

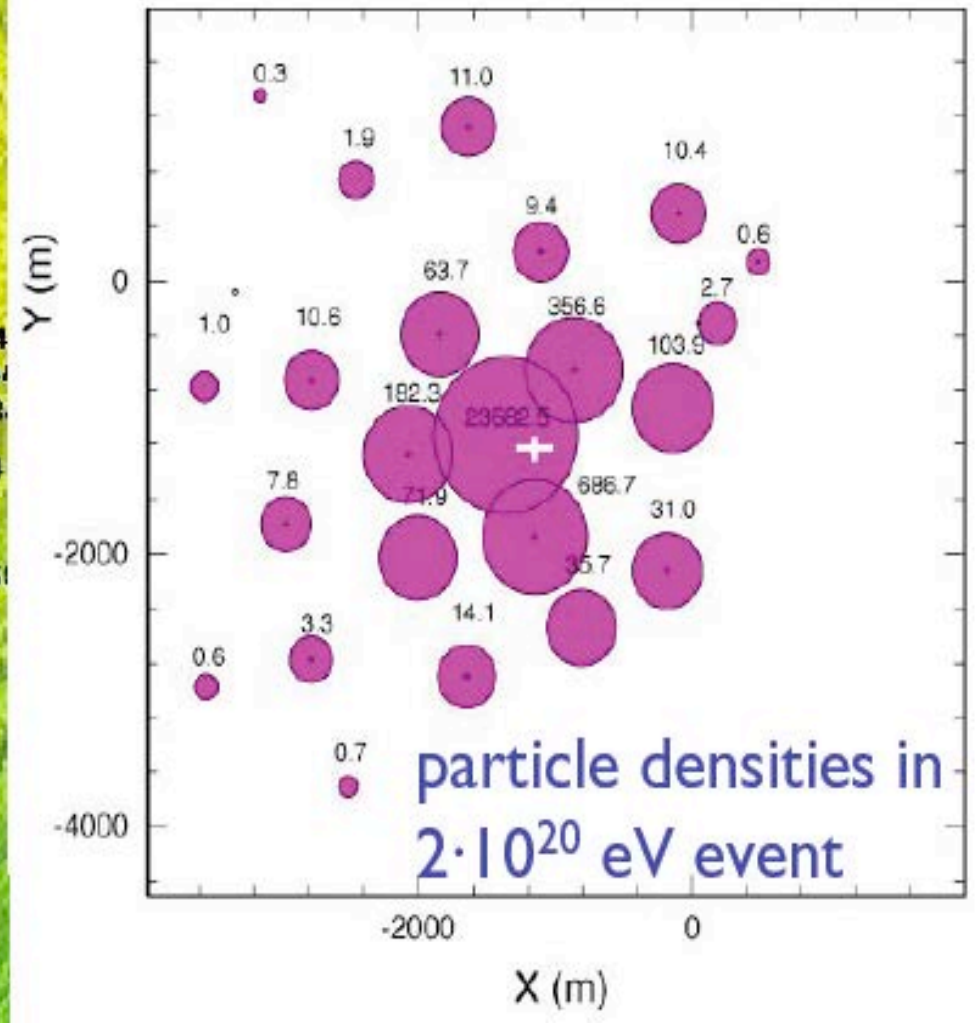

The AGASA Telescope Array (Japan)

Akeno Giant Air Shower Array (AGASA) group has published its results on the discovery of 8 air-shower events with the primary energies beyond 10^{20}eV out of 9 years observation.

Space becomes opaque to particles with energies in excess of several times 10^{19}eV because of the 2.7K cosmic microwave background.

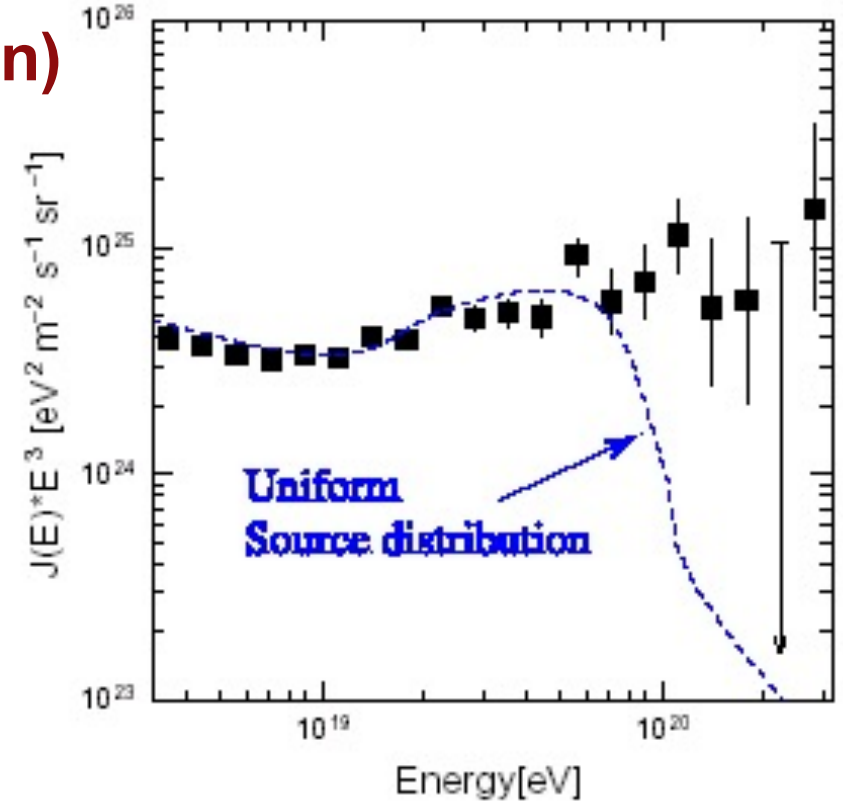

Fig. 3. The energy spectrum of cosmic rays with events up to 60°. The arrows are Poisson upper limits of 90% C.L. The dashed curve is the expected energy spectrum for sources uniformly distributed in the universe taking account of the energy resolution of the AGASA experiment.

The energy spectrum observed by AGASA using events with zenith angles up to 60° is shown in Fig.3, multiplied by E^3 in order to emphasize the detailed structure of the steeply falling spectrum. Error bars represent the Poisson upper and lower limits at 68% and arrows are 90% confidence level (C.L.) upper limits. There is no cutoff around GZK energy ($\sim 4 \times 10^{19}$eV) and the spectrum extends up to a few times 10^{20}eV. The updated spectrum is consistent with that by Takeda *et al.* (1998).

Greisen and Zatsepin and Kuzmin independently pointed out that CMB radiation would make space opaque to cosmic rays of very high energy (GZK mechanism). This limitation implies that the sources for these extremely high energy particles need to be less than about 50Mpc from the Earth. Particles with energies in this range are expected to be deflected very little by magnetic fields within or beyond the galaxy. Yet none of these high energy cosmic rays points back to a possible known source.

An overview of present/future C.R. detectors

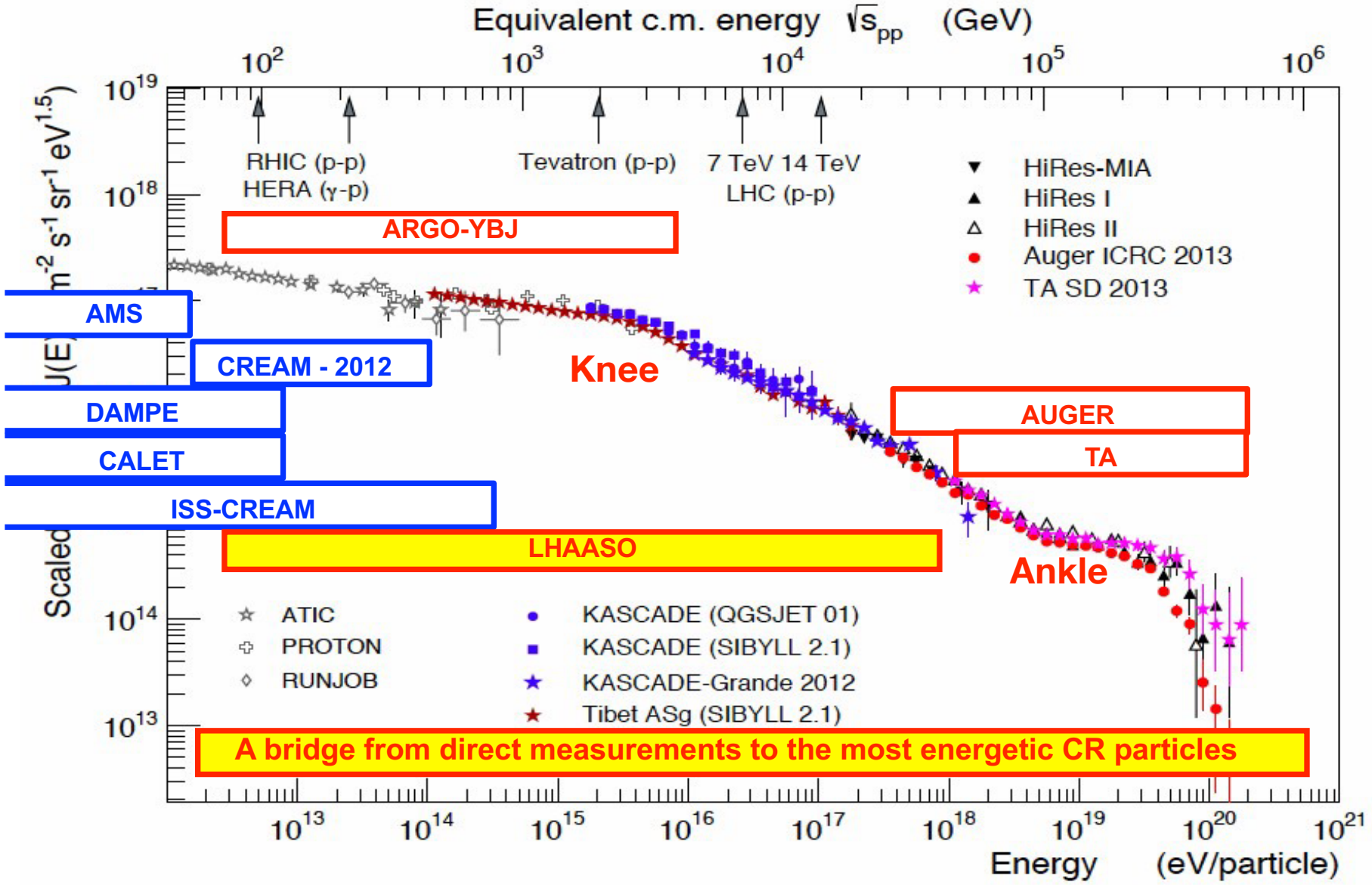

LHAASO: Water Cherenkov Detector Array

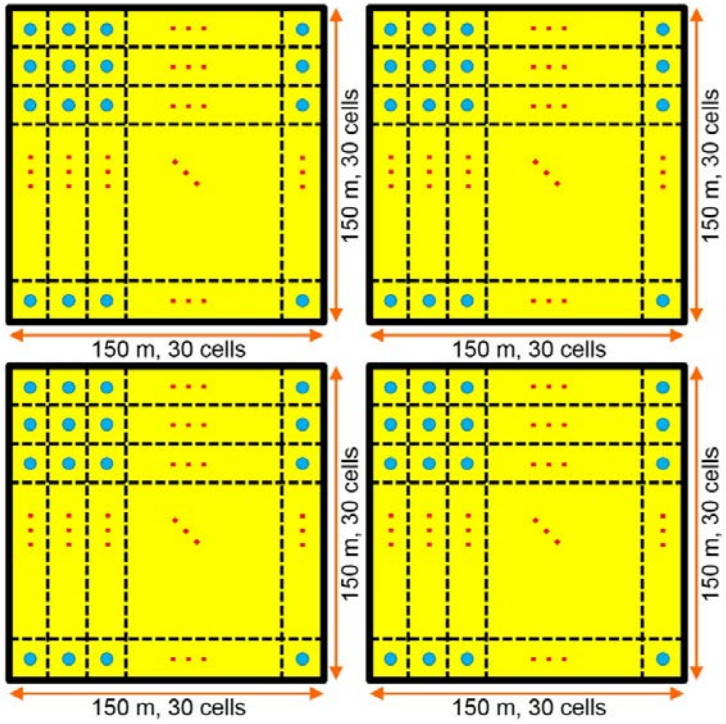

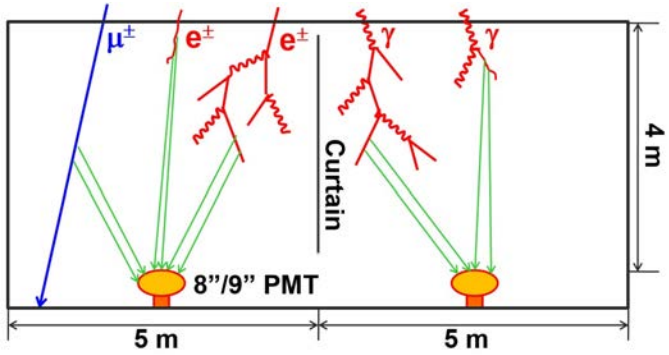

Item	Value
Cell area	25 m^2
Effective water depth	4 m
Water transparency	> 15 m (400 nm)
Precision of time measurement	0.5 ns
Dynamic range	1-4000 PEs
Time resolution	<2 ns
Charge resolution	40% @ 1 PE 5% @ 4000 PEs
Accuracy of charge calibration	<2%
Accuracy of time calibration	<0.2 ns
Total area	90,000 m^2
Total cells	3600

Lhaaso; Electromagnetic particle Detector

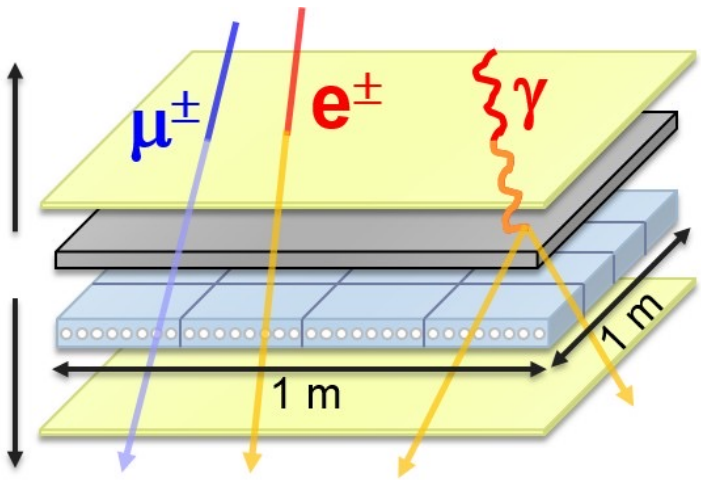

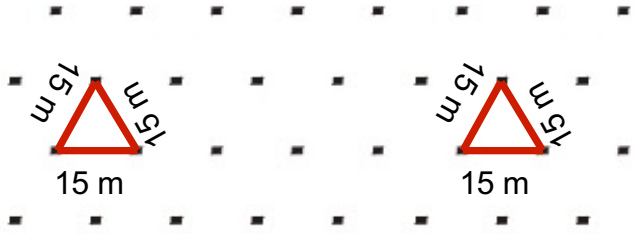

Item	Value
Effective area	1 m^2
Thickness of tiles	2 cm
Number of WLS fibers	8/tile × 16 tile
Detection efficiency (> 5 MeV)	>95%
Dynamic range	1-10,000 particles
Time resolution	<2 ns
Particle counting resolution	25% @ 1 particle 5% @ 10,000 particles
Aging	>10 years
Spacing	15 m
Total number of detectors	5635

LHAASO: Muon Detector

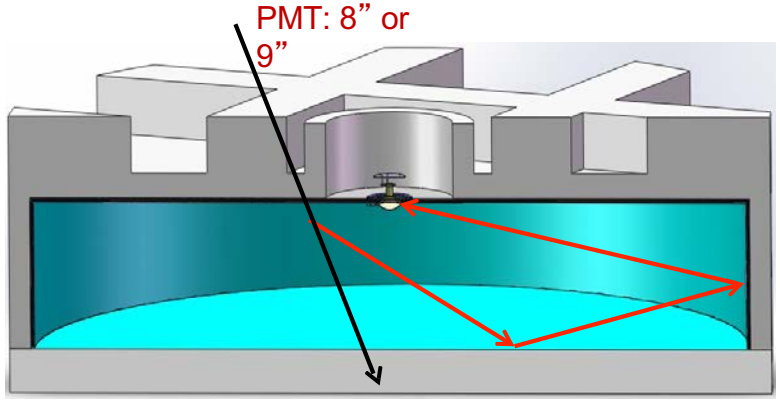

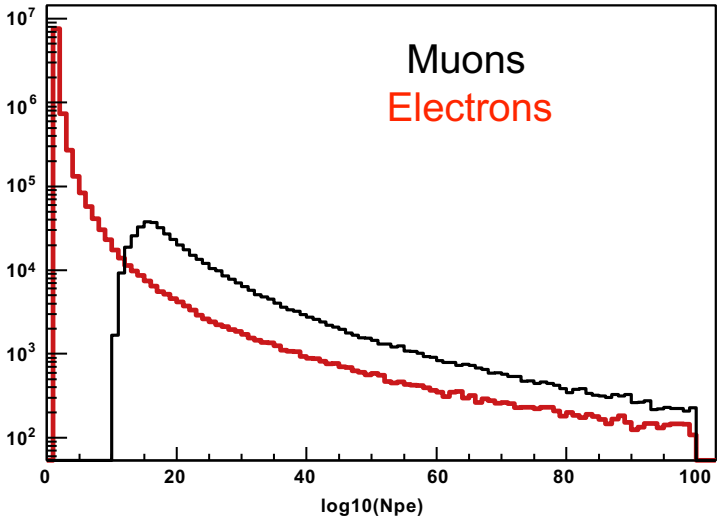

Photoelectron distribution at R>100m from the shower core

Item	Value
Area	36 m^2
Depth	1.2 m
Molasses overburden	2.5 m
Water transparency (att. len.)	> 30 m (400 nm)
Reflection coefficient	>95%
Time resolution	<10 ns
Particle counting resolution	25% @ 1 particle 5% @ 10,000 particles
Aging	>10 years
Spacing	30 m
Total number of detectors	1221

LHAASO: Wide field of view Cherenkov Telescope Array

24 telescopes (Cherenkov/Fluorescence)

- 5 m2 spherical mirror
- 16x16 PMT array
- FOV: 14ºx 14º
- Elevation angle: 60º

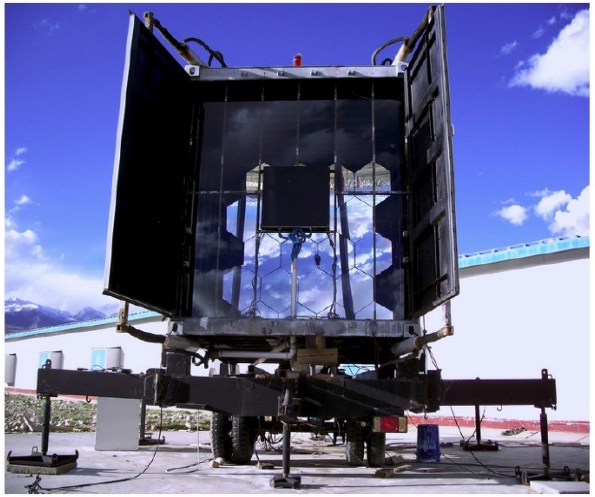

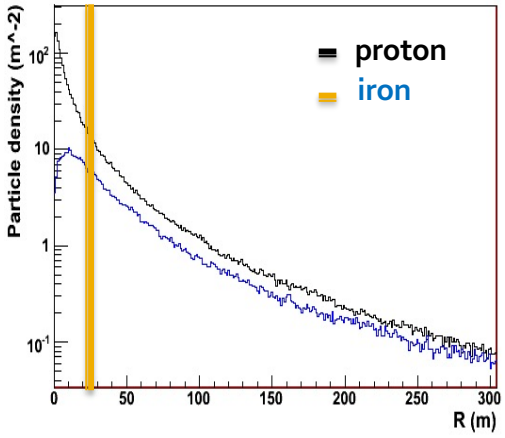

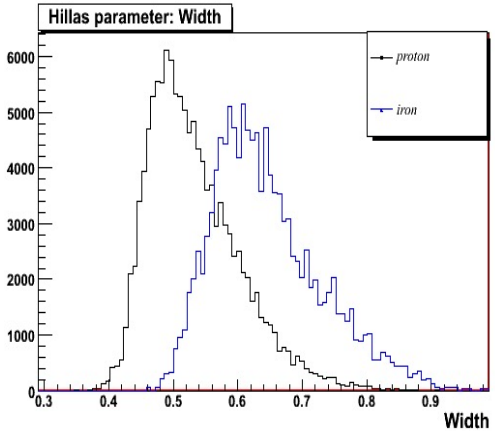

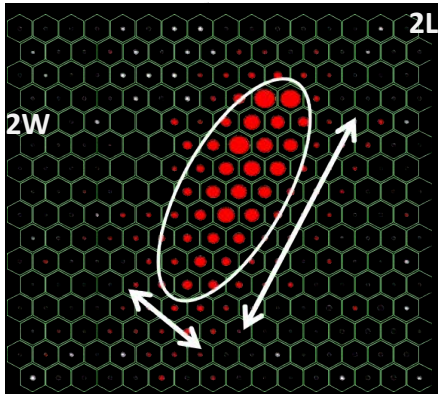

LHAASO: Shower Core Detector Array

425 close-packed burst detectors, located near the centre of the array, for the detection of high energy secondary particles in the shower core region.

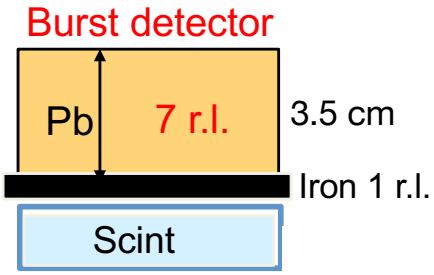

The burst detectors observe the electron size (burst size) under the lead plate induced by high energy e.m. particle in the shower core region

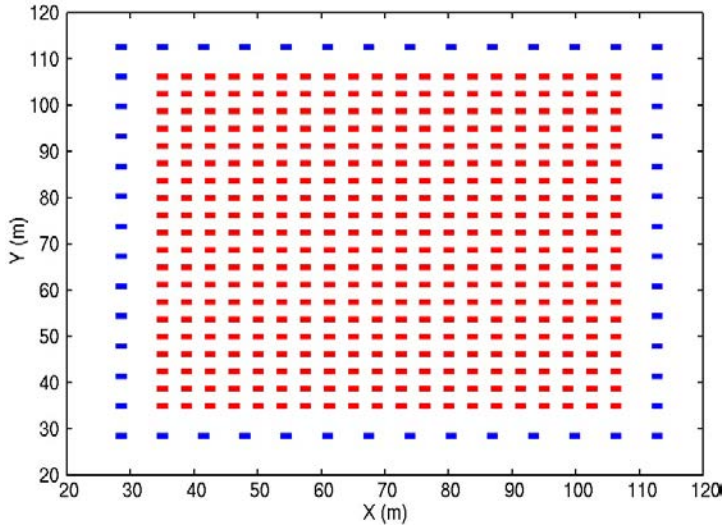

Each burst detector is constituted by 20 optically separated scintillator strips of 1.5 cm x 4 cm x 50 cm read out by two PMTs operated with different gains to achieve a wide dynamic range (1- 10 ^{6} MIPs).

Number of SCD: 0.5m^2 x 452
Cover Area: 5170m^2
Energy region: 30 TeV 10 PeV
Core position resolution: 1.5 m @50 TeV

Lead plate (80 cm X 50 cm X 7 rl)
Iron plate (1 m X 1 m X 1 rl)

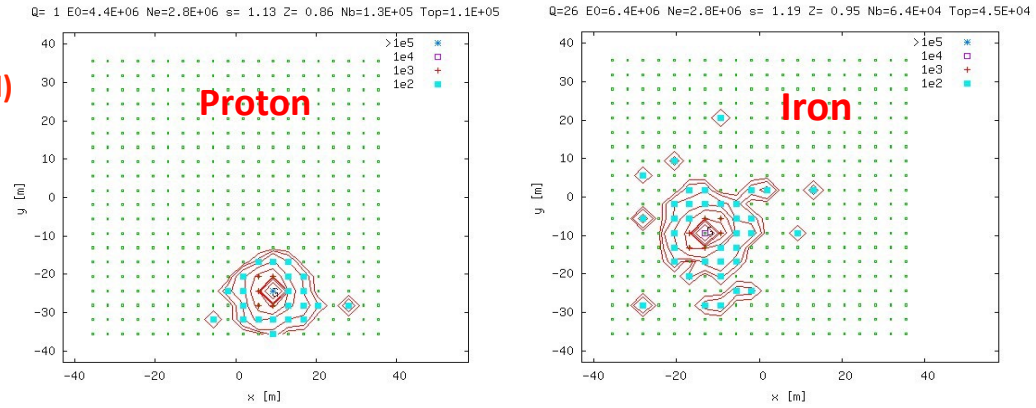

Charged primary Cosmic Rays for E >> TeV

So far we have mainly discussed experiments measuring gamma fluxes:

- very good tool for astronomy
- large background due to the much more intense charged component

High energy charged primary cosmic rays carry many information:

- what happens for E~10^{15} eV
- does the primary CR composition changes with energy ?? Can our detector distinguish a light CR (proton, He, …) from an heavy one (Fe, …) ?
- are these CR of galactic origin or there is an extragalactic component ?

What kind of experimental technique can answer to all these questions ?

LHAASO sensitivity for Crab-like sources

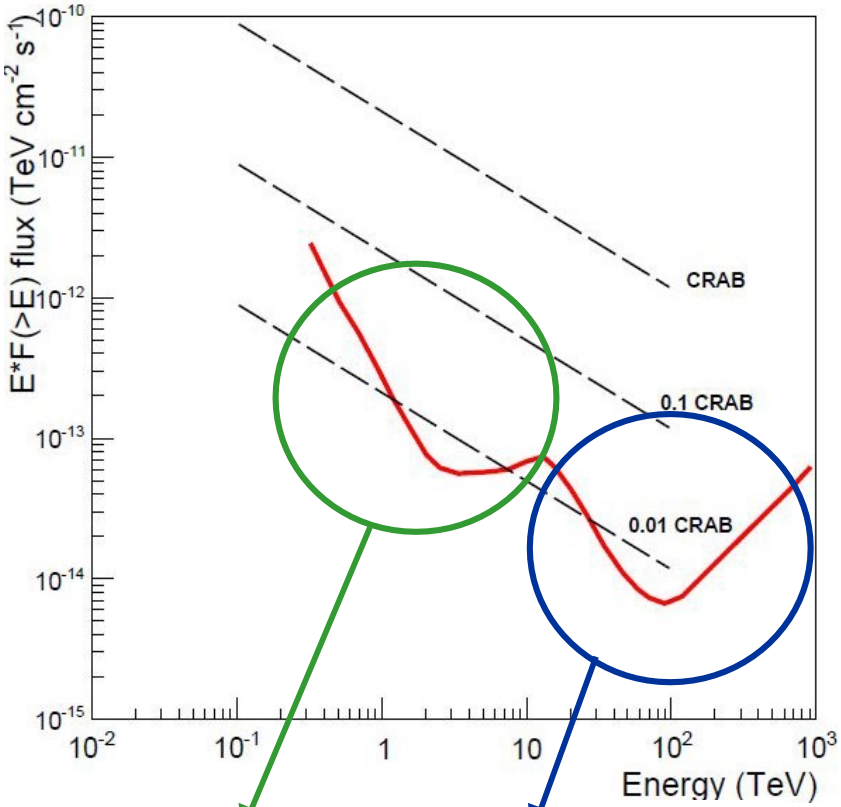

WCDA

KM2A (EDs + MDs)

WCDA discrimination

gamma

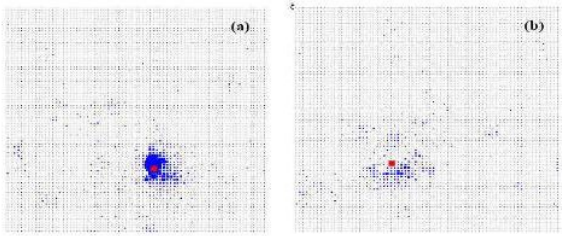

proton

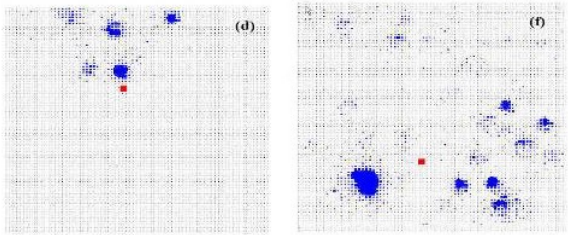

WCDA angular resolution

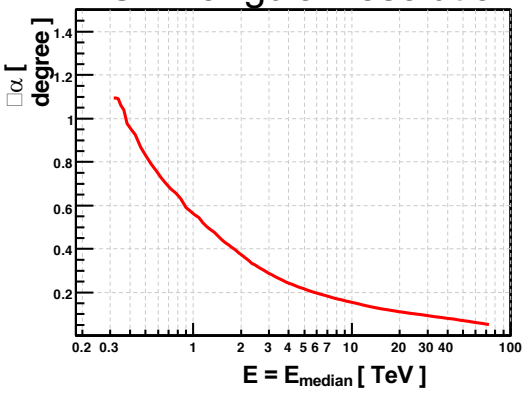

KM2A discrimination

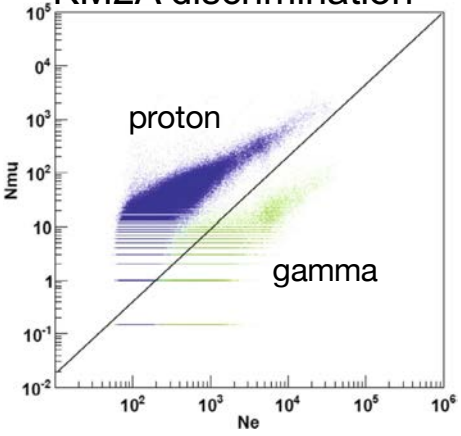

All particle energy spectrum

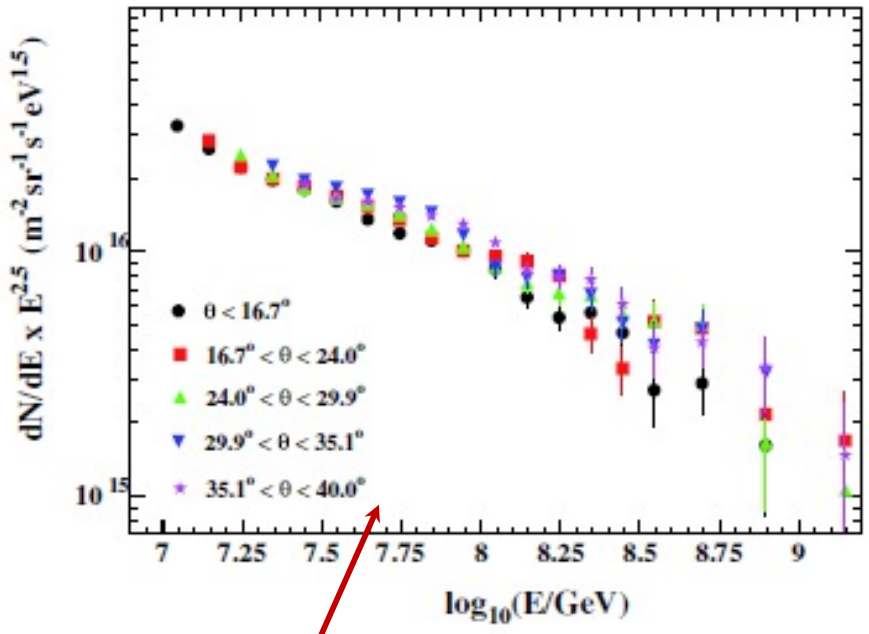

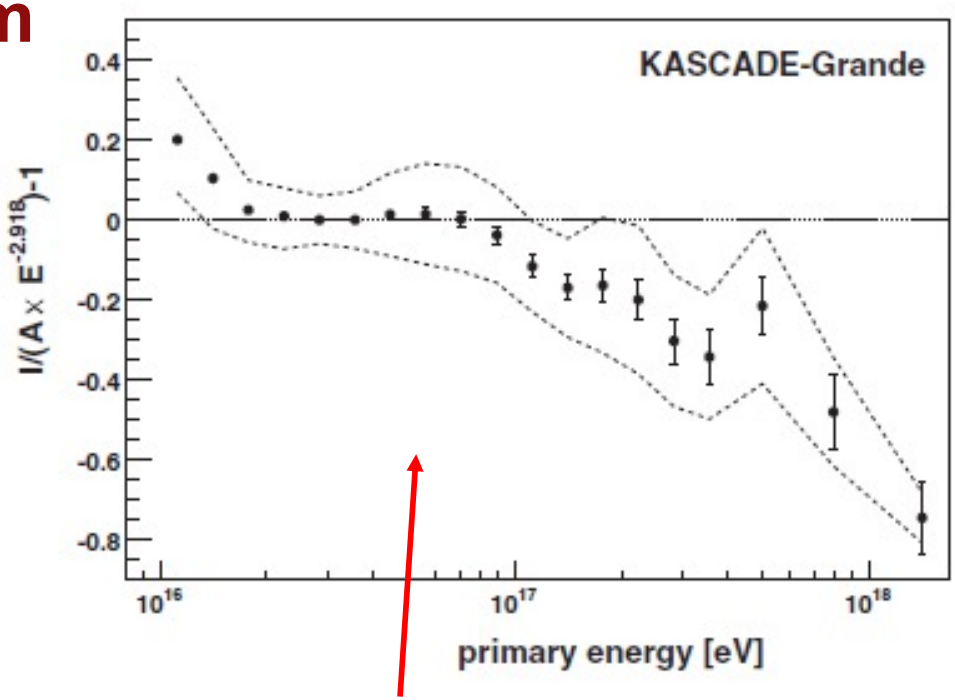

Energy spectra measured in the five angular bins

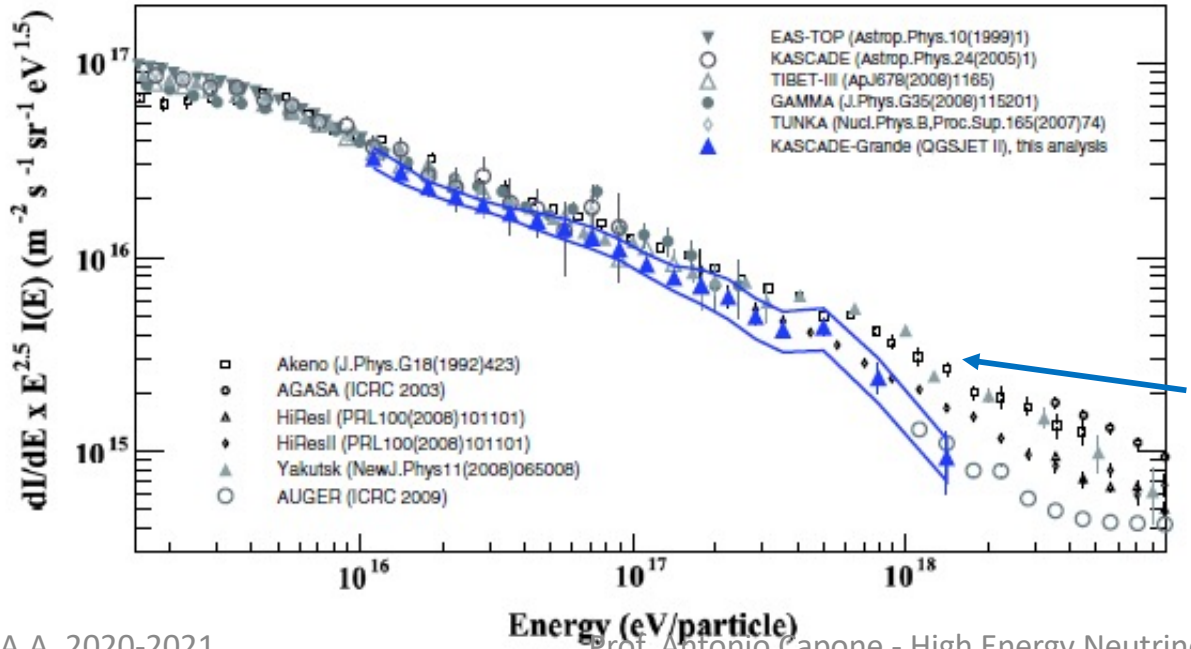

- **Spectrum cannot be described by a single power law**
- **Hardening above 10^{16} eV**
- **Steepening close to 10^{17} eV significance 2.1σ**

Comparison of the KG spectrum with different experiments

Astroparticle Physics 36, (2012) 183

KASCADE summary (1)

- KASCADE-Grande data taking stopped in November 2012.
- All particle spectrum:
  - Hardening ~10^{16} eV
  - Steepening ~8×10^{16} eV

- Steepening of the heavy primaries specrum at $10^{16.92 \pm 0.04}$ eV. Slope index changes from 2.76 ± 0.02 to 3.24 ± 0.05

- Hardening of the light primaries spectrum at $10^{17.08 \pm 0.08}$ eV. Slope index changes from 3.25 ± 0.05 to 2.79 ± 0.08

- $E_b(\text{light}) \neq E_b(\text{heavy})$
- $\gamma_1(\text{light}) = \gamma_2(\text{heavy})$
- $\gamma_2(\text{light}) \approx 2.7$

KASCADE summary (2)

KASCADE : energy spectra of single mass groups

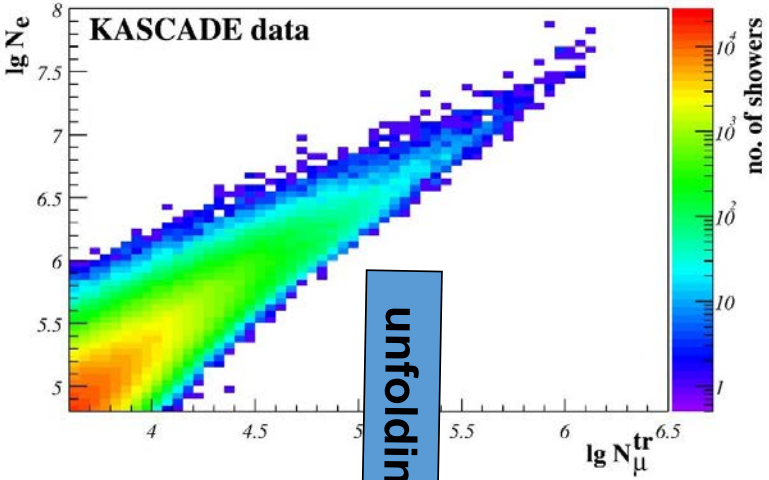

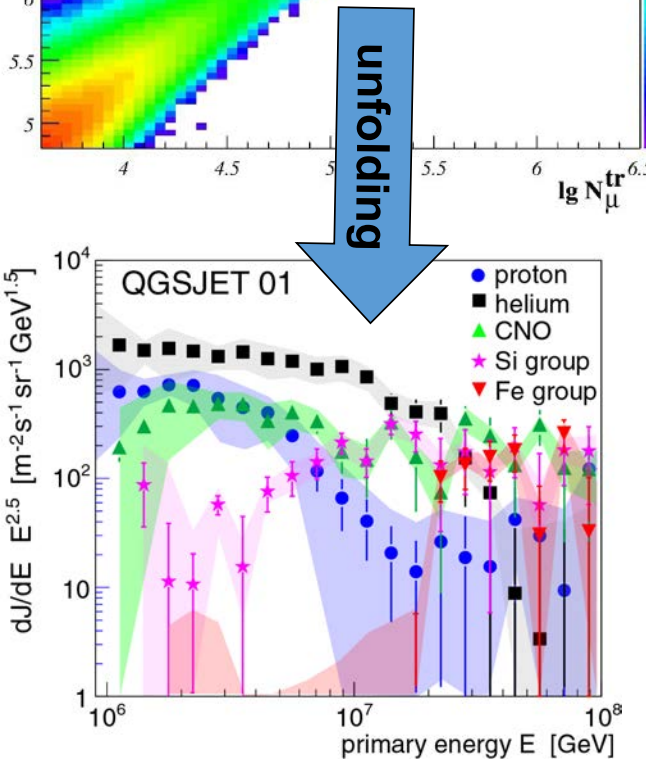

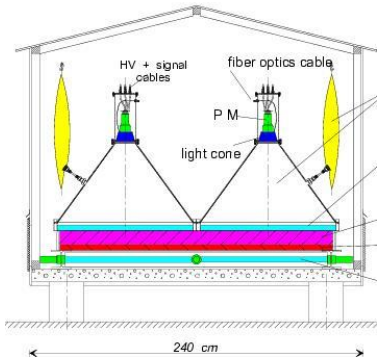

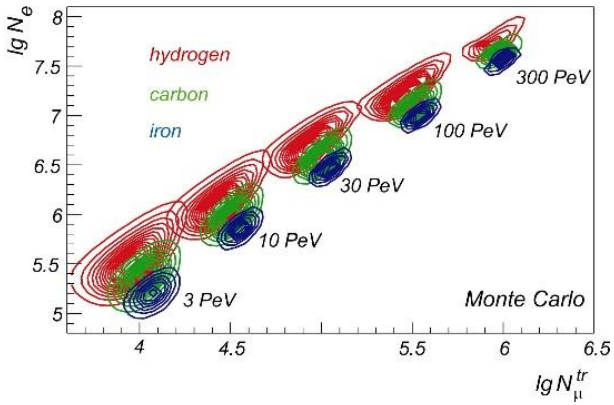

Searched: E and A of the Cosmic Ray Particles

Given: N_e and N_μ for each single event

➔ **solve the inverse problem**

$$\frac{dJ}{d\lg N_e\, d\lg N_\mu^{tr}} = \sum_A \int_{-\infty}^{+\infty} \frac{dJ_A}{d\lg E}\, p_A(\lg N_e, \lg N_\mu^{tr} \mid \lg E)\, d\lg E$$

- kernel function obtained by Monte Carlo simulations (CORSIKA)
- contains: shower fluctuations, efficiencies, reconstruction resolution